Report No. FHWA-KS-02-7
FINAL REPORT

ACCELERATED TESTING FOR STUDYING PAVEMENT DESIGN AND PERFORMANCE (FY 2001)

Evaluation of the Performance of Permeable and Semi-Permeable Unbound Grandular Bases under Portland Cement Concrete Pavement (PCCP) Slabs and Alternate Load Transfer Devices for Joint Repair

Hani G. Melhem
Roger Swart
Sandy Walker
Kansas State University

NOVEMBER 2003

KANSAS DEPARTMENT OF TRANSPORTATION

Division of Operations
Bureau of Materials and Research

1	Report No. FHWA-KS-02-7	2 Government Accession No.	3	Recipient Catalog No.
4	**Title and Subtitle** ACCELERATED TESTING FOR STUDYING PAVEMENT DESIGN AND PERFORMANCE (FY 2001) Evaluation of the Performance of Permeable and Semi-Permeable Unbound Grandular Bases under Portland Cement Concrete Pavement (PCCP) Slabs and Alternate Load Transfer Devices for Joint Repair		5	**Report Date** November 2003
			6	**Performing Organization Code**
7	**Author(s)** Hani G. Melhem, Roger Swart and Sandy Walker		8	**Performing Organization Report No.**
9	**Performing Organization Name and Address** Kansas State University; Department of Civil Engineering 2127 Fiedler Hall Manhattan, Kansas 66506		10	**Work Unit No. (TRAIS)**
			11	**Contract or Grant No.** C1232
12	**Sponsoring Agency Name and Address** Kansas Department of Transportation Bureau of Materials and Research, Research Unit 2300 Southwest Van Buren Street Topeka, Kansas 66611-1195		13	**Type of Report and Period Covered** Final Report July 2000 – June 2001
			14	**Sponsoring Agency Code** RE-0165-01

15 Supplementary Notes
For more information write to address in block 9.

16 Abstract

The objectives of this research are to determine the effect of unbound drainable base types on the performance of PCCP and the efficiency of fiber-reinforced polymer (FRP) dowels, compared to epoxy coated steel dowels, when retrofitted to re-establish the load transfer in damaged non-doweled joints. The experiment was conducted at the Accelerated Testing Laboratory at Kansas State University, and consisted of constructing two pavements, one with permeable base and another with semi-permeable base, and subjecting them to full-scale accelerated pavement test. Water was periodically spread at the surface of the pavement to simulate the effect of rainfall, induce the accumulation of water in the base and to allow the comparison of the drainage capability and the performance of the two unbound bases. The measured stresses and strains as well as the distresses observed on the two pavements clearly indicated a better performance for the permeable granular base. The semi-permeable base pavement exhibited severe cracking and pumping of fines from the base and subgrade. The joints and cracks in the semi-permeable base pavement were retrofitted with 1.5 inch FRP dowels and one inch steel dowels to re-establish the shear transfer. After an additional 25,000 passes were applied to the repaired pavement it was observed that the conventional steel dowels give a better performance than the FRP dowels.

17 Key Words	18 Distribution Statement
Accelerated Pavement Test, Dowels, Epoxy Coated Steel, Fiber Reinforced Polymer, FRP, Joint, PCCP, Portland Cement Concrete Pavement, Stress and Strain	No restrictions. This document is available to the public through the National Technical Information Service, Springfield, Virginia 22161

19 Security Classification (of this report) Unclassified	20 Security Classification (of this page) Unclassified	21 No. of pages 100	22 Price

Form DOT F 1700.7 (8-72)

ACCELERATED TESTING FOR STUDYING PAVEMENT DESIGN AND PERFORMANCE (FY 2001)

Evaluation of the Performance of Permeable and Semi-Permeable Unbound Grandular Bases under Portland Cement Concrete Pavement (PCCP) Slabs and Alternate Load Transfer Devices for Joint Repair

Final Report

Prepared by

Hani G. Melhem
Professor
Kansas State University

and

Roger Swart*

and

Sandy Walker*

*were with Kansas State University when report written

NOTICE

The authors and the state of Kansas do not endorse products or manufacturers. Trade and manufacturers names appear herein solely because they are considered essential to the object of this report.

This information is available in alternative accessible formats. To obtain an alternative format, contact the Office of Transportation Information, Kansas Department of Transportation, 915 SW Harrison Street, Room 754, Topeka, Kansas 66612-1568 or phone (785) 296-3585 (Voice) (TDD).

DISCLAIMER

The contents of this report reflect the views of the authors who are responsible for the facts and accuracy of the data presented herein. The contents do not necessarily reflect the views or the policies of the state of Kansas. This report does not constitute a standard, specification or regulation.

ABSTRACT

The objectives of this research are to determine the effect of unbound drainable base types on the performance of PCCP and the efficiency of fiber-reinforced polymer dowels, compared to epoxy coated steel dowels, when retrofitted to re-establish the load transfer in damaged non-doweled joints. The experiment was conducted at the Accelerated Testing Laboratory at Kansas State University, and consisted of constructing two pavements, one with permeable base and another with semi-permeable base, and subjecting them to full-scale accelerated pavement test. Water was periodically spread at the surface of the pavement to simulate the effect of rainfall, induce the accumulation of water in the base and to allow the comparison of the drainage capability and the performance of the two unbound bases. The measured stresses and strains as well as the distresses observed on the two pavements clearly indicated a better performance for the permeable granular base. The semi-permeable base pavement exhibited severe cracking and pumping of fines from the base and subgrade. The joints and cracks in the semi-permeable base pavement were retrofitted with 1.5 inch FRP dowels and one inch steel dowels to re-establish the shear transfer. After an additional 25,000 passes were applied to the repaired pavement it was observed that the conventional steel dowels give a better performance than the FRP dowels.

ACKNOWLEDGEMENTS

TABLE OF CONTENTS

LIST OF FIGURES

LIST OF TABLES

Chapter 1

Introduction

1.1 Report Organization

This manuscript is the final report that describes the research project conducted under Kansas Department of Transportation (KDOT) Contract C1232, "Accelerated Testing for Studying Pavement Design and Performance (FY 2001)", (KSU Research Project No. 5-34126). This contract is funded by the Midwest States Accelerated Testing Pooled Fund Program. States participating in this program are Iowa, Kansas, Missouri and Nebraska.

The purpose of the project is to conduct the experiment selected by the Midwest States Accelerated Testing Pooled Funds Technical Committee for the Fiscal Year 2001 (FY-01). The title of the experiment selected was "Effect of Moisture/Drainage on Non-Reinforced PCCP and Performance of FRP and Steel Dowels as Joint Repairs."

These experiments are the ninth and tenth experiment conducted at the Civil Infrastructures Systems Lab (CISL), formerly known as the Kansas State University Accelerated Testing Lab (ATL), and are therefore now identified as CISL-Exp#9 and CISL-Exp#10. The first two ATL experiments, ATL-Exp#1 and #2 were reported in Report No. FHWA-KS-97/5 [1], ATL-Exp#3 through #6 were reported in Report No. FHWA-KS-99-2 [2], ATL-Exp#7 is reported in Report No. FHWA-KS-99-7 [3], and ATL-Exp#8 is reported in Report No. FHWA-KS-02-6 [4].

This report describes the following aspects of CISL-Exp#9 and #10:

1. The test setup and testing strategies followed.

2. The pavement structure and material used for sub base and pavement construction.

3. The executed monitoring plan.

4. A description of the experiment: This includes the experimental work performed in terms of the total number of cycles applied to each specimen, testing conditions (loads, temperature, etc.), and the testing activity and corresponding time schedule.

5. A summary of the data collected, results from instrumentation, variations (curves/histograms) of the response data with the number of load cycles applied, and comparison of the responses of the different pavement constructions.

6. The conclusions drawn from the obtained results and observed performance.

7. Recommendations to the highway agencies for practical implementation and future experiments.

1.2   Project Overview

The goal of the research is to determine 1) the effect of unbound drainable base types on the performance of PCCP and 2) the efficiency of fiber-reinforced polymer dowels, compared to that of epoxy coated steel dowels, when retrofitted to re-establish the load transfer in damaged non-doweled joints.

The work described in this report examines the experimental aspects of the research study. This mainly entails the applications of full-scale axle loads to full-scale concrete pavement under controlled thermal conditions. The experimental work was conducted at the Civil Infrastructure Systems Laboratory (CISL) of Kansas State University (KSU). The experimental work includes monitoring and recording deflection, strain, soil pressure, and temperature in the pavement slabs tested.

This experimental investigation, together with the observed performance of similar situations on in-service highways and supplemented with additional analytical studies, can help

the state transportation and highway agencies establish or modify provisions for the use of unbound drainable bases under non-reinforced PCCP and that of retrofitted FRP or steel dowels for joint repairs. It may also lead to standard guidelines for instrumentation of in-service highway pavement in the States participating in the Pooled Fund Program. Further work could include numerical modeling, evaluation of mechanistic response, analysis of Falling Weight Deflectometer (FWD), and comparative studies with other research in the United States and abroad.

The effort outlined in this report encompasses the application of full-scale truck axle loads in a controlled environment, as dictated by the scope of this experiment. The loads cycles, surface temperature and moisture were applied according to a tight and detailed monitoring plan in order to obtain the necessary performance data: tensile strains, soil pressure, moisture content and pavement deflections. The monitoring plan is discussed in Section 3.1.13 and 3.2.5.

Chapter 2

Background

2.1 Premise of the Study

The monitoring of the condition of in-service road sections has clearly indicated that rigid pavements with inadequate subsurface drainage deteriorate faster than well-drained pavements. The effect of poor subsurface drainage is reflected in joint faulting, slab cracking, and increased roughness of the longitudinal profile. At high moisture levels in the base layer, the passing of wheel loads above the pavement causes pumping of the base material out through joints, cracks and pavement edges. The base material is softened, eroded and support is lost under the concrete slab. Since it is difficult to prevent water from infiltrating into the base layer, good drainage is imperative for assuring a long lasting pavement structure and reducing the maintenance costs over the life of the structure.

The purpose of building a drainable base is to drain as quickly as possible the water entering the pavement structure. This can be achieved by using a permeable, open-graded material as base material. The base layers can be constructed full-width and day lighted at the side slopes or designed to outlet into a collector drain installed beneath the shoulder. However, the more open-graded the material, the lower its stability to mechanical action. A layer with low stability is difficult to construct, does not provide enough support for the construction equipment when the top layer is constructed and for the concrete slab during trafficking. To improve stability, stabilized layers are a better solution for constructing an open-graded base layer when compared to granular layers, but the stabilization increases greatly the cost of the construction. Both asphalt binders and Portland cement may be used for stabilization.

A possible solution for improving stability of the base layer without increasing the construction cost is to use aggregates with more uniform gradation. But the more uniform gradation reduces the permeability of the base layer and the layer becomes semi-permeable. The proposed study aims to compare the performance of a permeable unbound granular base with that of a semi-permeable unbound granular base using full-scale accelerated pavement testing. The advantage of using the accelerated pavement test when compared to a field test is that the results of the comparison study are obtained in several months. In a field test, the results are obtained after observing the behavior of the witness road sections over at least five years.

2.2 Description of the Test Facility

A detailed description of the test facility can be found in "Development of an Accelerated Testing Laboratory for Highway Research in Kansas [1]."

2.3 Instrumentation

The following sensors were placed within the test sections and monitored during the experiment (in the test sections only):

1. Strain gages (Tokyo Sokki PML-60-2L)

2. Soil Moisture Sensors (Cole-Palmer Inst. P-99037-50)

3. Soil Pressure Cells (Geokon 3500-2-0100)

4. Thermocouples (fabricated in-house at KSU)

5. Displacement Transducers (Sensotech DLA BY132HP)

These types of sensors have been used previously and were successfully installed by CISL personnel according to the manufacturer's guidelines. Data was collected using existing data acquisition system developed at the CISL through previous research contracts. The hardware consists of several terminal blocks on a number of corresponding SCXII modules mounted on

the instrumentation chassis. Data acquisition boards are installed in PC computers with Pentium processors. The data acquisition software consists of the LabView package, which the Department of Civil Engineering has a license for 10 users. All data acquisition hardware and software are products of National Instruments, Inc.

Chapter 3

Description of the Test Experiments

3.1   Experiment #9

This section gives a detailed description of test experiment #9 including the pavement

construction, loading conditions, heat and cooling application, sensor installation and data

acquisition, and the performance monitoring plan.

3.1.1 Test Bed and Construction for Experiment #9

The test bed consists of a pit approximately 20 x 20-ft square and 6-ft deep. The walls of

this pit are reinforced concrete on the east, west and north sides. A heavy steel and wood

bulkhead, placed at the south side, is waterproofed with a rubber membrane. There is no integral

drainage system for the pit. An 8-in. to 12-in. layer of pea gravel is placed in the bottom of the

pit and covered by Geotextile. In the pit, a standpipe was constructed from the surface so that

water trapped in the bottom could be pumped out.

A wall was constructed at the centerline of the pit to separate the two pavements, so that

water from one subgrade would not enter the other subgrade, as shown in Figure 3.1. This wall

extends from the surface down to the top of the pea gravel, "the geotextile", and is anchored to

the end walls of the pit. The separation wall was made of 6-in. reinforced concrete and is

dependent on the fill from either side for its stability. When the separation wall was built it was

found that the pea gravel layer was full of water, apparently the result of gradual accumulation

from previous tests. This water had saturated the lower portion of the subgrade. Therefore, it was

necessary to remove the existing subgrade and dry it out before refilling the pit with the subgrade

material from the previous tests.
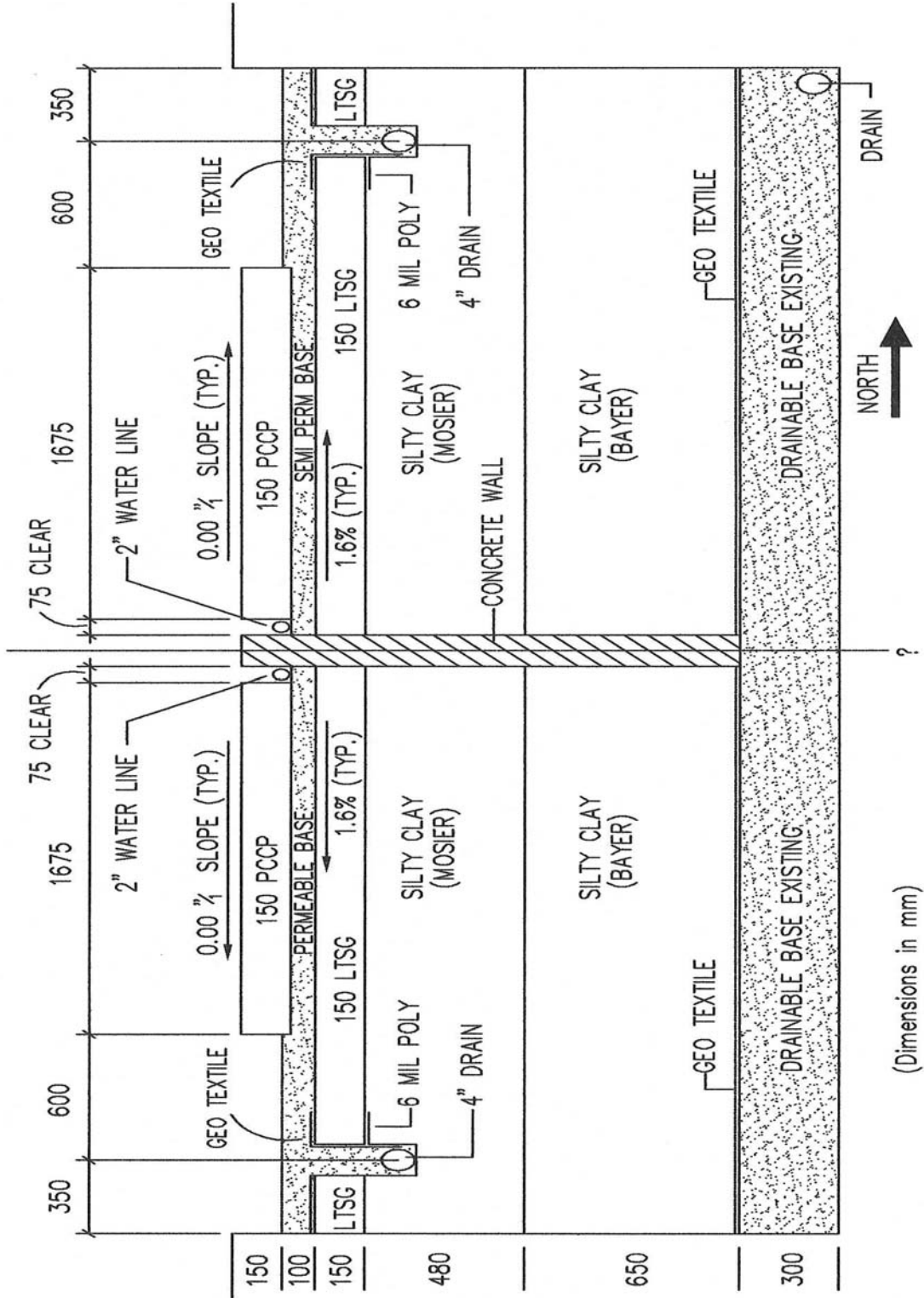
FIGURE 3.1: Cross Section of the Test Pit

8

3.1.2 Subgrade (Soil from the Previous Test)

The existing subgrade material was silty clay. Figure 3.2 shows the gradation curve of the existing subgrade soil. After being removed and dried, the subgrade soil was recompacted to a density greater than 90 percent maximum dry density (MDD), at near-optimum moisture content. The Proctor curve for this soil is shown in Figure 3.3. This compaction was done by hand with a whacker type vibrating compactor resulting in densities of the order of 94 to 95 percent maximum dry density. This subgrade was brought up to a depth of approximately 27-in., on both sides of the dividing wall, in 4-in. to 6-in. lifts. This minimized the stress on the wall and, more importantly, maintained uniformity in the moisture and density of the subgrade on both sides of the wall.

3.1.3 Subgrade (Added Soil from the Mosier Pit)

Since it was not possible to add more of the same subgrade soil, a new soil from the Mosier Quarry was added to the pits to bring the subgrade to the desired level. Soil tests were performed to determine the soil type and Proctor density. Figures 3.4 and 3.5 show the gradation and Procter curves, respectively, for the added soil. The subgrade was brought up in 4-in. to 6-in. compacted layers, to a level of 10 inches below the pit surface.

3.1.4 Lime Treated Subbase

Lime was rototilled into the top 6-in. of the subgrade and cured according to KDOT specifications (5). The total amount of lime added to the two pits was 1140 lbs, corresponding to a lime content of 6 percent. See Table 3.1 for the selection of the optimum lime content as a function of the pH of the stabilized soil. After the curing period the lime treated subgrade was compacted to approximately 95 percent density and cut to grade.
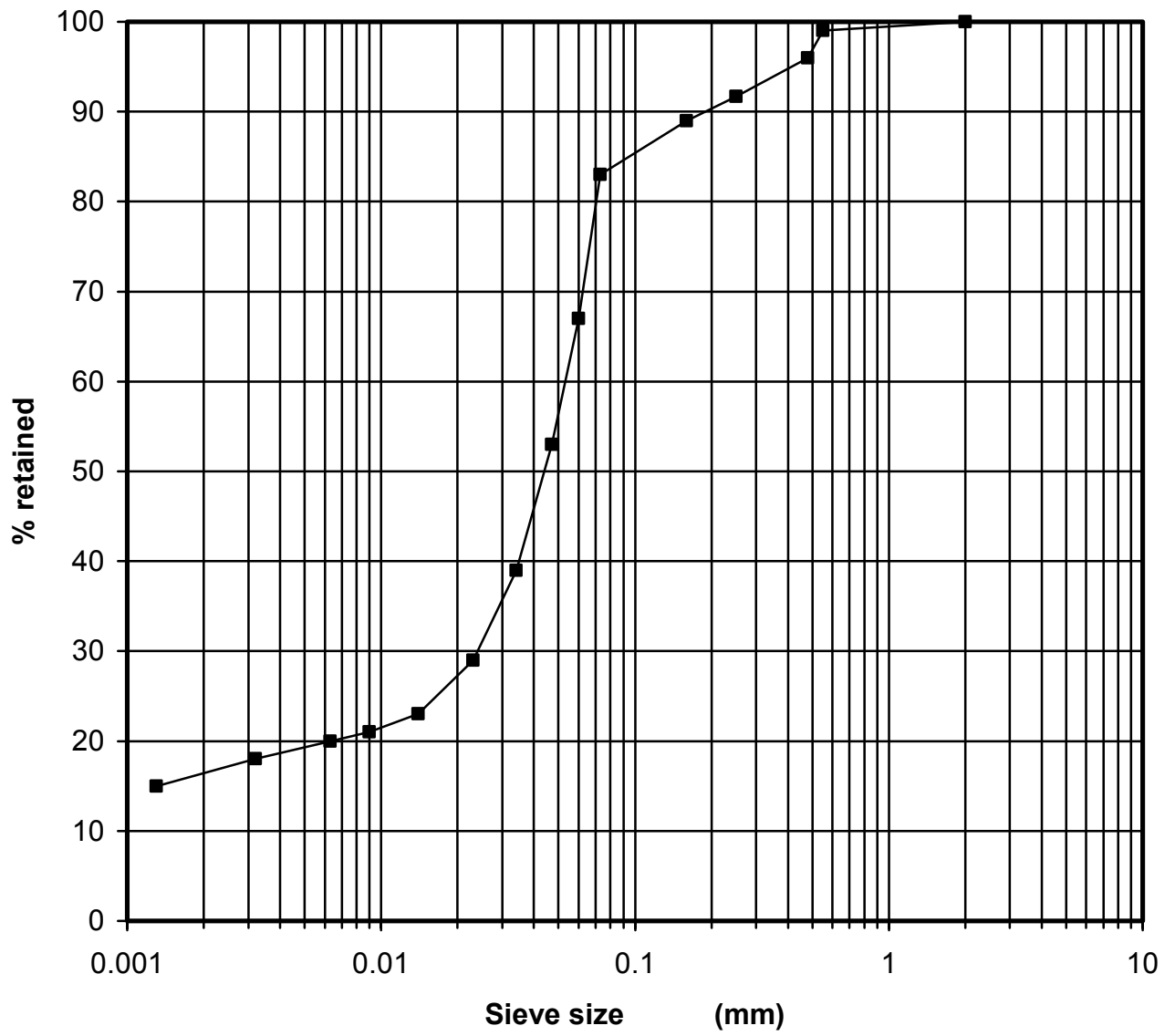
FIGURE 3.2: Gradation Curve for the existing Subgrade Soil

FIGURE 3.3: Proctor Curve for the existing Subgrade Soil
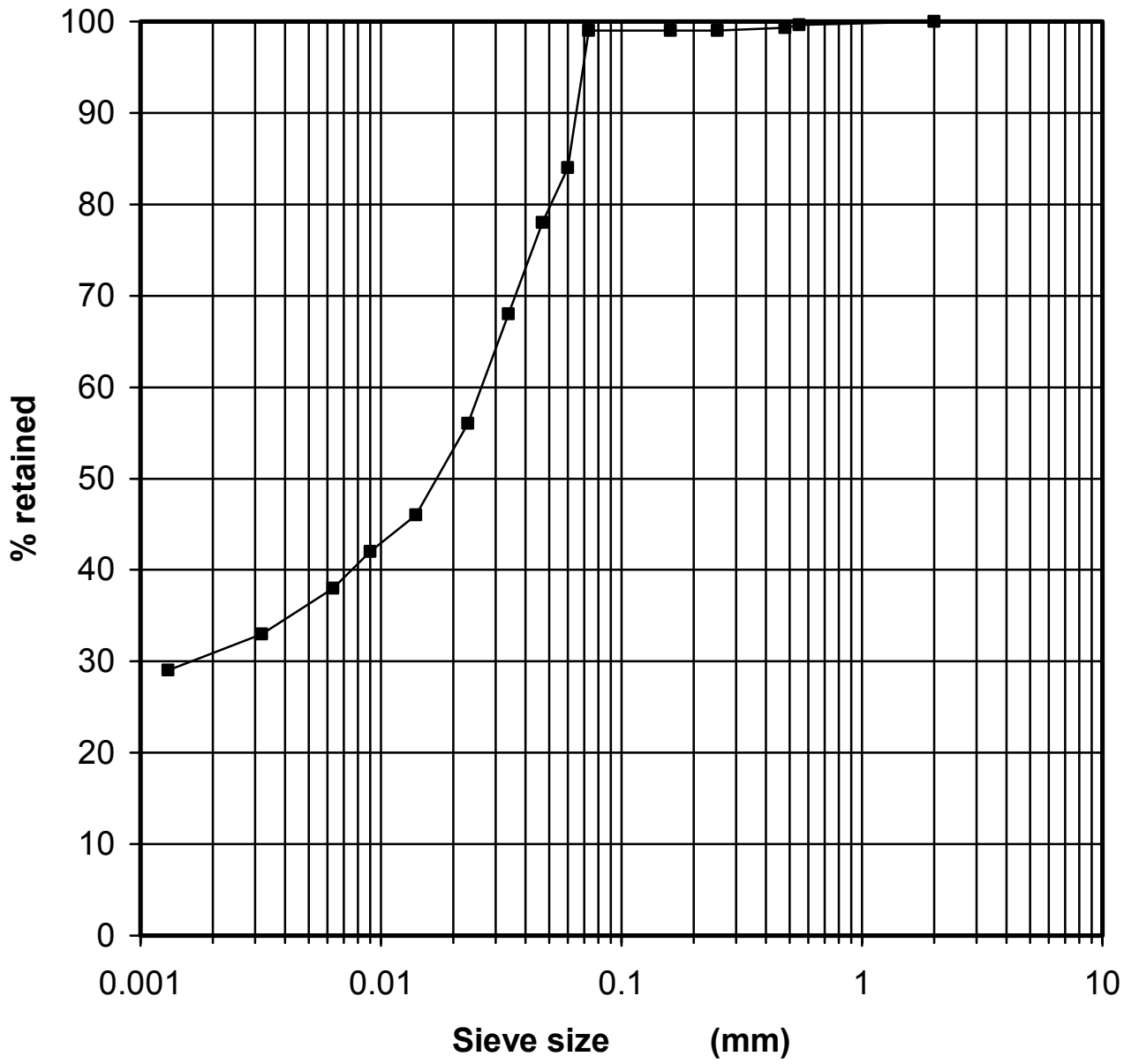
FIGURE 3.4: Gradation Curve for the Mosier Pit Soil

KANSAS DEPARTMENT OF TRANSPORTATION
REPORT OF SOIL COMPACTION TESTS

| SUBMITTED BY | ATL | ADDRESS | Manhattan | LAB. NO | 00-2234 |
| PROJECT | EN 2274-00 (808) | COUNTY | NA | DATE | 6-20-00 |

SAMPLE NUMBER: 3C
MAXIMUM DRY DENSITY:
1,612.0 Kg/m³
OPTIMUM MOISTURE:
19%
LIQUID LIMIT: 43
PLASTIC LIMIT: 15
PLASTICITY INDEX: 28

2.50
2.60
2.70

DRY DENSITY, Kg/cubic meter

MOISTURE CONTENT, %
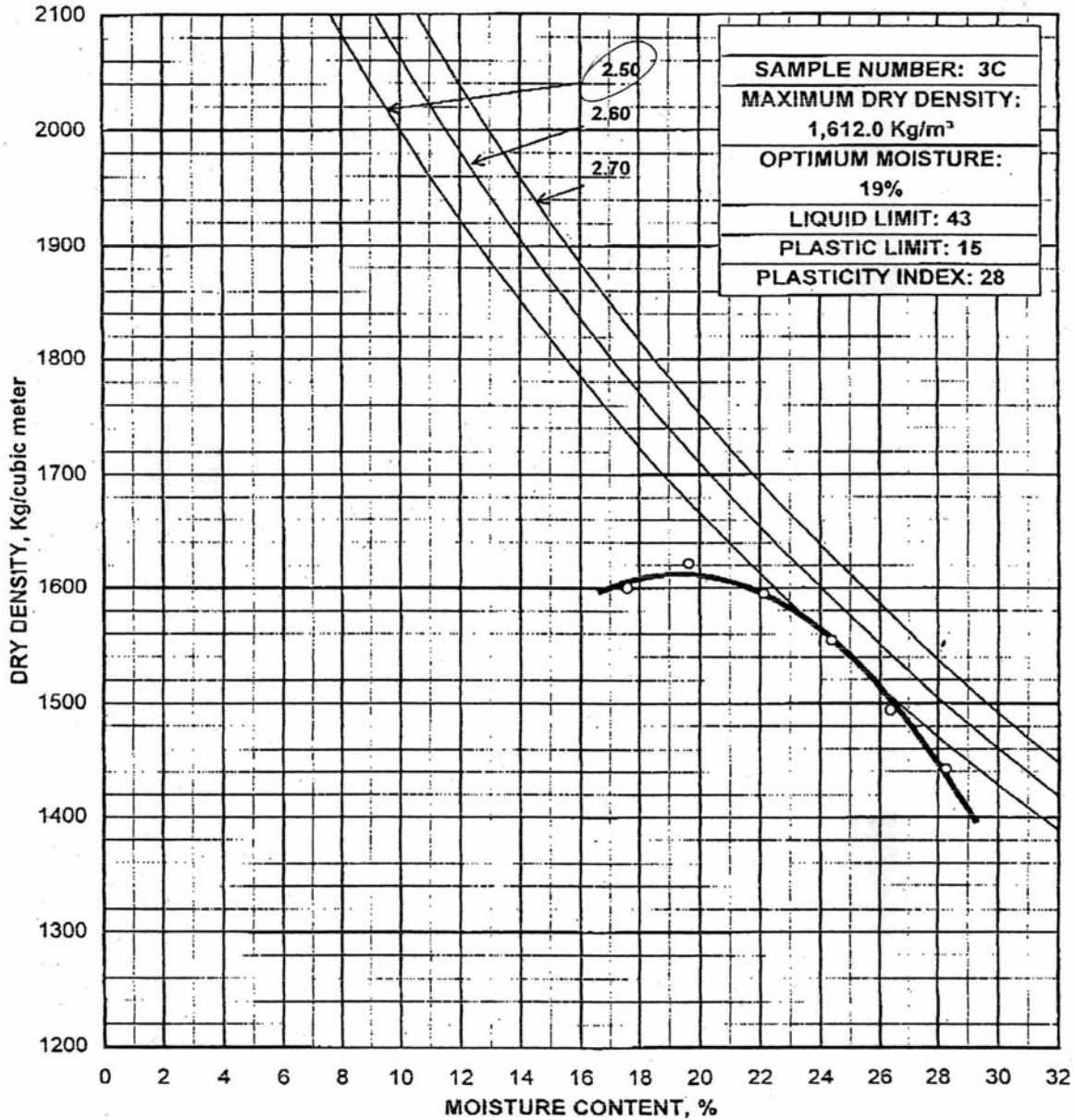
TEST METHOD AASHTO-T99
REMARKS

L. S. Ingram, P.E.
Chief, Bureau of Materials and Research
BY
James J. Brennan, Soils Engineer
D.O.T. Form No. 638

FIGURE 3.5: Proctor Curve for the Mosier Pit Soil

13

TABLE 3.1: Determination of the Optimum Lime Content

Lab Number: 00-2234

Percent Lime	pH
Raw	8.12
2%	11.88
3%	12.11
4%	12.17
5%	12.18
6%	12.20
7%	12.20
8%	12.22
9%	12.23
10%	12.22
11%	12.22
12%	12.20
13%	12.20

3.1.5 Side Drain

During the curing period a side drain, which consisted of an impervious membrane that covered the interior of the ditch, was filled with ¾-in. rock (see Figure 3.1). A strip of geotextile was placed at the edge of the drain and down past the depth of the lime-treated subbase. This helped to minimize the discharge of soil into the drain trench if the lime-treated subbase would become saturated and begin transferring water through the base instead of collecting it and discharging it at the top of the lime-treated subbase.

3.1.6 Permeable and Semi-Permeable Base

The permeable and semi-permeable base was placed on top of the lime treated subbase. These materials were to conform to KDOT Specification CA-5, "*Free Draining Aggregate for the Permeable Base,*" and Missouri Department of Transportation (MoDOT) Type 5 Aggregate for the semi-permeable base. These aggregate bases were made by mixing crushed ledge limestone of four commercial products in various proportions to meet the gradation requirements of these specifications. Table 3.2 gives the gradations of these materials as taken from the pit. Table 3.3 provides the calculations to obtain the aggregate mixed materials to meet KDOT Specification CA-5 for the permeable base. Figure 3.6 shows the associated gradation of a sample of the mixed KDOT CA-5 material as it was used.

Table 3.4 provides the calculations to obtain the aggregate mixed materials to meet the Type-5 Missouri specification for the semi-permeable base. Figure 3.7 shows the associated gradation of a sample of the mixed Type 5 material as it was used.

Figures 3.6 and 3.7 show the desired as well as the measured gradations as it was being placed in the pits. These gradations were measured from placed material in the pit in three locations for each pavement. The material was brought to grade and compacted with a vibratory plate compactor. Screenings were placed on top of the base and compacted with a plate compactor to act as a bond breaker.

TABLE 3.2: Gradation of Commercial Materials from Pit (% retained)

Sieve Size	3/4"coarse aggregate	3/8"coarse aggregate	1/8" screening	Crusher Run	Permeable	Semi-Permeable
3/4"	29.8	N/A	N/A	N/A	19.9	11.92
1/2"	83.9	N/A	N/A	6	55.9	36
3/8"	92.4	8.5	N/A	17.4	64.4	43.9
#4	94.4	58.4	1.5	38.1	82.4	53.3
#8	94.9	84.4	69.2	52.7	91.4	72.9
#16	95.2	91.6	90.3	60.6	94	80.4
#30	95.3	92.9	91.7	65.4	94.5	82.6
#40	95.5	93.2	92.1	67.5	94.8	83.6
#50	95.6	93.5	92.3	68.9	94.9	84.3
#100	95.8	94	92.7	71.7	95.2	85.5
#200	96.2	94.4	93.1	73.8	95.6	86.6

3.1.7 Permeability of the Base Materials

The gradation data of the semi-permeable material and the possible range of gradation for material passing the 200 sieve are shown in Table 3.5 and Figure 3.8, respectively. These are the average gradations of the semi-permeable material. No calculations were made on the CA-5 permeability, but calculations were made on the Missouri Type 5 material using the SOILPROP program provided by KDOT. The estimated permeability is between 530 and 630 m/day (see Appendix B). No permeability tests were performed on the two base materials.

TABLE 3.3: Design and Measured Gradations-Permeable Base

Size	Target	Sample 1	Sample 2	Sample 3	Average	KS Spec. Min	KS Spec. Max
1"	0	0	0	0	0		
3/4"	19.9	9.6	19.2	12.7	13.8	8	20
1/2"	55.9	41.1	56.0	54.4	50.5	36	56
3/8"	64.4	61.2	65.0	67.0	64.4	54	74
#4	82.4	87.0	80.8	88.8	85.5	79	99
#8	91.4	92.1	90.8	93.7	92.2	92	100
#16	94.0	93.2	92.4	94.4	93.3	92	100
#30	94.5	93.6	92.9		93.7		
#40	94.8	93.8	93.0		93.8		
#50	94.9	93.9	93.1		93.9		
#100	95.2	94.1	93.3		94.1		
#200	95.6	94.4	93.6		94.4	94	100
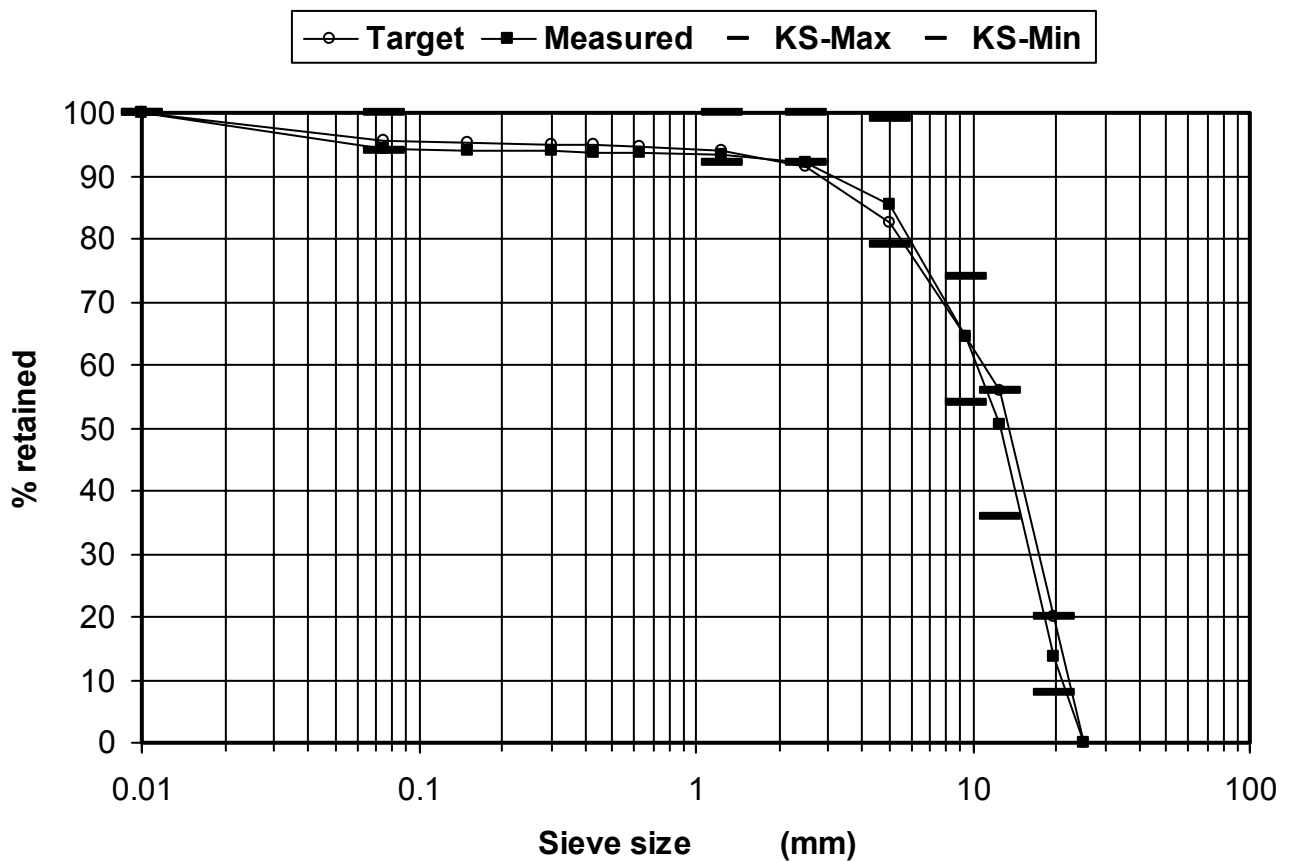
FIGURE 3.6: Design and Measured Gradations-Permeable Base

TABLE 3.4 Design and Measured Gradation-Semi-Permeable Base

Size	Target	Sample 1	Sample 2	Sample 3	Average	MO Spec. Min	MO Spec. Max
1"	0	0	0	0	0	0	0
3/4"	11.92	5.1	7.8	4.6	5.8		
1/2"	36	25.7	31.4	19.5	25.5	10	40
3/8"	43.9	40.6	39.2	29.9	46.6		
#4	53.3	52.7	50.8	39.3	47.6	40	60
#8	72.9	73	70.9	64.2	69.4		
#16	80.4	80.8	78.6	75.1	78.2		
#30	82.6	83	81.2	78.4	80.9	65	85
#40	83.6	83.9	82.2	79.7	81.9		
#50	84.3	84.5	83	80.6	82.7		
#100	85.5	85.6	84.4	82.2	84.1		
#200	86.6	86.6	85.5	83.3	85.1	85	100
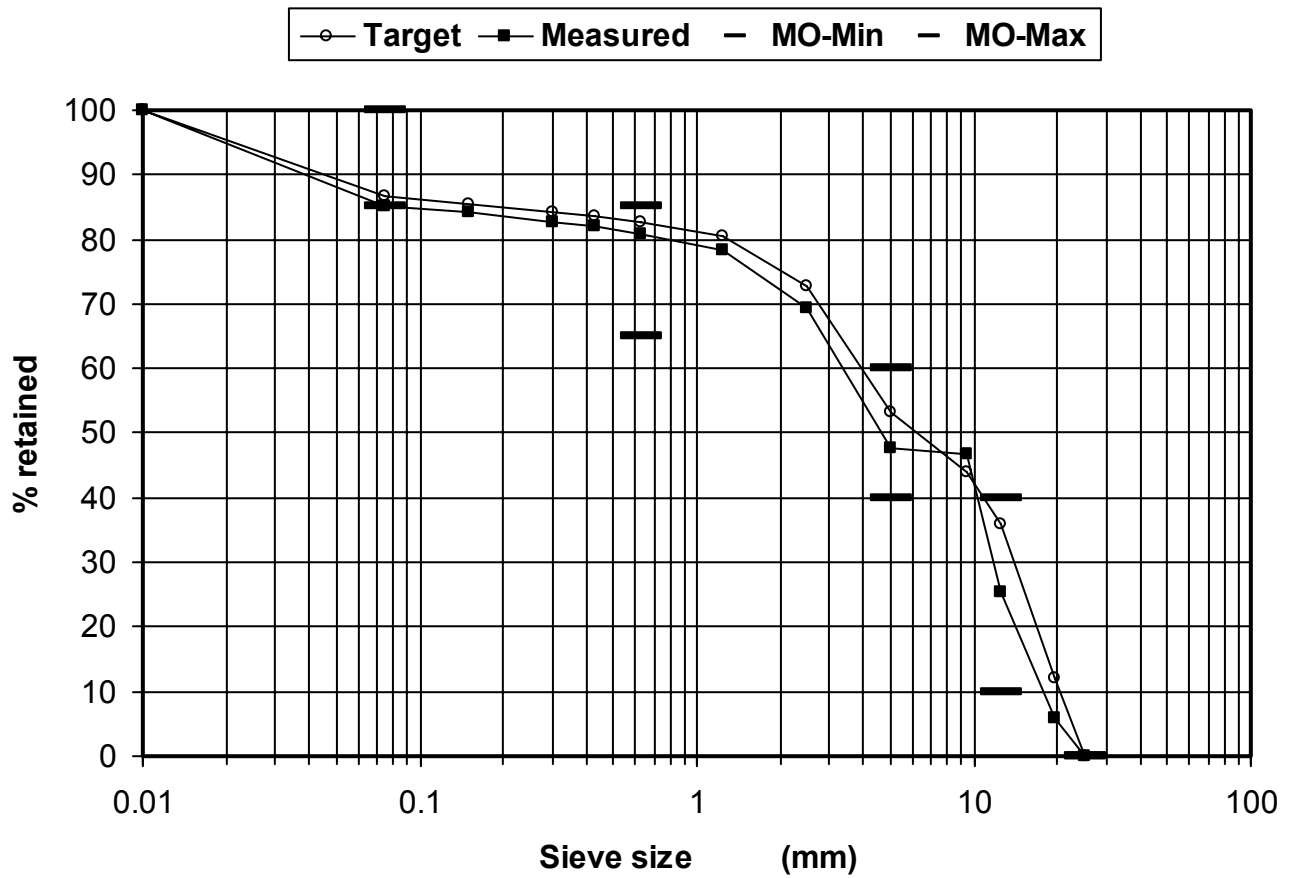
FIGURE 3.7 Design and Measured Gradation-Semi-Permeable Base

18

TABLE 3.5: Gradation for Semi Permeable Material

ASTM Class/Size		No Clay %/% Passing		2 % CLAY % / % PASS	
CLAY	<.002mm	0	0	2	2
FINE SILT	<.005	0	0	2	4
MED SILT	<.02	5	5	3	7
C SILT	<.05	6	11	5	12
VF SAND	<.10	3	14	2	14
F SAND	<.25	3	17	3	17
M SAND	<.5	1	18	1	18
C SAND	<1.0	2	20	2	20
VC SAND	<2.0	5	25	5	25
F GRAVEL	<12.0	46	71	46	71
COBBLE	>12.0mm	29	100	29	100
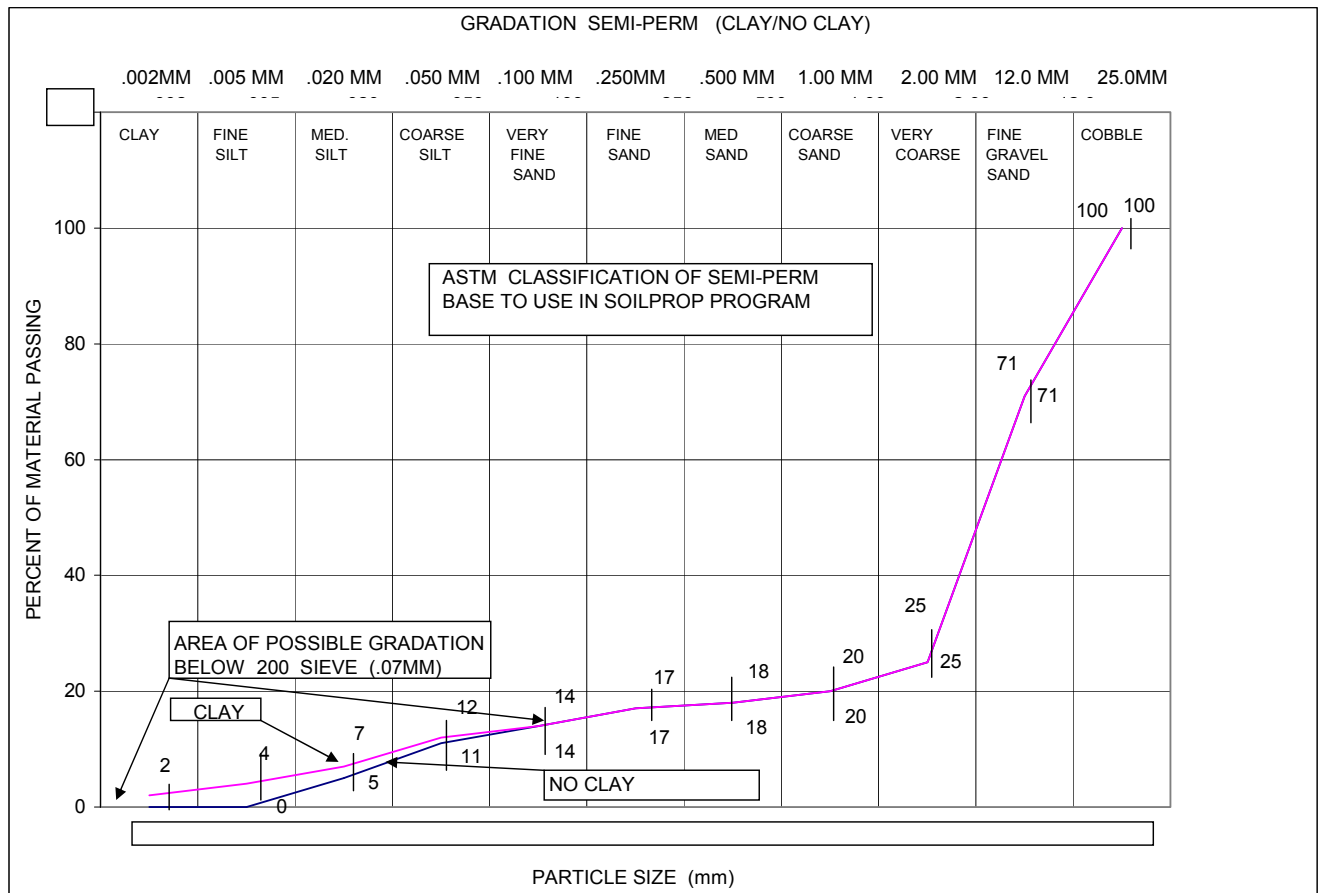
FIGURE 3.8: Gradation of Semi Permeable Material

19

3.1.8 Concrete Slab

Concrete slabs were placed in both pits and finished simultaneously out of the same batch of concrete. Strain sensors and thermocouples were placed in the slabs at this time. Table 3.6 shows the batch data and test information on the concrete used in the construction of the slabs. These slabs were restrained on the ends using reinforcing bars welded to the pit rail. Relief joints were sawed five feet from each end of the slabs, leaving a 10 foot section in the middle of each slab. The joints were cut 1 ¾-in. deep.

3.1.9 Sensor Installation, Placement and Data Acquisition

Several sensors were placed in the test sections to monitor pavement behavior. In addition to complement measurements obtained from these sensors, rolling wheel deflections and drop weight deflections were recorded.

- Pressure Cells

Two pressure cells (Geokon) were placed below the aggregate base level (26-in. from the surface). Two cells were placed in the middle of the slabs and two additional cells were placed in the location of the west transverse joint. The location of the pressure cells are shown in Figure 3.9. The corresponding channel designations are provided in Table 3.7. These particular types of sensors were successfully used in previous projects and have shown good performance and acceptable results. The sensors were installed according to the manufacture's guidelines.

- Thermocouples

Six thermocouples were placed at the interface between the top of the subgrade and the bottom of the slab (6-in. from the surface). Six other thermocouples were placed on top of the slab, once six thermocouples were placed in the slab. These thermocouples were fabricated by lab personnel. Figure 3.10 and Table 3.8 show, respectively, the location and corresponding

channel designations of the thermocouples placed as described. Similar thermocouples were used in previous experiments and produced acceptable results when compared to other conventional temperature measurement devices.

TABLE 3.6: Concrete Batch Data

TRUCK	USER LOGIN			TICKET NUM	TICKET ID	TIME	DATE
54	USER			32246	28471	13:15	07/26/00

LOAD SIZE	MIX CODE				SEQ	LOAD ID
5.00 YD	8108				N	29758

MATERIAL	DESIGN QTY	REQUIRED	BATCHED	VAR	% VAR	MOISTURE	ACT. WATER
A/E	1.75 OZ	8.75 OZ	10.00 +	1.25	14.295		
Ca-6	910 lb	4573 lb	4580	7	0.15%	0.505 M	2.73 gl
Cement 3	470 lb	2350 lb	2340	-10	-.43%		
Dara 65	18.80 oz	94.00 oz	94.00	0.00	0.00%		
Sand	2166 lb	11053 lb	11080	27	0.24%	2.06 % A	26.74 gl
Water	29.8 gl	114.6 gl	117.0 +	2.4	2.09 %		117.00 gl

NON-SIMULATED NUM BATCHES: 1
LOAD TOTAL : 18983 LB   WATER/CEMENT RATIO: 0.522T   WATER IN TRUCK 0.00 GL
SLUMP: 3.00"   TRIM WATER: 0.0 GL/YD

TEST CYLINDERS	MADE	TESTED	AGE	SLUMP	WEIGHT	STRENGTH
07-26-A	7/26/00	8/09/00	14	3 1/2"	27.5 LB	3622 PSI
07-26-B	7.26/00	8/23/00	28	3 1/2"	27.5 LB	4351 PSI
07-26-C (HOLD)						

TEST BEAMS	MADE	TESTED	AGE	SLUMP	WEIGHT	STRENGTH
07-26-A	7-26-00	8-09-00	14			364 PSI
07-26-A	7-26-00	8-23-00	28			579 PSI
7-26-C (HOLD)						

TABLE 3.7: Soil Pressure transducer Location/Channel Designations

Designation	Data Acquisition Channel	Vertical Location
Position 1, 46472	Ch24	12" below surface
Position 2, 46469	Ch25	12" below surface
Position 3, 46467	Ch27	26" below surface
Position 4, 46468	Ch28	12" below surface
Position 5, 46470	Ch26	12" below surface
Position 6, 46471	Ch29	26" below surface
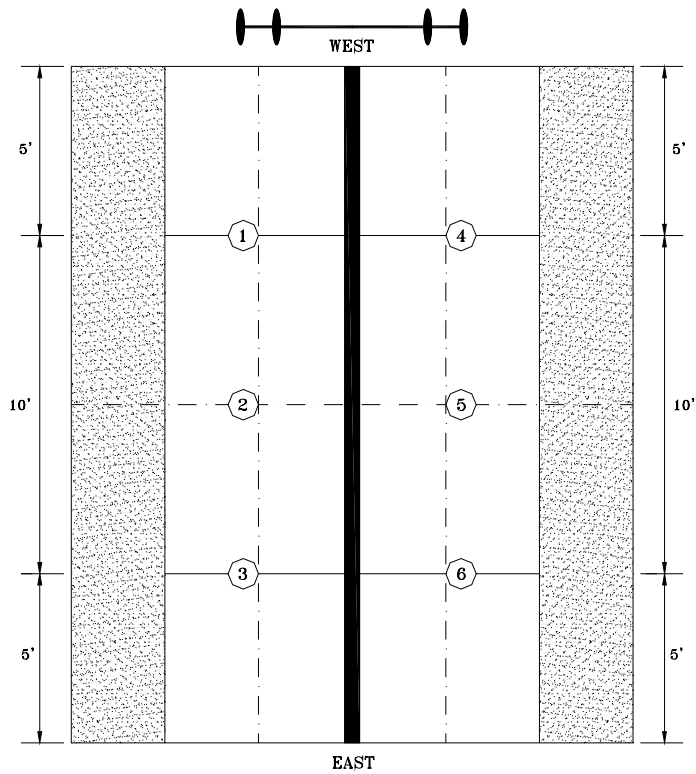
FIGURE 3.9: Soil Pressure Transducer Location
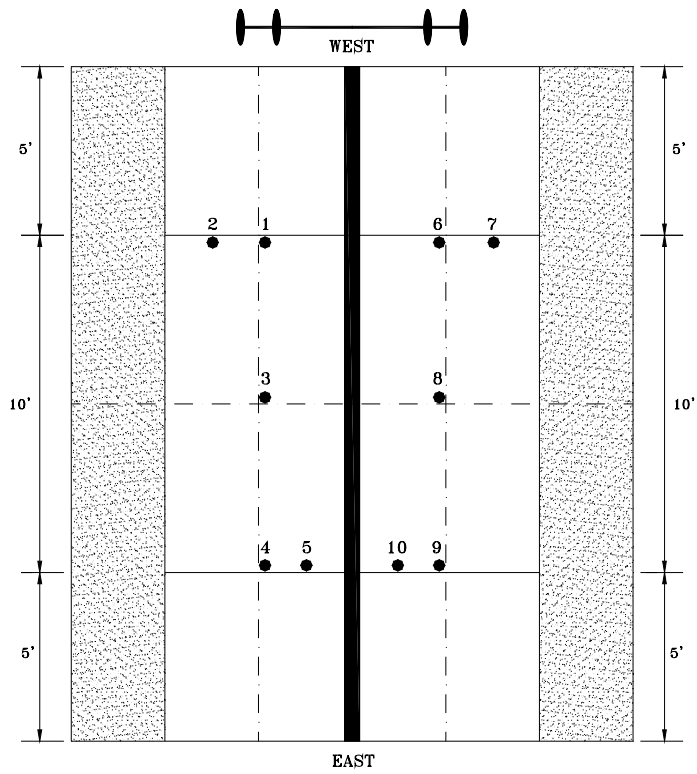
FIGURE 3.10: Thermocouple Transducer Locations

TABLE 3.8: Thermocouple Locations and Channel Designations

Designation	Data Acquisition Channel	Vertical Location
Position 1,TC1B	Ch 0	6" below surface
Position 1, TC1M	Ch 1	3" below surface
Position 2, TC2S	Ch 2	Surface
Position 3, TC3B	Ch 3	6" below surface
Position 3, TC3M	Ch 4	3" below surface
Position 3, TC3S	Ch 5	Surface
Position 4, TC4B	Ch 6	6" below surface
Position 4, TC4M	Ch 7	3" below surface
Position 5, TC5S	Ch 8	Surface
Position 6, TC6B	Ch 9	6" below surface
Position 6, TC6M	Ch 10	3" below surface
Position 7, TC7S	Ch 11	Surface
Position 8, TC8B	Ch 12	6" below surface
Position 8, TC8M	Ch 13	3" below surface
Position 8, TC8S	Ch 14	Surface
Position 9, TC9B	Ch 15	6" below surface
Position 9, TC9M	Ch 16	3" below surface
Position 10, TC10S	Ch 17	surface

- Strain Gages

Strain gages were installed in the slab longitudinally along the long axis of the slab at 1-in., 3-in. and 5-in. from the bottom of the slab as shown in Figure 3.11. Six strain gages were installed in the transverse direction at 1.25-in., 3.25-in., and 5.25-in. from the bottom of the slab as shown in Figure 3.11. Table 3.9 shows the channel designation for the strain gages.
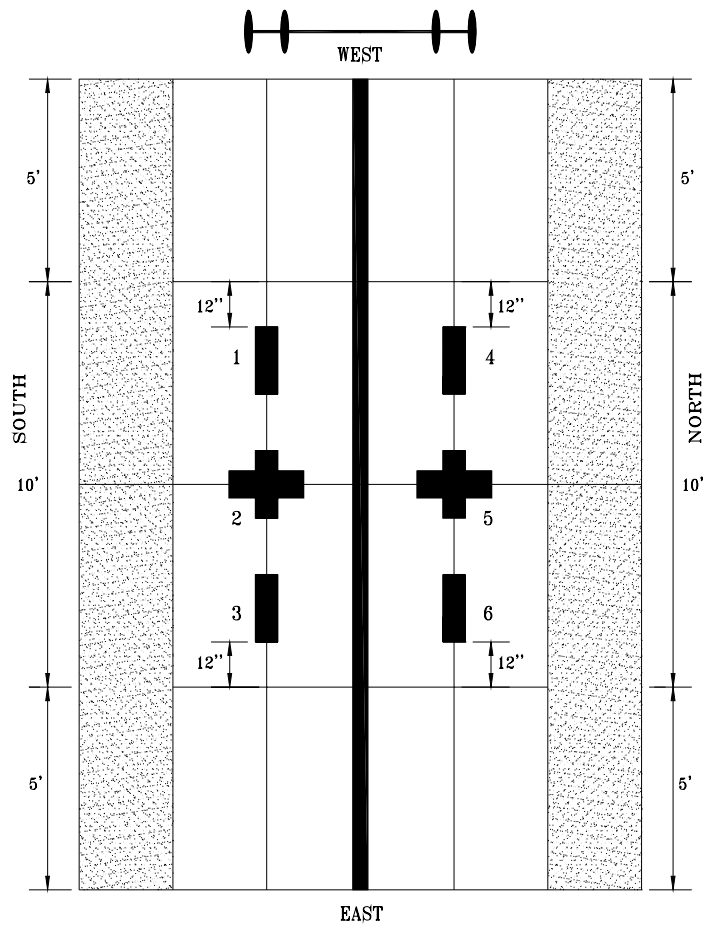
FIGURE 3.11: Strain Gauge Locations

TABLE 3.9: Strain Gauge Location and Channel Designations

Designation	Data Acquisition Chan.	Vertical Location
Position 1, LT1 (long)	Ch 0	1" below surface
Position 1, LM1	Ch 1	3" below surface
Position 1, LB1	Ch 2	5" below surface
Position 2, LT2 (long)	Ch 3	1" below surface
Position 2, LM2	Ch 4	3" below surface
Position 2, LB2	Ch 5	5" below surface
Position 2, TT2 (trans)	Ch 6	1.25" below surface
Position 2, TM2	Ch 7	3.25" below surface
Position 2, TB2	Ch 8	5.25" below surface
Position 3, LT3 (long)	Ch 9	1" below surface
Position 3, LM3	Ch 10	3" below surface
Position 3, LB3	Ch 11	5" below surface
Position 4, LT4 (long)	Ch 12	1" below surface
Position 4, LM4	Ch 13	3" below surface
Position 4, LB4	Ch 14	5" below surface
Position 5, LT5 (long)	Ch 15	1" below surface
Position 5, LM5	Ch 16	3" below surface
Position 5, LB5	Ch 17	5" below surface
Position 5, TT5 (trans)	Ch 18	1.25" below surface
Position 5, TM5	Ch 19	3.25" below surface
Position 5, TB5	Ch 20	5.25" below surface
Position 6, LT6 (long)	Ch 21	1" below surface
Position 6, LM6	Ch 22	3" below surface
Position 6, LB6	Ch 23	5" below surface

- Drop Weight and Rolling Wheel Load

Slab deflections were recorded under the influence of a drop weight and also under the rolling wheel load. Figure 3.12 shows the drop weight position and LVDT locations for the north (semi-permeable) and south slab (permeable). Channel designations are the same as the LVDT and drop weight numbers. In addition to this data the position of the wheel was recorded in the same file with the rolling wheel load/deflection.

NORTH PAVEMENT
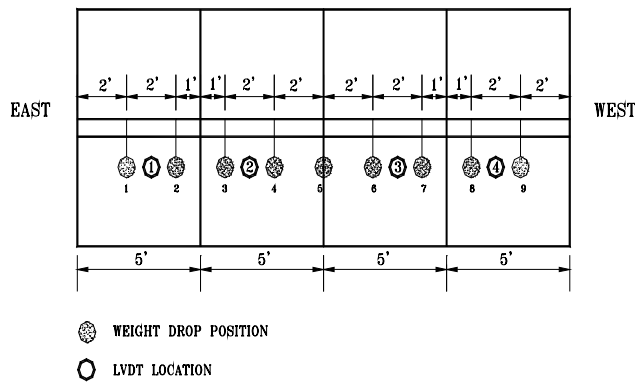
SOUTH PAVEMENT
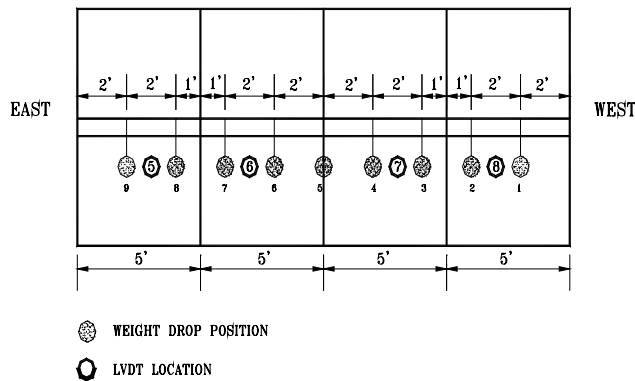
FIGURE 3.12: LVDT Position Diagram

3.1.10 Heating/Cooling

Heat was applied to the surface of the pavement specimens using thermal coil panels containing a glycol water fluid that heated or cooled the pavement from the top depending on the phase of the test. All heating and cooling was applied to the surface. Temperatures on the surface and inside the pavement were continuously monitored with thermocouples.

3.1.11 Addition of Water

A measured quantity of water was added directly to the subgrade through a system of pipes as shown in the diagram of Figure 3.13. The water that came through the subgrade was trapped in the subgrade system, then pumped out and its volume was measured.

3.1.12 Loading Conditions

Loading was applied using a dual wheel single axle with total load of 22 kips (97.86 kN). The centerline of the axle passes corresponds to the location of the line separating the two test slabs (i.e. in line with the full depth wall). A fixed wheel path (zero lateral wander) was maintained and uni-directional traffic (west-to-east) was applied throughout the test. The tire inflation pressure was maintained at 110 psi.

3.1.13 Operating Schedule and Recording of Data

Table 3.10 shows the operating schedule of the project, when test data was collected, the heating and cooling cycles, and the water additions and recovery. At the beginning, this test schedule was plagued by equipment breakdowns and the proposed schedule was not followed. Major modifications were made to the machine; the pneumatic operation was changed to a full hydraulic operation. Operating instructions and drawings for the current machine will be provided in a separate document.
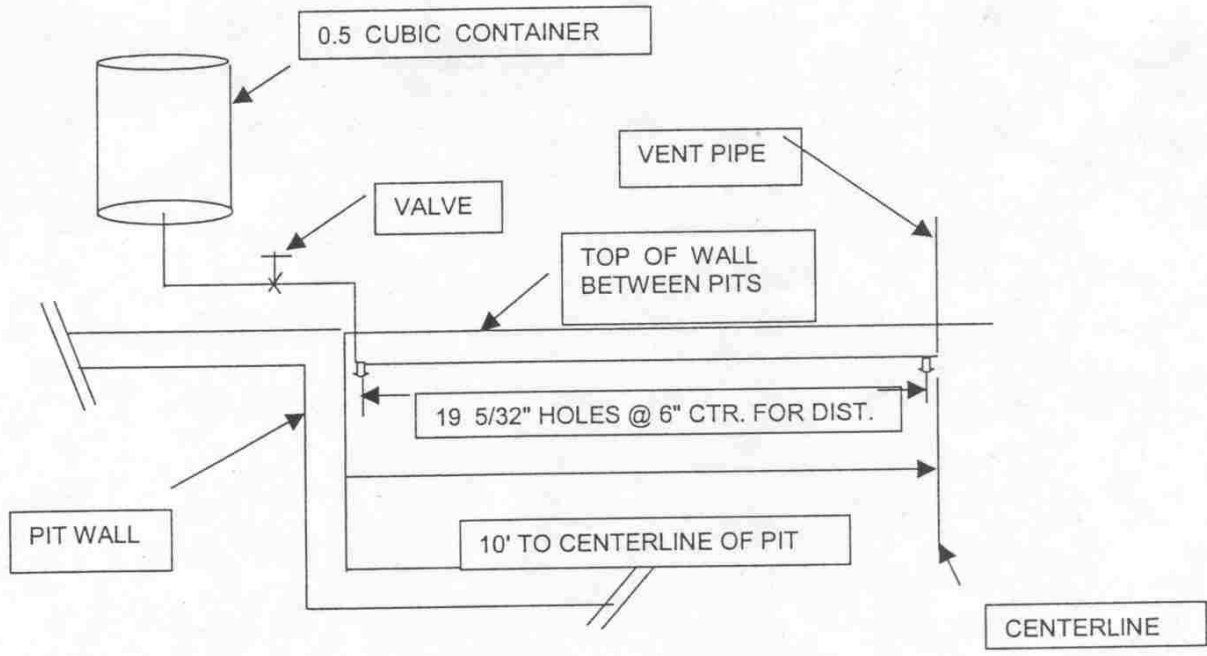
FIGURE 3.13: Water Pipe Diagram

TABLE 3.10: Log of Operation and Testing Experiment #9

DATE	DAY	CYCLES	REMARKS	TEMP	WATER INPUT/RECOVERY — PERM	SEMI-PERM	ROLLING WHEEL OIL LEAKING	DROP WEIGHT	SOIL PRESSURE	STRAIN
SEPT.	29	F	252	START			*	*	*	*
	30	S								
OCT	1	S								
	2	M	2,794							
	3	T	4,511	5,000			*	*	*	*
	4	W	6,570							
	5	T	7,490	10000			*	*	*	*
	6	F	12,030	Broke Down						
	7	S		Repaired						
	8	S								
	9	M								
	10	T		20,000			*	*	*	*
	11	W								
	12	T								
	13	F	20,102							
	14	S	23,381							
	15	S								
	16	M	24,588	25,000				*	*	*
	17	T	25,044							
	18	W	29,911	30,000					*	*
	19	T	33,856	Broke Down						
	20	F		Repaired (wire)						
	21	S								
	22	S								
	23	M	33,856							
	24	T	34,904	35,000					*	*
	25	W	36,926	Broke Down						
	26	T		Parts(cyl.)						
	27	F								
	28	S								
	29	S								
	30	M								
	31	T								
NOV	1	W								
	2	T								
	3	F								
	4	S								
	5	S								
	6	M	36,926	Repaired						
	7	T	37,065							

* Recorded Temperature: A-Ambient temp., C-Cooling, H-Heating, X-Change H-C or C-H

TABLE 3.10: Log of Operation and Testing Experiment #9

DATE		DAY	CYCLES	REMARKS	TEMP	WATER INPUT/RECOVERY		RW LOH OLE A LED IL ING G	D W R E O I P G H T	S P OR I E L S S U R E	S T R A I N
						PERM	SEMI-PERM				
NOV	8	W	38,428	Stop for 40,000							
	9	T									
	10	F									
	11	S									
	12	S									
	13	M	39,937	40,000				*	*	*	*
	14	T	43,225								
	15	W	46,055								
	16	T	47,189	50,000				*	*	*	*
	17	F	52,166	Broke Cable							
	18	S		Repair Cable							
	19	S									
	20	M	54,869	Broke Cyl							
	21	T	56,693								
	22	W									
	23	T									
	24	F									
	25	S		Repair Cyl.							
	26	S									
	27	M	56,693								
	28	T	56,854								
	29	W	60,000	60,000	A			*		*	*
NOV	30	T			A						
DEC	1	F			A						
	2	S	60,040		A						
	3	S	61,599		A						
	4	M	62,870	Broke Cyl.	A						
	5	T			A						
	6	W			A						
	7	T			A						
	8	F			A						
	9	S			A						
	10	S		Repair Cyl.	A						
	11	M	65,931		A						
	12	T	67,146		A						
	13	W	68,318		A						
	14	T	71,023		A						
	15	F	73351		A						
	16	S			A						
	17	S			A						

31

TABLE 3.10: Log of Operation and Testing Experiment #9

DATE		DAY	CYCLES	REMARKS	TEMP	WATER INPUT/RECOVERY		RW LOH OLE A LED I L N G	D W R E O I P G H T	S P OR I E L S S U R E	S T R A I N
						PERM	SEMI-PERM				
DEC	18	M	77,534		A						
	19	T	77,799								
	20	W	79,681	80,000				*		*	*
	21	T		Vacation							
	22	F		*							
	23	S									
	24	S									
	25	M		*							
	26	T		Vacation	A						
	27	W	80,127		C						
	28	T	82,916	Broke Axle	C						
	29	F	87,079		A						
	30	S									
DEC	31	S									
JAN	1	M									
	2	T									
	3	W									
	4	T									
	5	F									
	6	S									
	7	S									
	8	M									
	9	T									
	10	W									
	11	T									
	12	F									
	13	S									
	14	S									
MLK	15	M		Change Axle							
	16	T									
	17	W									
	18	T									
	19	F	87,079	Repaired	A						
	20	S			A						
	21	S			A						
	22	M	87,127		C						
	23	T	90,685		C						
	24	W	92,998		C						
	25	T	96,940		C						
	26	F		100,000	C			*		*	*

TABLE 3.10: Log of Operation and Testing Experiment #9

DATE		DAY	CYCLES	REMARKS	TEMP	WATER INPUT/RECOVERY		RWL OHOLEALEDILNG	DWROIPGHT	SPORIESSURE	STRAIN
						PERM	SEMI-PERM				
JAN	27	S			C						
	28	S			C						
	29	M	100,062		X						
	30	T	103,488		H						
JAN	31	W	106,044		H						
FEB	1	T	110,304	Vacation	H						
	2	F		*	H						
	3	S									
	4	S									
	5	M		*							
	6	T		*							
	7	W		*							
	8	T		*							
	9	F		*							
	10	S									
	11	S									
	12	M		Vacation							
	13	T	113,057		H						
	14	W	117,313	120,000	H			*	*	*	*
	15	T		Wait for Cool	H						
	16	F		*							
	17	S									
	18	S									
	19	M	120,047		X						
	20	T	123,127		C						
	21	W	127,459		C						
	22	T	132,345		C						
	23	F	136,689		C						
	24	S			C						
	25	S			C						
	26	M	140,000		X						
	27	T	142,793		H						
FEB	28	W	146,412		H						
MAR	1	T	150,688		H						
	2	F	155,542		H						
	3	S			H						
	4	S			H						
	5	M	160,001		X						
	6	T	164,221		C						
	7	W	168,139		C	4.00/2.37	4.00/0.41				

TABLE 3.10: Log of Operation and Testing Experiment #9

DATE		DAY	CYCLES	REMARKS	TEMP	WATER INPUT/RECOVERY		RW OH LEADILING	D OH RO P OIL	S OR I E L S S U R E	S T R A I N
						PERM	SEMI-PERM	RW OH LEADILING	D W RE O I P G H T	S P OR I E L S S U R E	S T R A I N
MAR	8	T	172,599		C	4.00/3.28	4.00/1.85				
	9	F	176,754	180,000	C	4.00/3.45	4.00/2.01	*	*	*	*
	10	S			A						
	11	S			A						
	12	M		WORK ON	A	4.00/2.55	4.00/1.60				
	13	T		HYDRAULICS		4.00/2.88	4.00/1.70				
	14	W				4.00/3.28	4.00/2.60				
	15	T				4.00/2.80	4.00/2.75				
	16	F				4.00/1.75	4.00/1.30				
	17	S									
	18	S									
	19	M				4.00/2.73	4.00/1.65				
	20	T				4.00/2.70	4.00/1.73				
	21	W				4.00/2.78	4.00/1.90				
	22	T				4.00/2.63	4.00/1.85				
	23	F				4.00/2.70	4.00/1.75				
	24	S									
	25	S									
	26	M				4.00/2.48	4.00/1.58				
	27	T	180,175			4.00/2.85	4.00/1.95				
	28	W	180,402			4.00/3.43	4.00/3.19				
	29	T	184,617			4.00/2.80	4.00/2.37				
	30	F	188,831			4.00/2.90	4.00/2.25				
MAR	31	S									
APR	1	S									
	2	M	193,019			4.00/2.03	4.00/0.84				
	3	T	197,293			4.00/3.40	4.00/2.13				
	4	W	201,550			4.00/2.96	4.00/2.25				
	5	T	205,879			4.00/2.80	4.00/2.15				
	6	F	210,059			4.00/2.55	4.00/1.80				
	7	S									
	8	S									
	9	M	214,155			8.00/6.42	8.00/5.63				
	10	T	217,712		H						
	11	W	221,976		H	8.00/6.48	8.00/5.41				
	12	T	225,438		H	8.00/6.85	8.00/5.93				
	13	F	229,436		H	8.00/7.55	8.00/7.35				
	14	S			H						
	15	S			H						
APR	16	M	223,310		H	8.00/7.20	8.00/6.61				

TABLE 3.10: Log of Operation and Testing Experiment #9

DATE		DAY	CYCLES	REMARKS	TEMP	WATER INPUT/RECOVERY		RW OH LED OIL LEAKING	DROP WEIGHT	SPOILS PRESSURE	STRAIN
						PERM	SEMI-PERM				
APR	17	T	237,575		H	6.00/5.10	8.00/4.25				
	18	W	241,830		X	8.00/6.88	8.00/5.95				
	19	T	246,016		C	8.00/6.45	8.00/5.90				
	20	F	250,242	START CRACK	C	8.00/7.05	8.00/5.60				
	21	S		PUMPING NL	C						
	22	S			C						
	23	M	255,472	BREAKDOWN	C	8.00/6.39	8.00/4.35				
	24	T		ORDER PART		6.00/5.15	6.00/4.15				
	25	W		*no late reading		6.00/3.3*	6.00/3.28*				
	26	T									
	27	F									
	28	S									
	29	S									
APR	30	M									
MAY	1	T									
	2	W									
	3	T									
	4	F									
	5	S									
	6	S									
	7	M									
	8	T									
	9	W									
	10	T									
	11	F									
	12	S									
	13	S									
	14	M									
	15	T									
	16	W									
	17	T									
	18	F	258,399	REPAIR		4.00/2.60	4.00/0.95				
	19	S									
	20	S									
	21	M		260,000		6.00/5.75	6.00/4.00	*	*	*	*
	22	T	260,094			8.00/8.15	8.00/8.20				
	23	W	264,091			8.00/8.00	8.00/7.50				
	24	T	267,949			8.00/8.63	8.00/6.59				
	25	F	272,092	Break Axle		4.00/4.15	4.00/3.00				
	26	S		Bracket							

TABLE 3.10: Log of Operation and Testing Experiment #9

DATE		DAY	CYCLES	REMARKS	TEMP	WATER INPUT/RECOVERY		RW LOH OLE A LED IL N G	D RO P	W E I G H T	S OR I L S U R E	S T R A I N
						PERM	SEMI-PERM					
MAY	27	S										
	28	M	273,178	Repair		8.00/7.80	8.00/5.85					
	29	T	276,733			8.00/8.60	8.00/6.50					
	30	W	280,691			8.00/8.65	8.00/6.30					
MAY	31	T	284,065			6.00/6.70	6.00/4.25					
JUNE	1	F	287,840			3.00/3.35	3.00/2.00					
	2	S										
	3	S										
	4	M	291.957			2.00/1.89	2.00/1.63					
	5	T	295,830			2.00/1.60	2.00/1.17					
	6	W	299,664									
	7	T		300,000								

3.2   Experiment #10

This section gives a detailed description of test experiment #10 including the pavement replacement, dowel bar retrofit, sensor installation and data acquisition, loading conditions, and the performance monitoring plan.

3.2.1 Pavement Replacement

Experiment #10 used the distressed pavements tested in experiment-#9. A section of pavement approximately 5 ¾-ft. long was removed from the north PCCP, located between 24-in. and 95-in. from the east wall and roughly centered over the East transverse joint. This location coincides with the transverse cracks which developed in the slabs during experiment-#9. Saw cuts were made along the transverse cracks and the section was broken–up and removed. Figure 3.14 shows the saw marks and east transverse joint prior to removal. The existing base from experiment-#9 was covered with a layer of sand and compacted to assume uniform support under the new concrete slab. Prior to replacing the concrete, all longitudinal cracks in the distressed PCCP from experiment-#9 were epoxy injected by KDOT personnel. Figure 3.15 shows the removed section of PCCP and epoxy injection. A thin bond breaker was placed at each end of the distressed PCCP prior to placing the new concrete section. The new 6-in. thick section was placed and allowed to cure for seven days.

3.2.2 Dowel Bar Retrofit

The north PCCP was retrofit with a combination of steel dowels and fiber reinforced polymer (FRP) dowels. Steel dowels were placed in the east end of the new section of the north PCCP. The steel dowels were one inch diameter and placed following KDOT specifications. The west end of the new section was retrofit with 1 ½-in. diameter FRP dowels. The retrofit using FRP dowels followed the guidelines of the KDOT specification for retrofitting steel dowels.

37

Another transverse crack which developed in the north PCCP during experiment-#9 was retrofit with 1-in. diameter FRP dowels. This crack was located approximately 30-in. from the west end of the north PCCP. The transverse crack, which developed at 40k cycles in experiment-#9 and repaired with epoxy stitches, was left as is for testing in experiment #10. Figures 3.16–3.18 show the 1-in. steel, 1 ½-in. FRP and 1-in. FRP dowels placed in the north PCCP, respectively. There was no dowel bar retrofit in the south PCCP.

FIGURE 3.14: Saw Cuts and East Transverse Joint before Removal

FIGURE 3.15: Removed Section of North Slab and Epoxy Injection
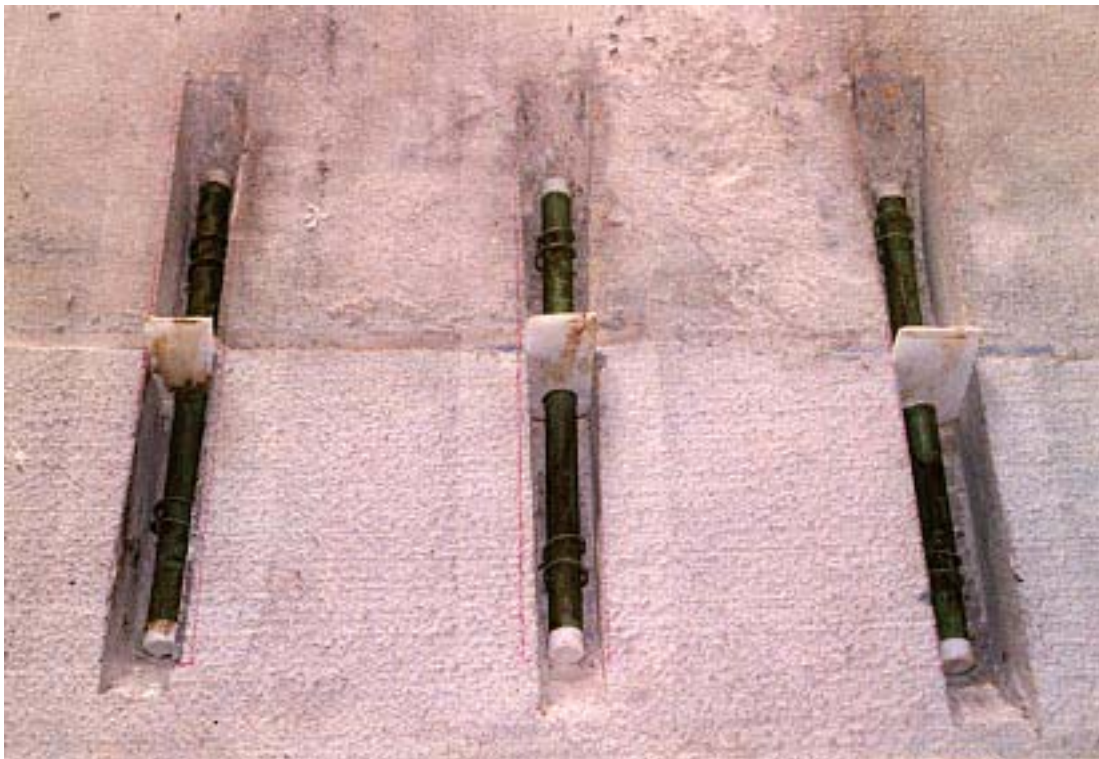
FIGURE 3.16: Steel Dowels (1-in. diameter)

FIGURE 3.17: Fiber Reinforced Dowels (1.5-in. diameter)
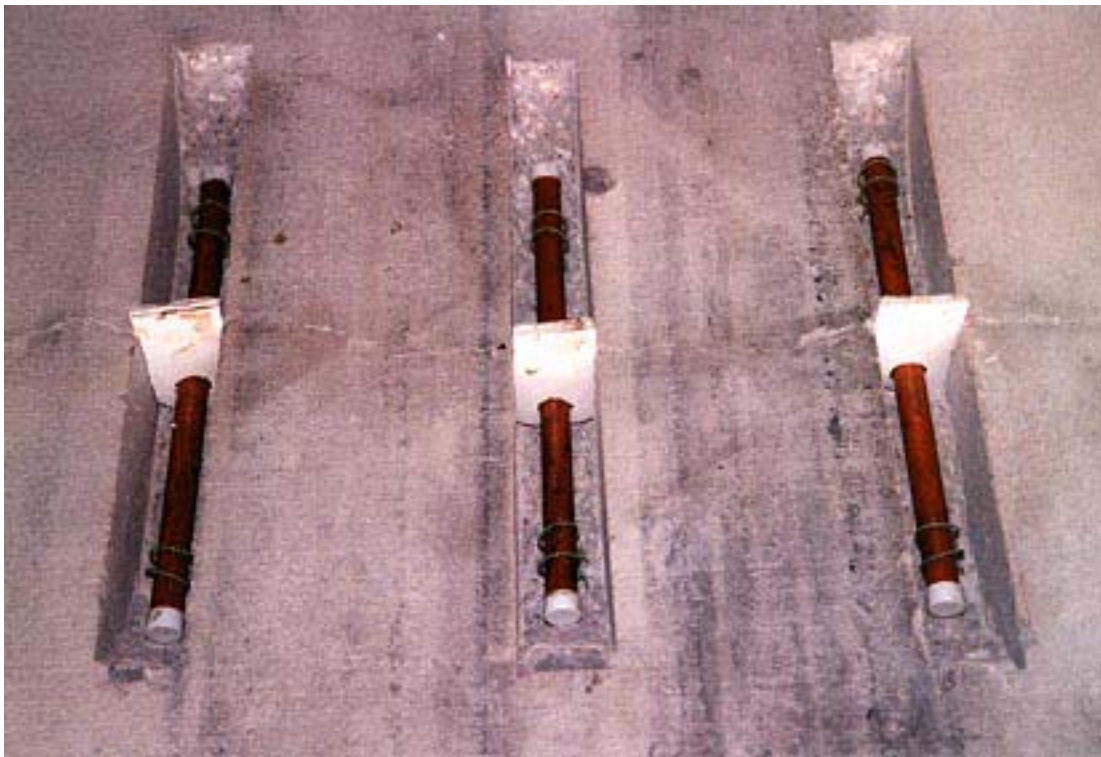
FIGURE 3.18: Fiber Reinforced Dowels (1-in. Diameter)

3.2.3 Sensor Installation and Data Acquisition

All existing sensors from experiment #9 were used. A new strain gauge was installed in the middle of the replaced section of the North PCCP. LVDTs were placed as follows:

- on each side of the transverse joints retrofitted with dowel bars (6)

- on each side of the original West transverse joint in the North slab (2)

- one next to the stitches constructed in experiment #9.

These LVDTs were attached to a rigid bar, located approximately two feet from the longitudinal centerline of the north slab. With the exception of temperature and drop weight tests, the data collected for experiment #10 is similar to that collected for experiment #9.

3.2.4 Loading Conditions

The loading conditions for experiment #10 are the same as described in section 3.1.3 for experiment #9.

3.2.5 Test and Monitoring Plan

Unidirectional 22 kip single axle loads were applied to the north and south slabs at room temperature. The experiment was monitored daily for visual changes. Deflection, strain and vertical stress data was taken daily. The test duration was 10 days and a total of 21,355 cycles were accumulated. Table 3.11 summarizes the test and monitoring plan.

Table 3.11 Log of Operation and Testing Experiment #10

DATE		DAY	CYCLES	REMARKS	TEMP	WATER INPUT/RECOVERY		ROLLING WHEEL LOAD	DROP WEIGHT	SOIL PRESSURE	STRAIN
						PERM	SEMI-PERM				
JULY	12	T	300,000			4.0/1.9	4.0/1.0	*		*	*
	13	F	300,619			4.0/2.45	4.0/2.2	*		*	*
	16	M	302,604			3.0/1.52	3.0/1.0	*		*	*
	17	T	305,051			2.0/2.68	2.0/1.45	*		*	*
	18	W	306,882			4.0/2.2	4.0/1.5	*		*	*
	19	T	309,236			4.0/3.05	4.0/1.75	*		*	*
	20	F	311,769			4.0/3.38	4.0/1.65	*		*	*
	23	M	314,205			4.0/4.1	4.0/1.65	*		*	*
	24	T	316,553			4.0/1.85	4.0/0.8	*		*	*
				321,355							

Chapter 4

Test Results and Observations

4.1 Experiment #9

4.1.1 Stresses and Strains in Pavement

-Vertical Stresses

Vertical stress in the subbase was monitored for the six locations described in section 3.1.9. The maximum vertical stresses recorded are provided in Table 4.1. The pressure transducer located at the west end of the north pavement failed during the experiment, therefore no data was collected. Figures 4.1 to 4.3 show vertical stress vs. cycles for the west end, midspan and east end locations, respectively. The stress in the west end of the south subbase shows increasing values up to 120k cycles and then drops significantly through the end of the testing. The vertical stresses at midspan initially increase in both the north and south subbases, then decrease in value to 120k cycles. A significant increase in stress occurs at 180k cycles. The stress in both north and south subbases at the east end of the pit are very low (~0 psi), a result of being placed 26-in. below the pavement surface. The stress in the north subbase at the east end jumps to 3 psi between 260k-300k cycles, due to the failure of the pavement in the vicinity. From Figures 4.2 and 4.3 it is observed that the larger compressive stresses were measured under the north lane indicating a weak semi-permeable base.

43

TABLE 4.1: Maximum Vertical Stresses (in psi)

Cycles	South Slab West end, 12" Below base	South Slab Midspan, 12" Below base	North Slab Midspan, 12" Below base	North Slab East end, 26" Below base	South Slab East end, 26" Below base
0k	0.62	0.96	1.35	0.075	0.0245
5k	1.12	1.25	1.82	0.09785	0.03328
10k	1.19	1.45	1.83	0.10165	0.02608
20k	1.42	1.34	2.24	0.11238	0.0322
25k	1.18	1.54	0.91	0.131	0.0356
0k	0.97	1.07	0.60	0.13415	0.3633
35k	1.56	1.49	0.15	0.08443	0.03223
40k	2.00	1.23	0.54	0.08278	0.03893
50k	1.99	0.94	0.59	0.08345	0.04015
60k	2.16	0.69	0.65	0.09123	0.04605
80k	1.85	0.50	0.44	0.09908	0.029
100k	2.86	0.49	0.32	0.09648	0.03363
120k	1.67	0.45	0.39	0.14673	0.0432
180k	0.69	1.84	2.45	2.99165	0.0446
260k	0.00	0.00	1.35	0.00365	0.0031
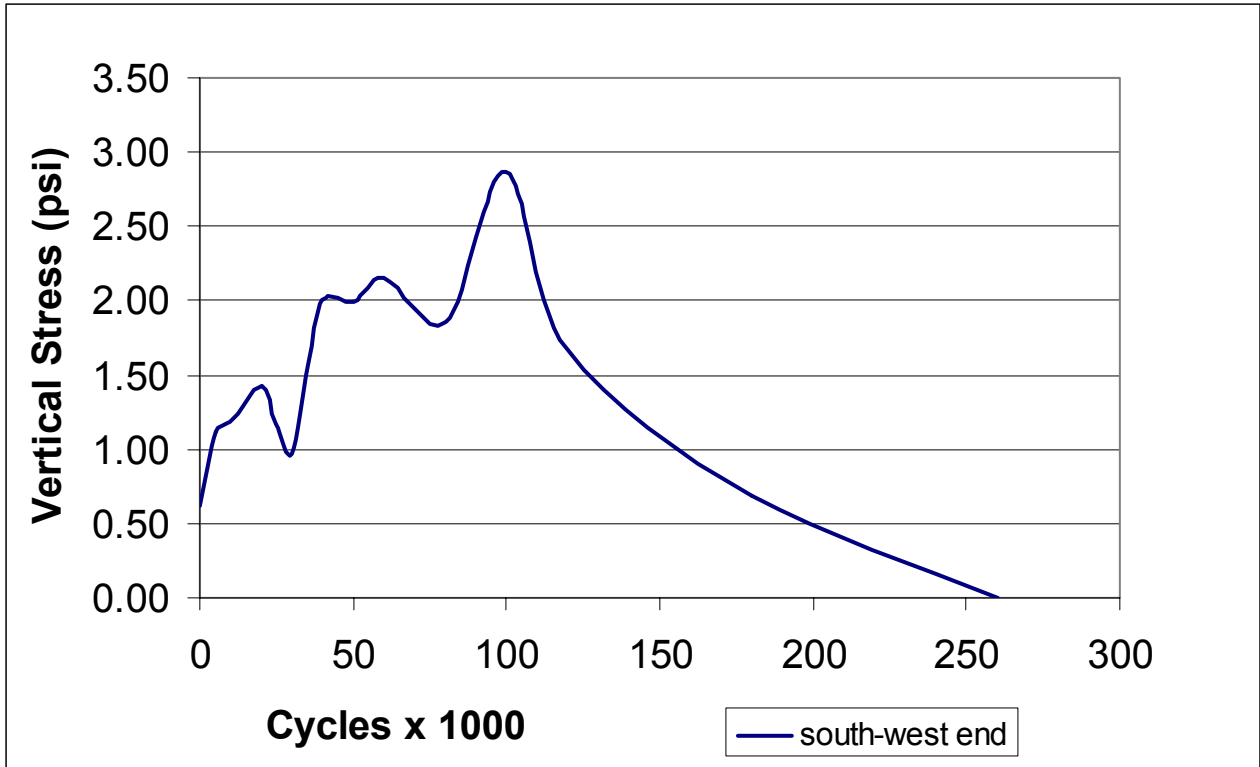
FIGURE 4.1: Vertical Stress vs. Cycles (West End)
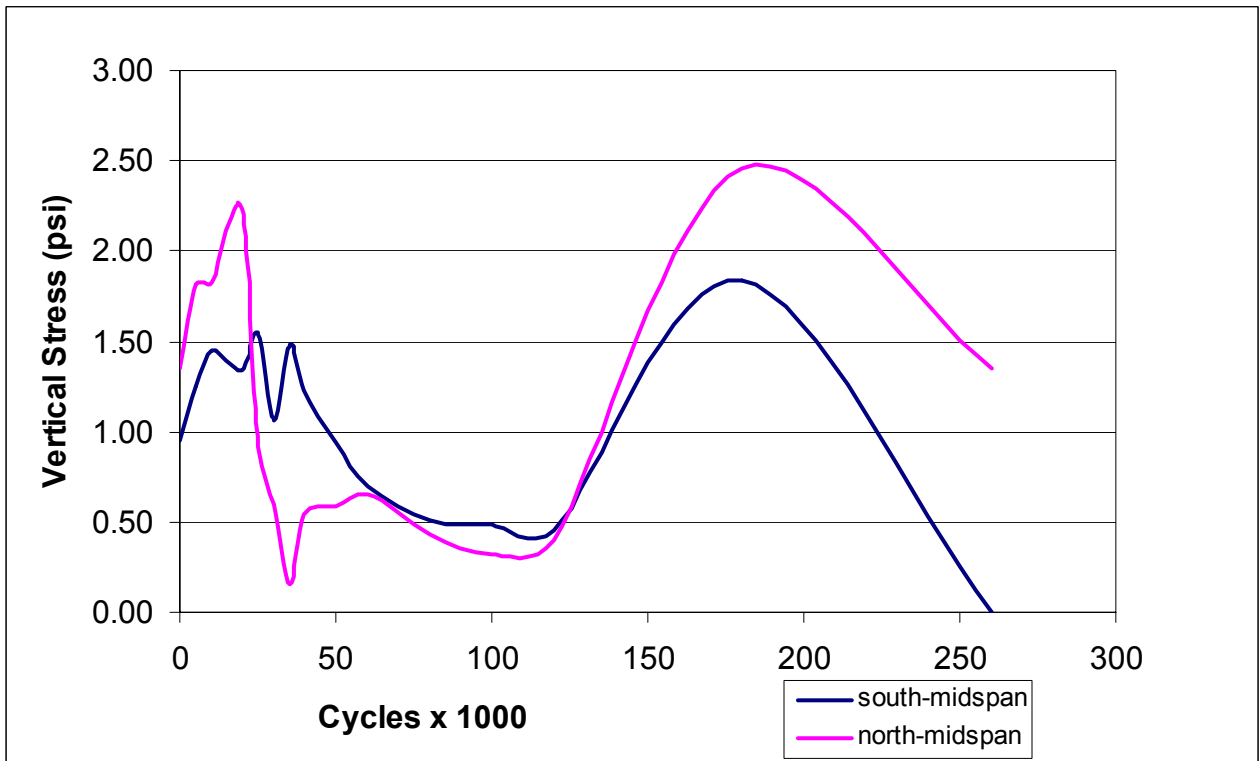
FIGURE 4.2: Vertical Stress vs. Cycles (Midspan)

45
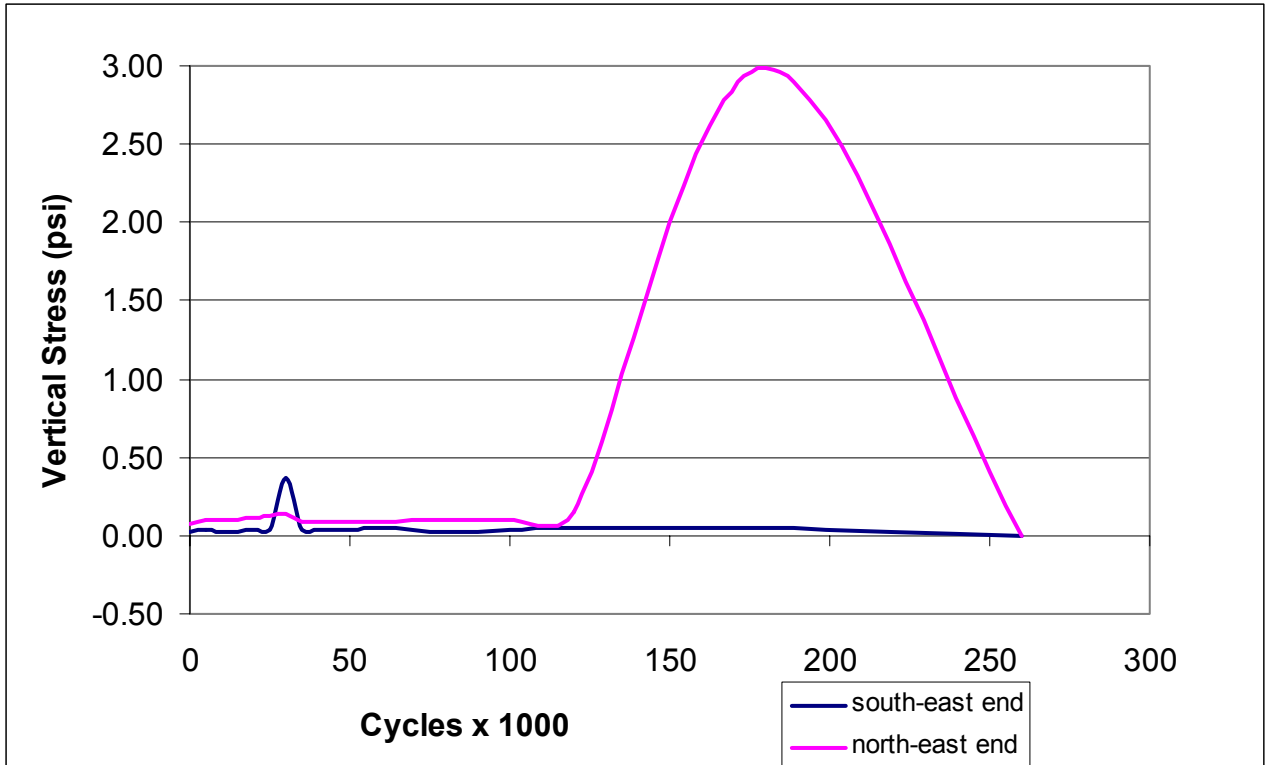
FIGURE 4.3: Vertical Stress vs. Cycles (East End)

-Strains

Strains were monitored at 12 different locations in both the north and south pavements as described in section 3.1.9, Table 3.8, and locations shown in Figure 3.11. The maximum strain values for positions #1 and #4 (west end) are provided in Table 4.2. The first four columns of this table give the strains in both pavements for the top and bottom positions as the wheel approaches locations #1 and #4. The last four columns show the strains in both pavements as the wheels leave locations #1 and #4. Figures 4.4 and 4.5 show the strains at the top and bottom positions for locations #1 and #4 as the wheels approach and after leaving, respectively.

TALBE 4.2: Maximum Strains at Locations #1 and #4 (in µ€)

Wheel Approach					Wheel Leaving			
South Top 1"depth	South Bottom 5"depth	North Top 1"depth	North Bottom 5"depth	Cycles X1000	South Top 1"depth	South Bottom 5"depth	North Top 1"depth	North Bottom 5"depth
-187.70	153.71	-186.47	148.22	0	41.49	-29.83	65.24	-41.94
-209.28	166.89	-40.86	32.26	5	28.30	-21.45	149.13	-106.09
-201.77	160.61	-32.25	25.11	10	17.64	-13.65	143.07	-103.72
-195.00	158.02	-32.66	24.38	20	21.04	-17.26	136.08	-101.22
-173.40	143.12	-36.69	31.35	25	37.53	-29.09	146.50	-103.49
-181.40	146.47	-34.35	34.78	30	36.40	-28.53	137.00	-83.66
-177.68	144.60	-42.06	42.36	35	48.16	-34.64	136.88	-81.03
-170.20	145.97	-38.10	32.93	40	52.15	-30.47	139.50	-88.25
-175.44	152.61	-56.42	37.56	40(AR)*	55.70	-28.23	212.25	-118.12
-176.40	146.61	-55.72	39.45	50	56.54	-35.32	208.62	-120.93
-179.51	147.88	-64.95	45.58	60	54.55	-33.91	199.22	-121.16
-104.49	67.20	51.16	-37.93	80	142.00	-99.33	306.48	-208.94
-117.72	100.74	-55.29	45.94	100	104.71	-83.10	167.87	-99.06
-92.05	73.57	67.51	17.49	120	194.19	-112.20	325.47	-185.68
-62.38	35.62	-52.54	25.86	180	248.33	-176.81	261.67	-188.05
-74.72	74.40	-89.07	58.42	260	267.69	-144.61	289.82	-208.72

* AR - After Repair

It is observed that the strains on the top surface tend to increase as the wheel approaches the gauge locations and the strains on the bottom surface decrease. The same trends are observed as the wheel load leaves the gauge locations.
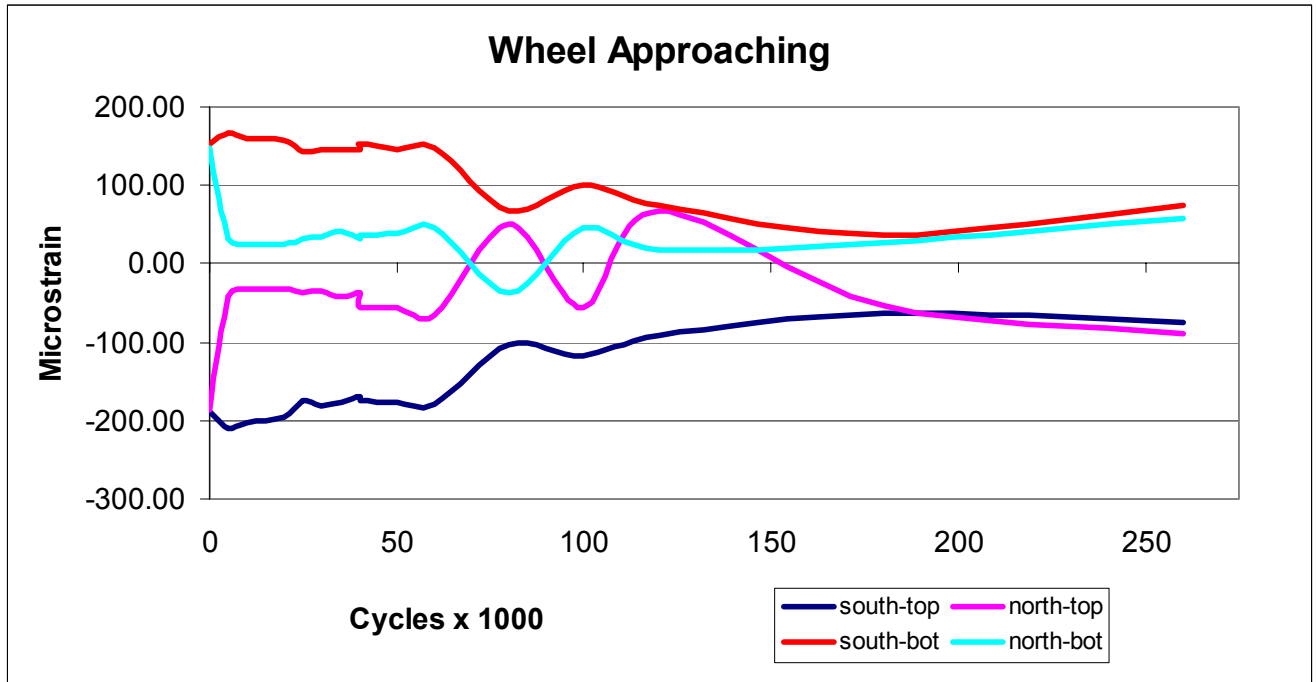
FIGURE 4.4: Strain vs. Cycles for Locations #1 and #4
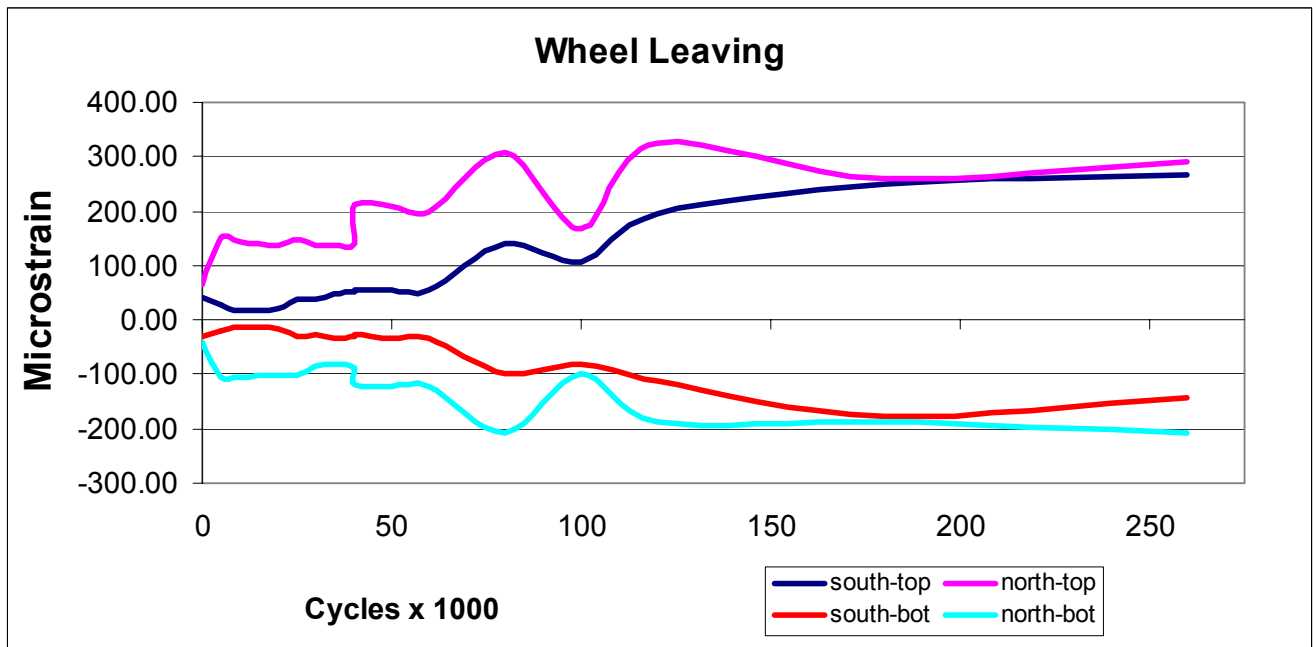
FIGURE 4.5: Strain vs. Cycles for Locations #1 and #4

Longitudinal and transverse strains were monitored in both pavements at midspan. Tables 4.3 and 4.4 give the strain values for the top and bottom positions in both pavements at locations #2 and #5 for the longitudinal and transverse directions, respectively. The first four columns are the wheel approaching strain values and the last four columns are for the wheel leaving, respectively.

TABLE 4.3: Maximum Longitudinal Strains for Locations #2 and #5 (in µ€)

	Wheel Approach				Wheel Leaving			
South Top	South Bottom	North Top	North Bottom	Cycles X1000	South Top	South Bottom	North Top	North bottom
-21.66	-87.62	172.43	-135.18	0	-95.78	156.68	-223.74	197.77
-27.27	-100.55	209.19	-163.12	5	-92.03	150.51	-151.68	125.04
-32.95	-102.23	224.68	-178.75	10	-98.27	134.21	-143.18	117.60
-35.77	-102.73	230.32	-190.10	20	-102.21	141.42	-135.73	107.12
-31.80	-102.18	198.99	-157.80	25	-104.48	128.54	-161.42	129.54
-26.13	-100.52	249.87	-203.93	30	-103.38	145.97	-115.85	92.15
-28.93	-95.88	217.50	-181.37	35	-119.68	146.86	-148.09	121.45
-24.96	-98.73	224.74	-190.48	40	-113.45	130.68	-132.96	104.13
-24.96	-99.85	146.55	-163.41	40AR*	-111.74	139.08	-201.93	144.37
-23.81	-93.65	173.30	-190.42	50	-111.70	140.16	-183.63	127.10
-24.94	-93.12	191.75	-192.05	60	-108.83	148.61	-179.26	129.33
-4.52	-29.62	147.20	-120.97	80	-88.73	131.30	-190.05	136.42
-32.79	-86.52	115.14	-103.72	100	-114.21	107.16	-179.61	138.64
-20.89	-32.34	122.53	-104.74	120	-103.32	110.37	-190.41	131.62
-32.19	-56.32	97.52	-95.43	180	-157.59	142.73	-233.91	186.80
-56.24	-72.28	70.61	-81.59	260	-180.55	215.11	-275.12	295.43

* AR – After Repair

Figures 4.6 and 4.7 show the longitudinal strains at the top and bottom positions for locations #2 and #5 as the wheels approach and after leaving, respectively. Figures 4.8 and 4.9

show the transverse strains at the top and bottom positions for locations #2 and #5 as the wheels

approach and after leaving, respectively.

TABLE 4.4: Maximum Transverse Strains for Locations #2 and #5 (in µ€)

Wheel Approach					**Wheel Leaving**			
South Top	South Bottom	North Top	North Bottom	Cycles X1000	South Top	South Bottom	North Top	North bottom
126.42	34.62	-25.89	41.52	0	-205.08	95.33	-111.63	107.16
132.04	43.00	-10.92	1.11	5	-198.68	100.14	-106.96	116.23
132.64	50.35	2.30	-4.45	15	-176.513	100.70	-108.13	117.36
130.32	50.87	3.45	-7.22	20	-182.74	109.08	-108.09	120.57
124.60	51.42	4.03	-3.89	25	-173.02	116.96	-122.45	149.45
126.30	45.77	4.03	-1.11	30	-180.41	115.27	-125.40	158.37
121.20	44.62	4.02	1.66	35	-182.70	129.34	-145.32	176.06
119.46	41.77	6.90	-1.11	40	-170.71	120.79	-131.70	162.60
117.17	39.50	-31.03	7.77	40AR*	-173.54	119.06	-140.80	171.40
112.64	34.45	-21.83	4.44	50	-181.53	121.88	-132.74	158.61
117.09	40.03	1.72	4.99	60	-181.64	116.70	-131.66	155.70
44.86	13.42	-9.20	6.61	80	-168.10	102.30	-101.18	107.35
78.52	53.13	-1.15	3.84	100	-112.11	135.31	-112.63	128.00
50.56	-5.03	-2.87	21.94	120	-143.75	130.10	-110.25	110.78
67.01	-28.44	11.49	-7.67	160	-149.96	195.25	-178.71	237.57
113.97	7.20	-31.47	-14.90	260	-158.82	798.94	-107.00	3159.70
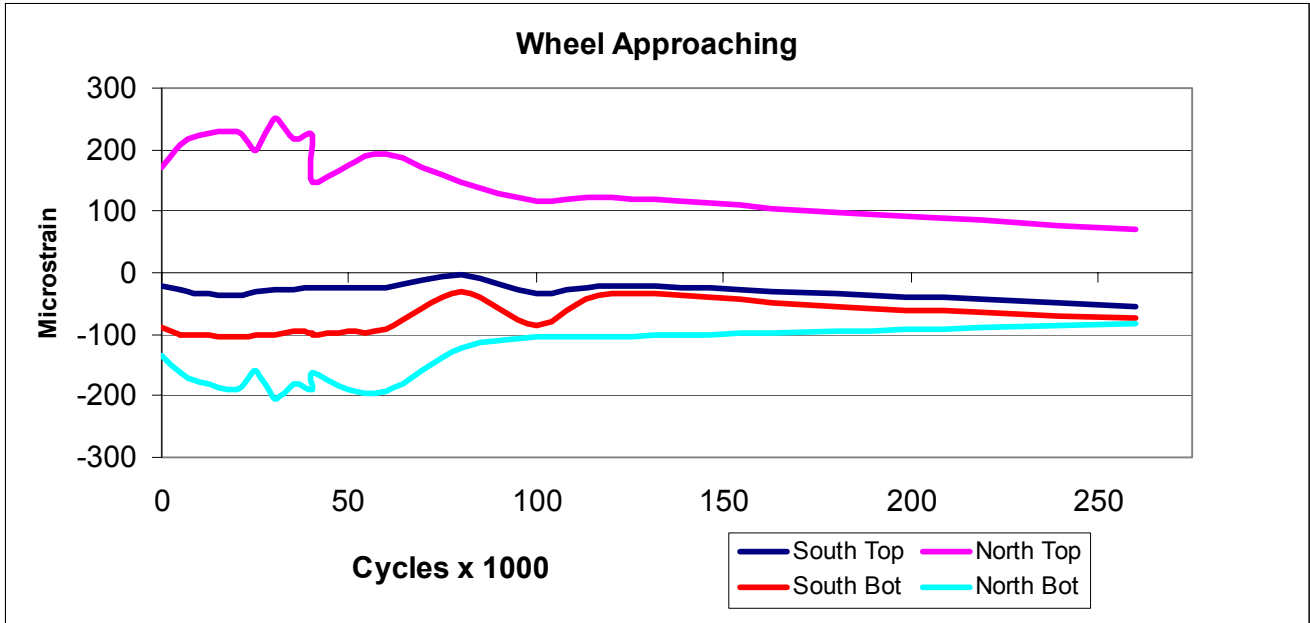
FIGURE 4.6: Longitudinal Strains vs. Cycles for Locations #2 and #5
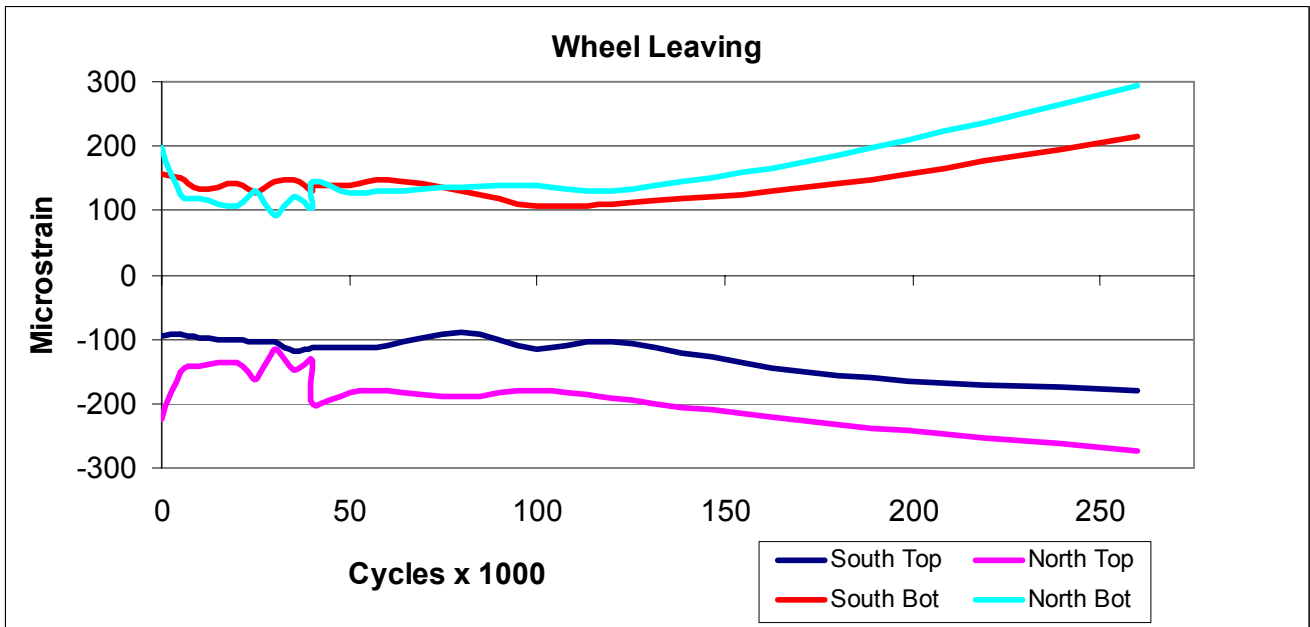
FIGURE 4.7: Longitudinal Strains vs. Cycles for Locations #2 and #5
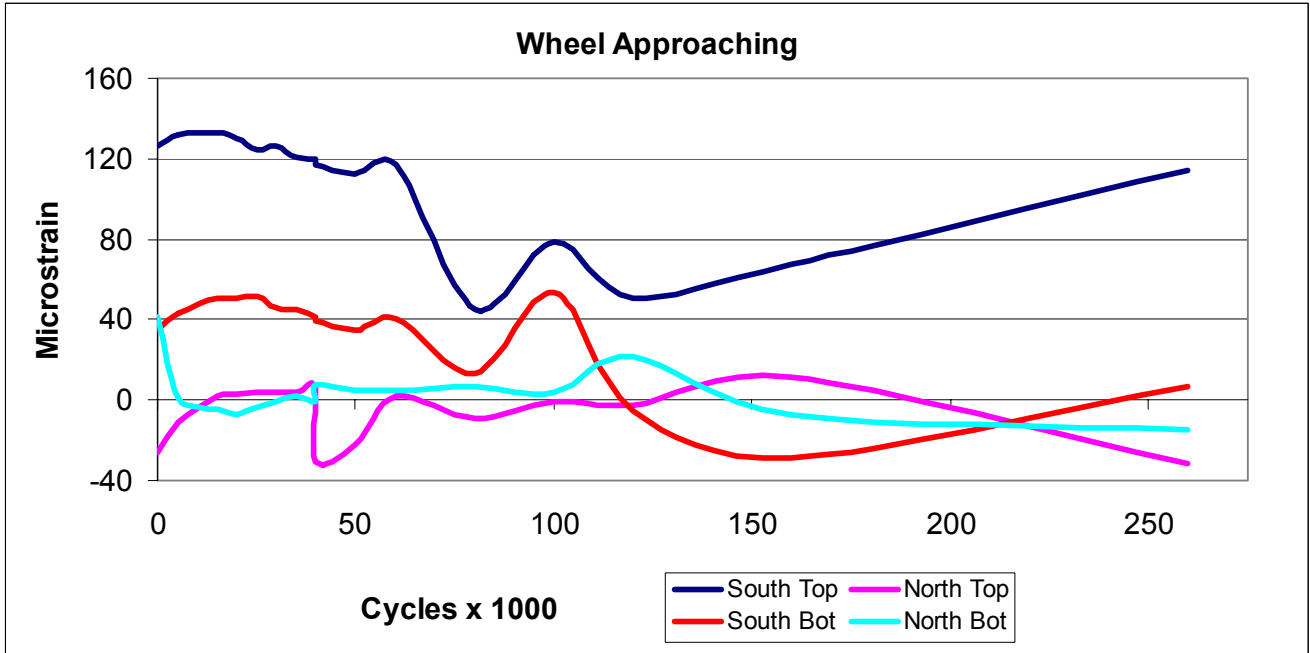
FIGURE 4.8: Transverse Strains vs. Cycles for Locations #2 and #5
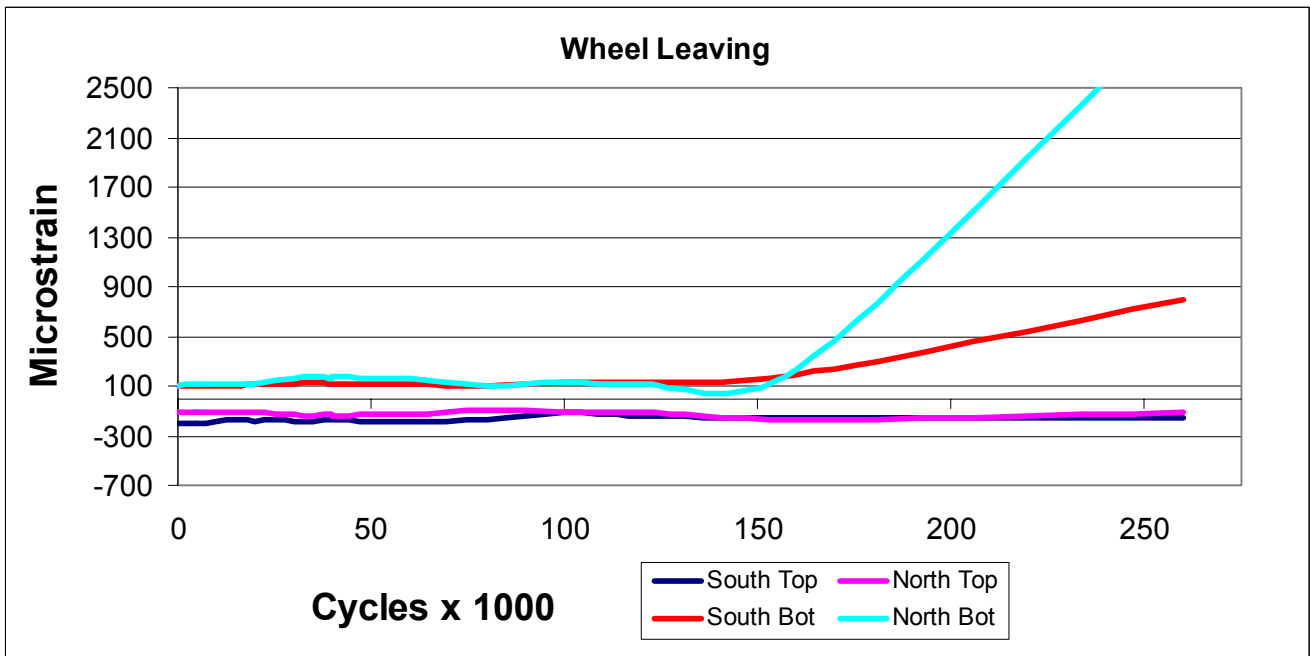
FIGURE 4.9: Transverse Strains vs. Cycles for Locations #2 and #5

The longitudinal strains for positions #2 and #5 tend to decrease on the top surface and increase on the bottom surface in both pavements for the wheel loads approaching and passed.

The transverse strains in the south pavement initially decrease for both top and bottom surface locations, and then increase until the end of testing. The transverse strain in the north pavement decrease for the duration of the testing, revealing the severe degradation of the semi-permeable base.

Table 4.5 gives the strain values for the top and bottom positions in both pavements at locations #3 and #6. The first four columns are the wheel approaching strain values and the last four columns are for the wheel leaving. Figures 4.10 and 4.11 show the longitudinal strains at the top and bottom positions for locations #3 and #6 as the wheels approach and after leaving, respectively.

TABLE 4.5: Maximum Strains at Locations #3 and #6 (in µ€)

Wheel Approach					Wheel Leaving			
South Top	South bottom	North top	North bottom	Cycles x1000	South Top	South Bottom	North top	North bottom
180.18	-0.19	177.27	-138.08	0	-176.07	-0.19	-168.23	162.83
136.49	-0.19	149.74	-129.09	5	-180.27	-0.19	-176.62	149.90
84.80	-0.19	139.64	-113.42	10	-195.05	-0.19	-160.95	143.20
76.78	-0.19	144.07	-114.38	20	-198.97	-0.19	-151.85	138.04
85.88	-0.19	145.70	-122.76	25	-187.06	-0.19	-124.30	112.79
74.57	-0.19	140.09	-111.04	30	-195.02	-0.19	-123.22	114.52
86.97	-0.19	145.22	-115.40	35	-190.28	-0.19	-140.74	131.06
93.22	-0.19	147.47	-120.51	40	-180.26	-0.19	-139.01	132.78
94.45	-0.19	145.11	-118.19	40AR*	-194.41	-0.19	-164.28	149.61
94.93	-0.19	139.62	-114.80	50	-195.00	-0.19	-176.10	163.52
91.60	-0.19	145.74	-117.62	60	-200.08	-0.19	-164.78	159.65
154.97	-0.19	234.29	-130.72	80	-138.99	-0.19	-158.91	89.97
83.45	-0.19	194.74	-86.99	100	-156.19	-0.19	-203.75	137.23
140.11	-0.19	285.68	-114.31	120	-134.99	-0.19	-136.03	123.30
160.63	-0.19	338.44	-160.92	180	-148.72	-0.19	-73.63	56.79
165.37	-0.19	535.38	-299.80	260	-150.68	-0.19	167.50	85.10
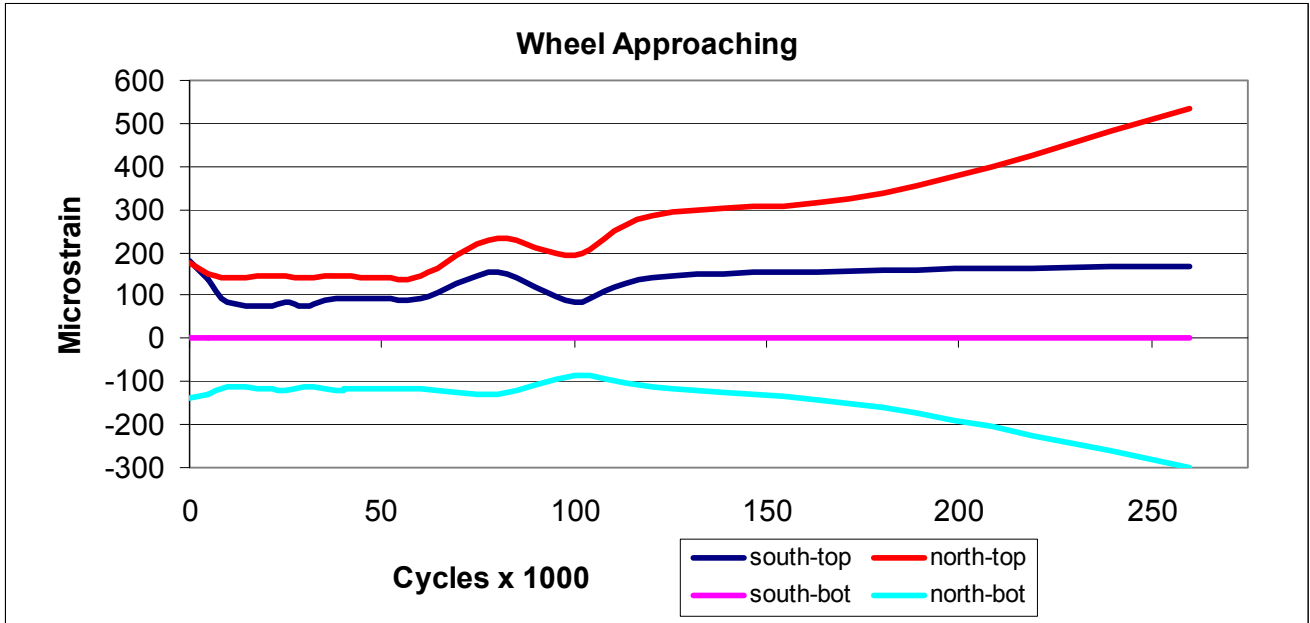
FIGURE 4.10: Strain vs. Cycles for Locations #3 and #6
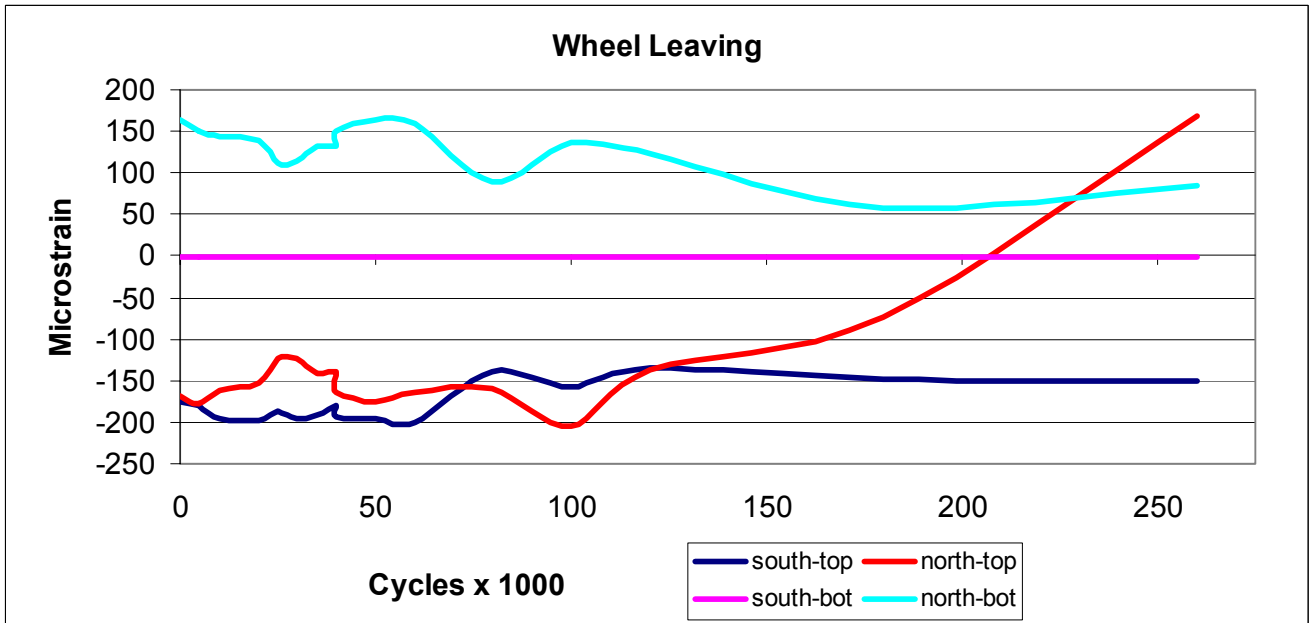
FIGURE 4.11: Strain vs. Cycles for Locations #3 and #6

The strains on the top surface of both north and south pavements at positions #3 and #6 increases as the wheel load approaches and passes for the duration of the testing. The strains on the bottom surface of the north pavement decrease for the duration of the test. The gage for the

bottom surface of the south pavement did not work properly during the testing. It was only observed that strains alternated from compressive to tensile (or tensile to compressive) as the wheel loads approached and then passed the gage locations in both the north and south pavements.

4.1.2 Temperature

The temperature profiles for experiment #9 are shown in Figures 4.12 to 4.17. Temperatures were monitored on the surface, 3-in. below the surface and 6-in. below the surface. Figures 4.12 to 4.14 show the profile for the south pavement and Figures 4.15 to 4.17 for the north pavement. It is clear that a temperature gradient exists from the top surface to 6-in. below the surface whether in a hot or cold cycle, and the gradients are higher at the joints than at the center of the slab.
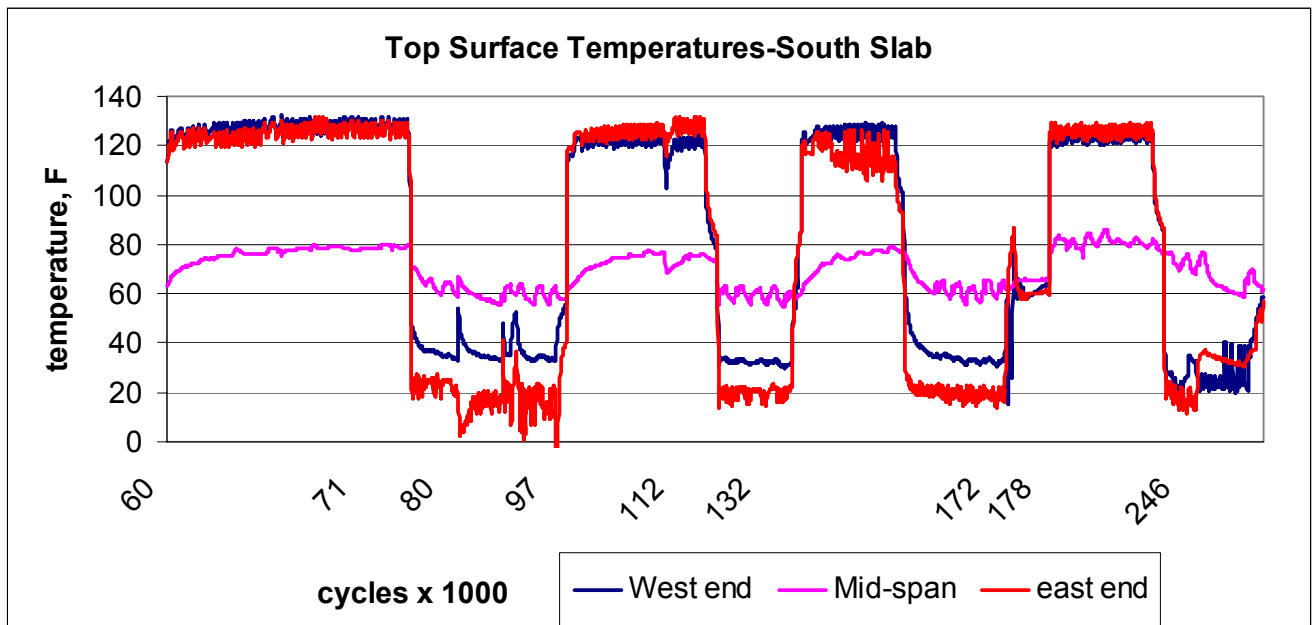
FIGURE 4.12: Temperature Profile, South Pavement, Top Surface
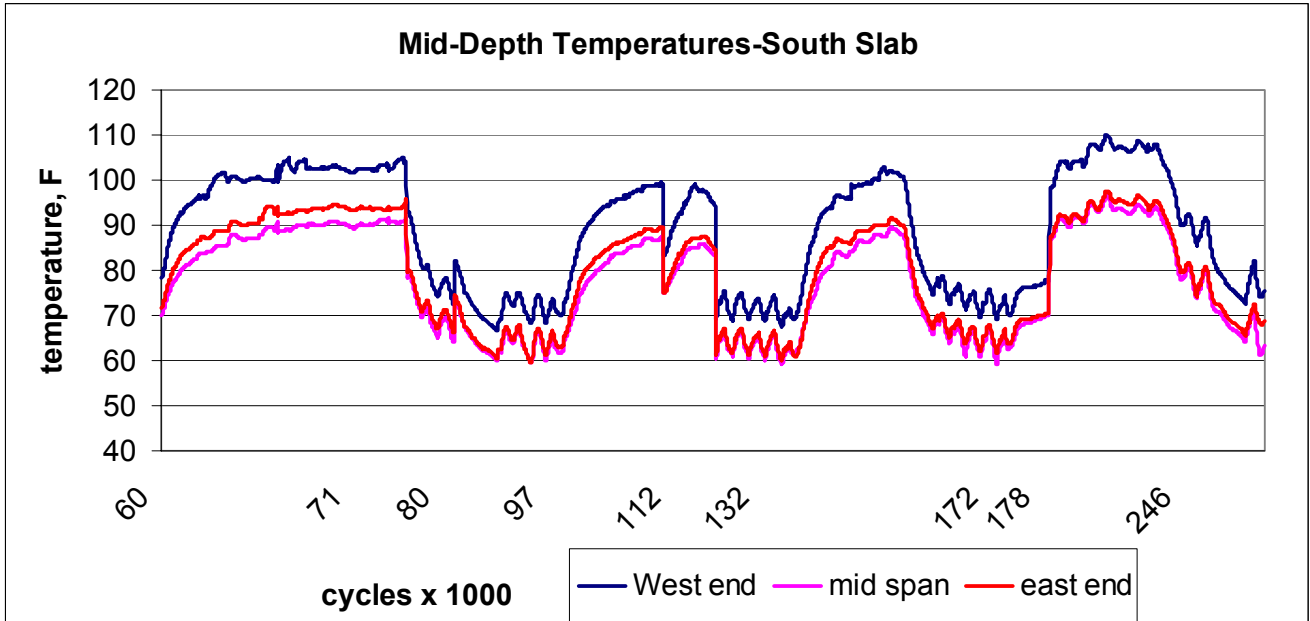
FIGURE 4.13: Temperature Profile, South Pavement, Mid-depth
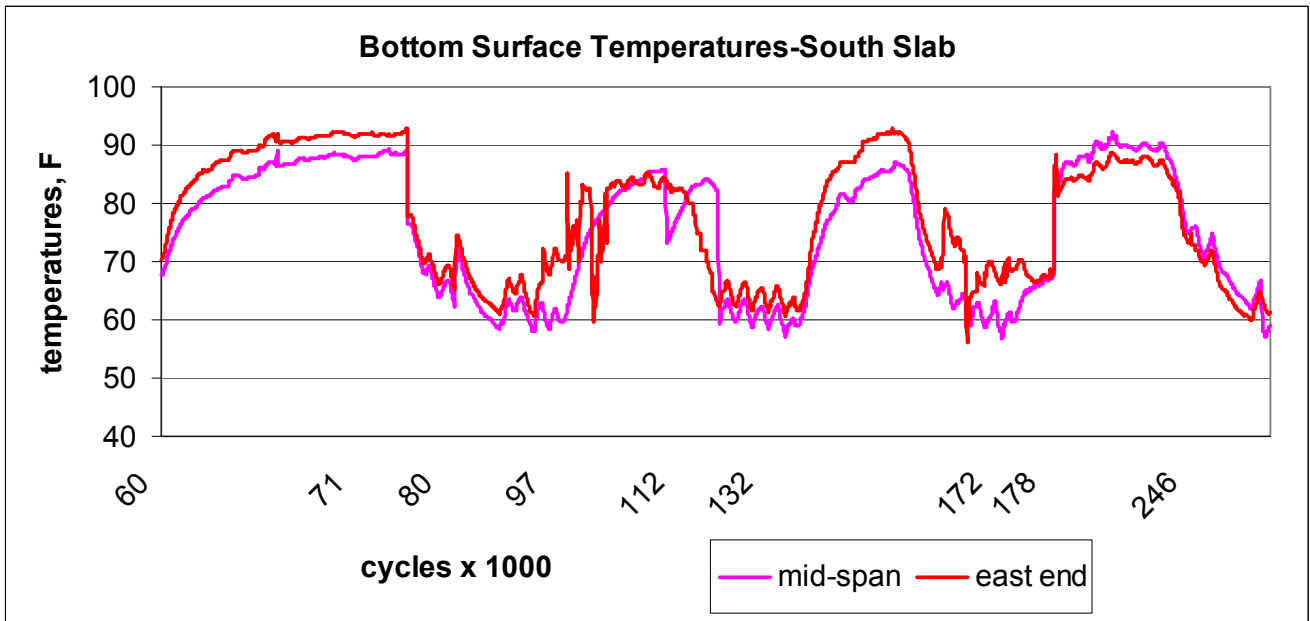
FIGURE 4.14: Temperature Profile, South Pavement, Bottom Surface
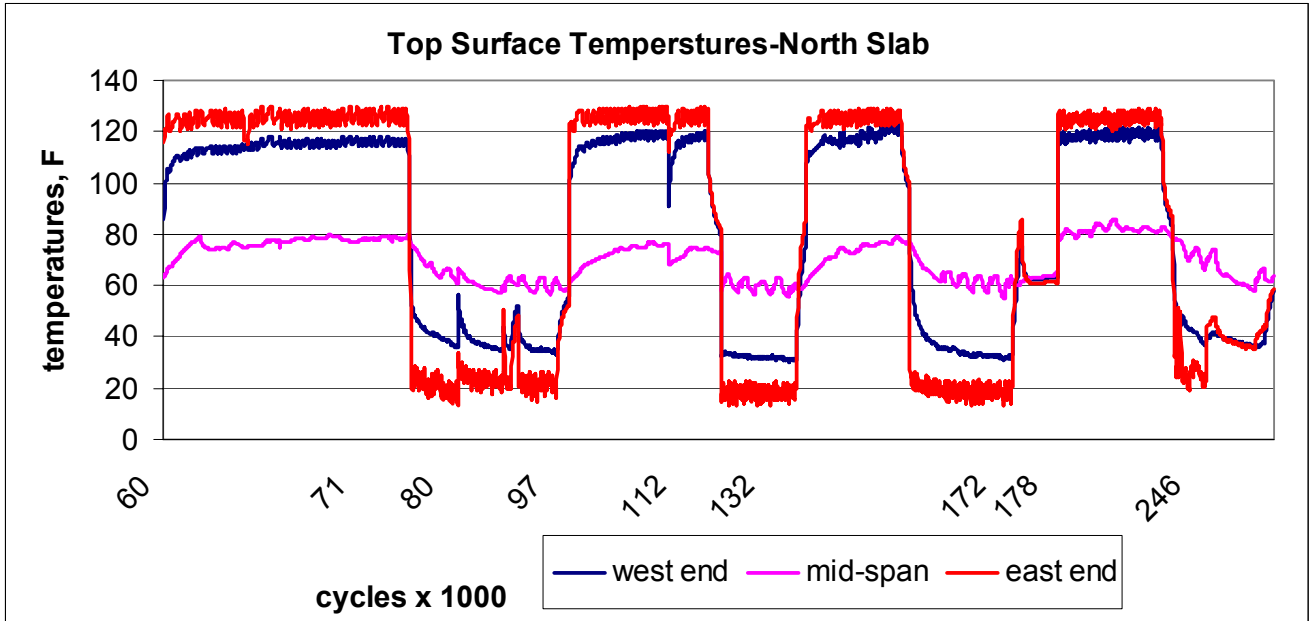
FIGURE 4.15: Temperature Profile, North Pavement, Top Surface
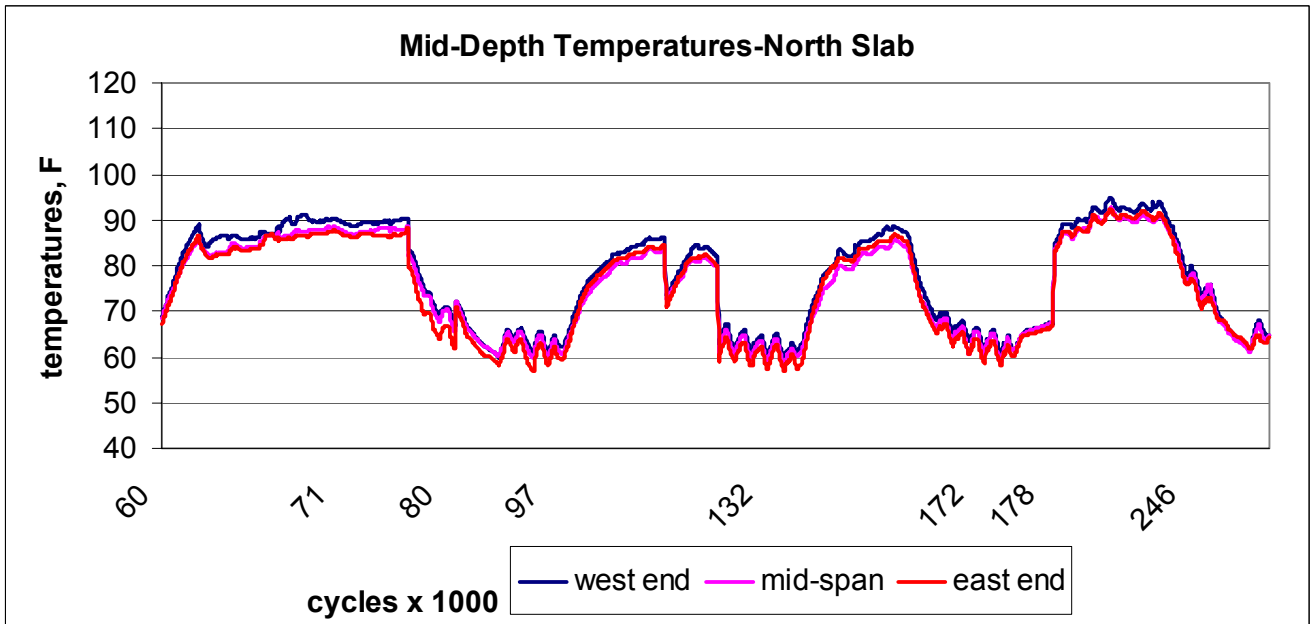
FIGURE 4.16: Temperature Profile, North Pavement, Mid-Depth

57
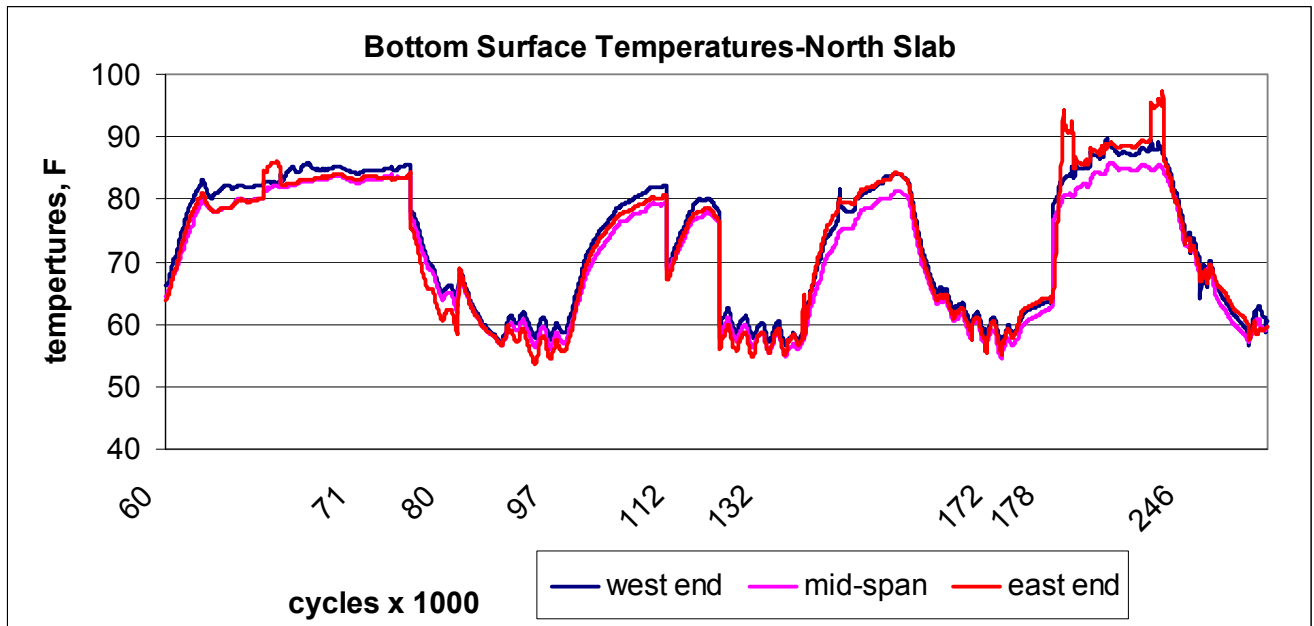
FIGURE 4.17: Temperature Profile, North Pavement, Bottom Surface

4.1.3 Vertical Deflection

The vertical deflection in both the south and north pavements was monitored using

LVDTs. The location of each LVDT is described in section 3.1.9 for the rolling wheel loads. A

typical deflection response for the north pavement is shown in Figure 4.18. As the wheel travels

west to east, LVDT #9 is first to deflect downward and LVDT #1 is last for downward

deflection, as observed in Figure 4.18. It is observed that as the wheels travel west to east, for

example, LVDT #6 deflects downward as the wheels pass and then deflect upward when the

wheels pass the location of LVDT #3. This behavior is observed for other LVDTs as well. The

maximum deflections, both upward and downward, for each LVDT are shown in Figures 4.19

and 4.20 for the south and north pavements, respectively.
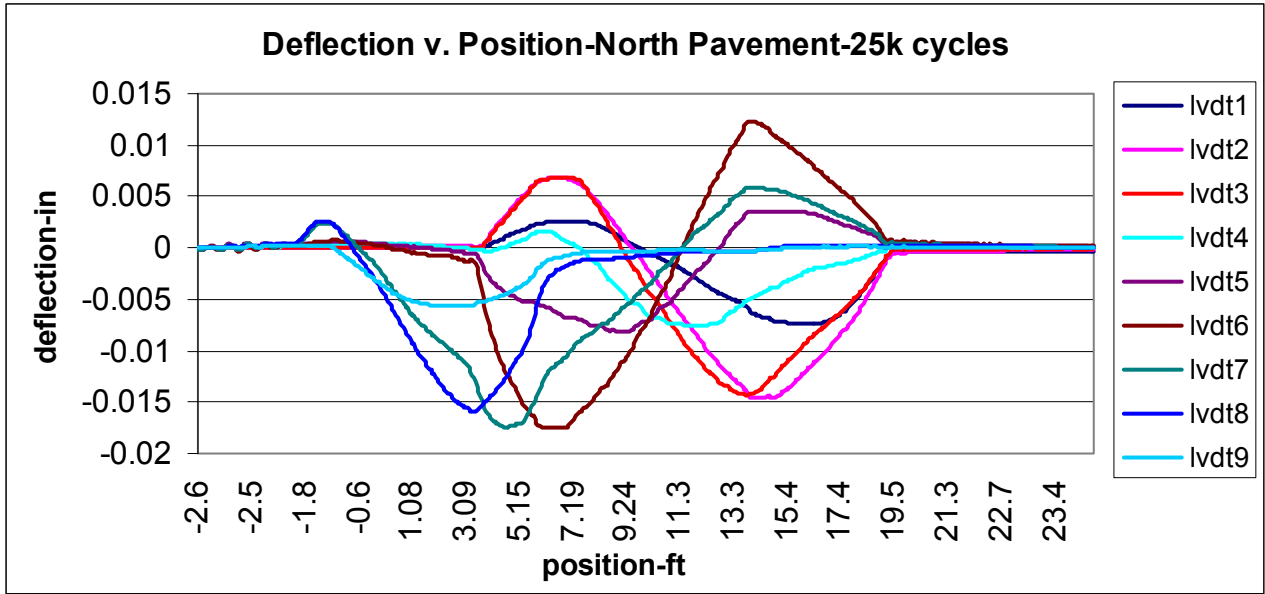
FIGURE 4.18: Deflection Profile in the North Pavement at 25k cycles
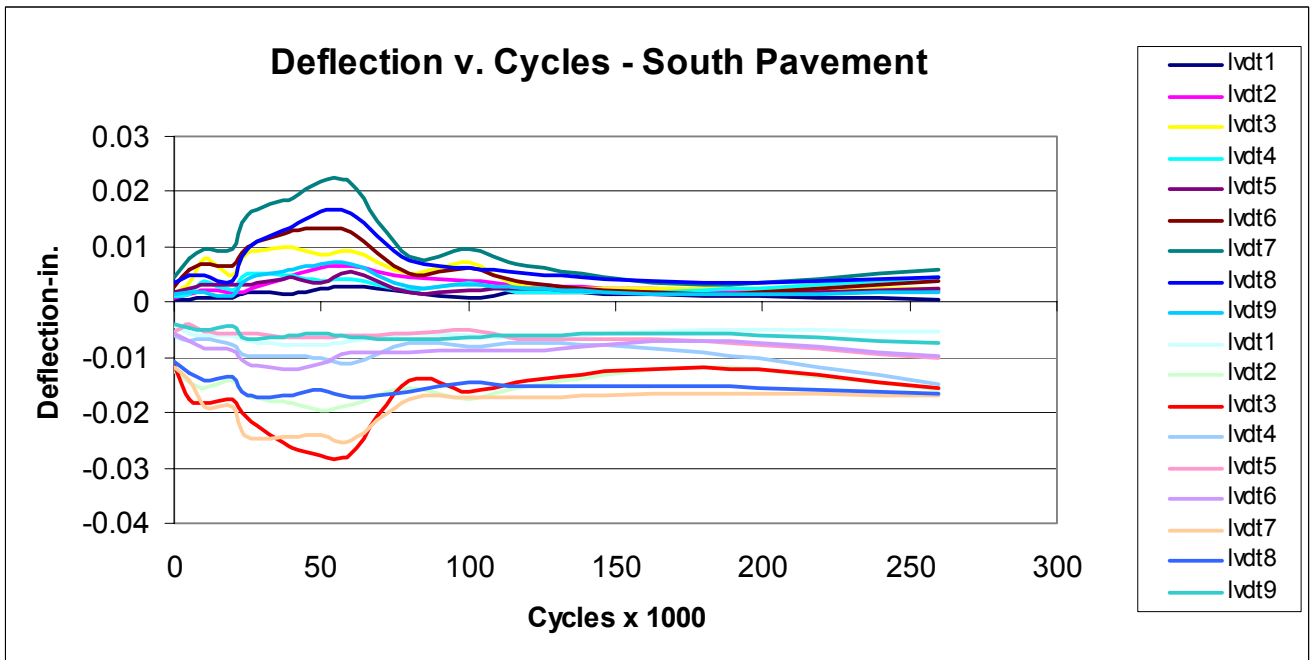
FIGURE 4.19: Max Deflections, South Pavement
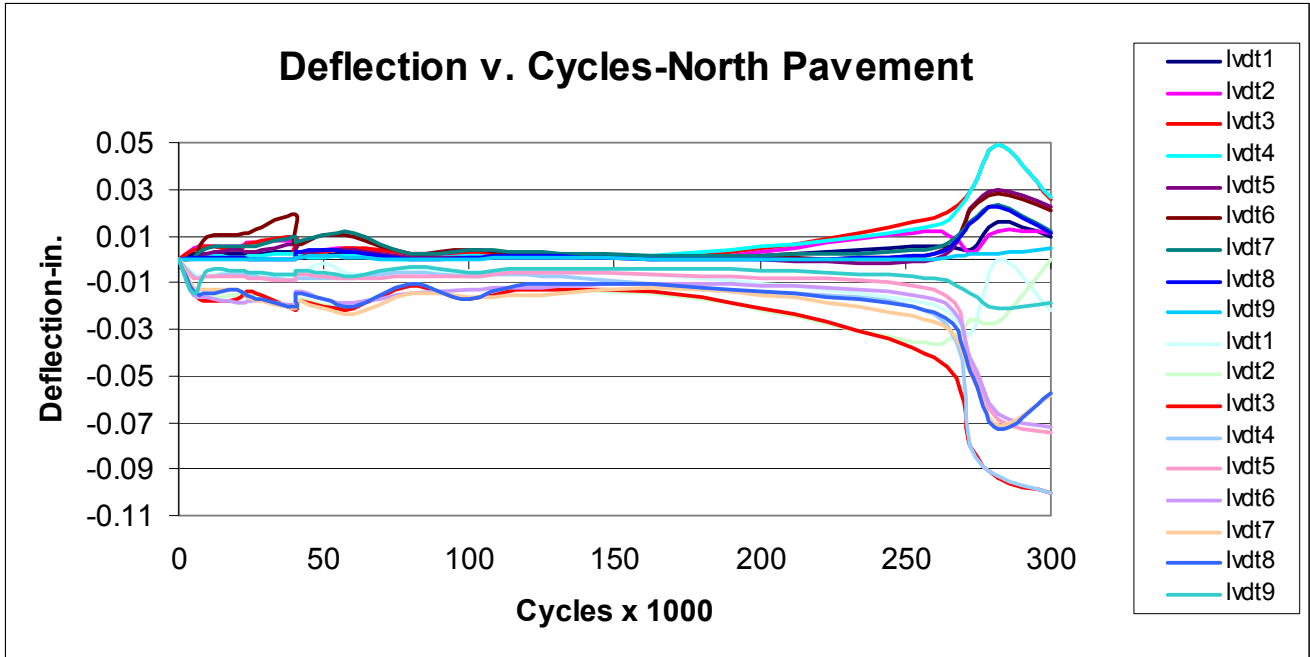
FIGURE 4.20: Max Deflections, North Pavement

4.1.4 Drop Weight

Drop weight tests were performed during experiment #9. The location of weight drops and LVDTs was described in section 3.1.9. The dominant frequency values are shown in Table 4.6 for the south and north pavements. The values in this table are based on weights dropped at positions 3 and 7, and deflection responses obtained from LVDT locations 2 and 8, respectively. Figure 4.21 shows the frequency response versus number of applied cycles.

TABLE 4.6: Drop Weight Dominant Frequency Values (in Hz)

Repetition	North Pavement	South Pavement
0	47.6074	48.8281
5	50.0488	46.3867
10	54.9316	34.1797
20	47.6024	37.8418
40	52.4902	29.2969
60	50.0488	25.6348
80	61.0352	62.2559
100	48.8281	62.2559
120	69.5801	59.8145
180	57.373	61.0352
260	46.3867	52.4902
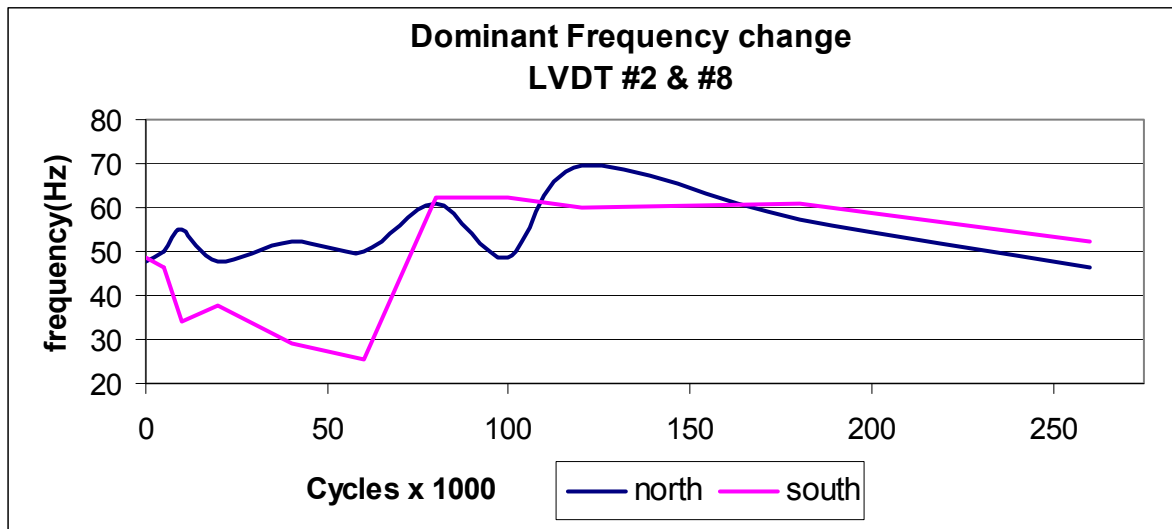
Figure 4.21: dominant Frequency vs. Cycles, Position #3 and #7, LVDT #2 and #8

4.1.5 Pavement Cracking (Experiment #9)

Pavement cracks developed during experiment #9 were monitored and documented for the duration of the experiment. Table 4.7 details the crack developments and the number of applied cycles. Figures 4.22 and 4.23 show the location of the cracks which occurred in the north and north pavements, respectively.

61

TABLE 4.7: Experiment #9 Cycles and Crack Descriptions

Cycles	Description/Comments
40,000	-North slab, 1st crack, through width, 28" east of west transverse joint -Repaired with 4 FRP plates (stitches)
180,000	-North slab, 2nd crack, through width, 37" west of east transverse joint -South slab, 12" transverse hair crack, 37" west of east transverse joint
200,000	-South slab, 1st crack, through width, 36" east of west transverse joint -South slab, 12" longitudinal hair crack, east from west transverse joint
250,000	-North slab, 3rd crack, through width, 33" east of east transverse joint -Pumping starts at east transverse joint from north slab
258,000	-North slab, 4th crack, through width, 28"west of west transverse joint -Pumping increases at east transverse joint, observed at west transverse joint -Cracks 2 and 4 begin to open/work in north slab
280,000	-North slab, longitudinal cracks, both directions from 2nd crack and from east joint to 3rd north slab crack

Severe pumping of the fines, both through the cracks and joints at the pavement surface (Figure 4.24), and the side drain (Figure 4.25) were observed in the north lane. The fine material from the semi-permeable base was pumped out. Since no pumping was observed in the south lane, it can be clearly concluded that the permeable base gives better performance than the semi-permeable base.
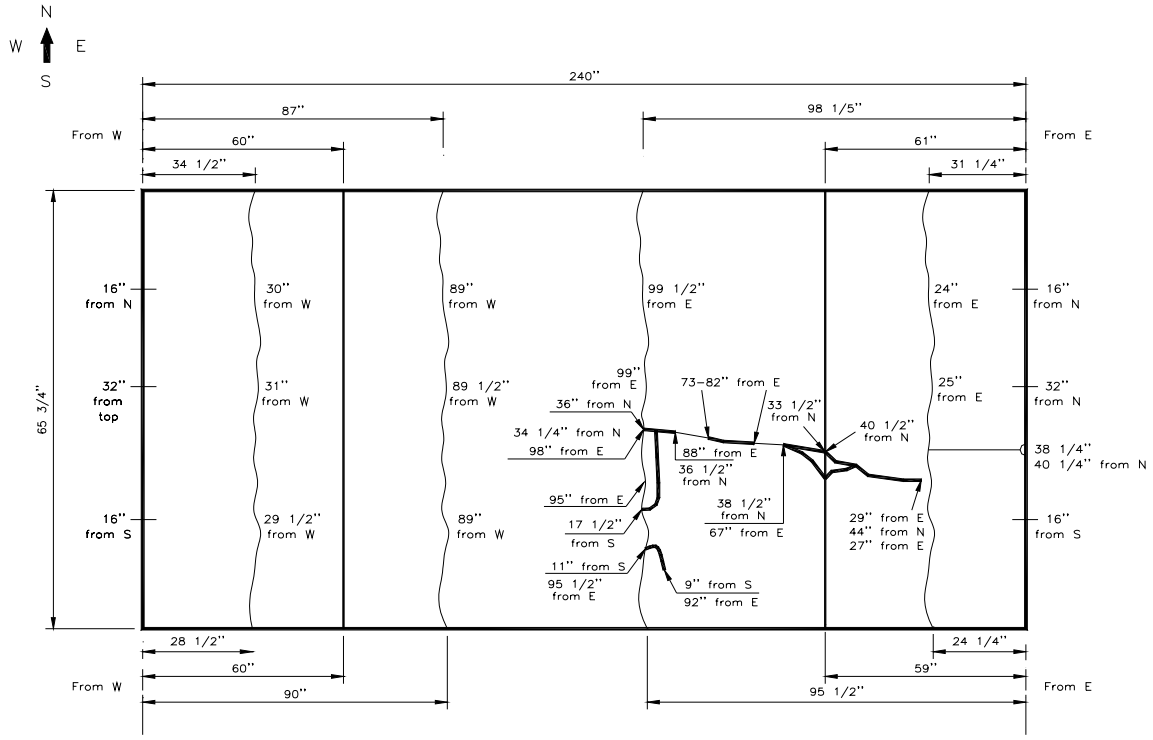
FIGURE 4.22: Crack Mapping for the North Pavement (Exp. #9)
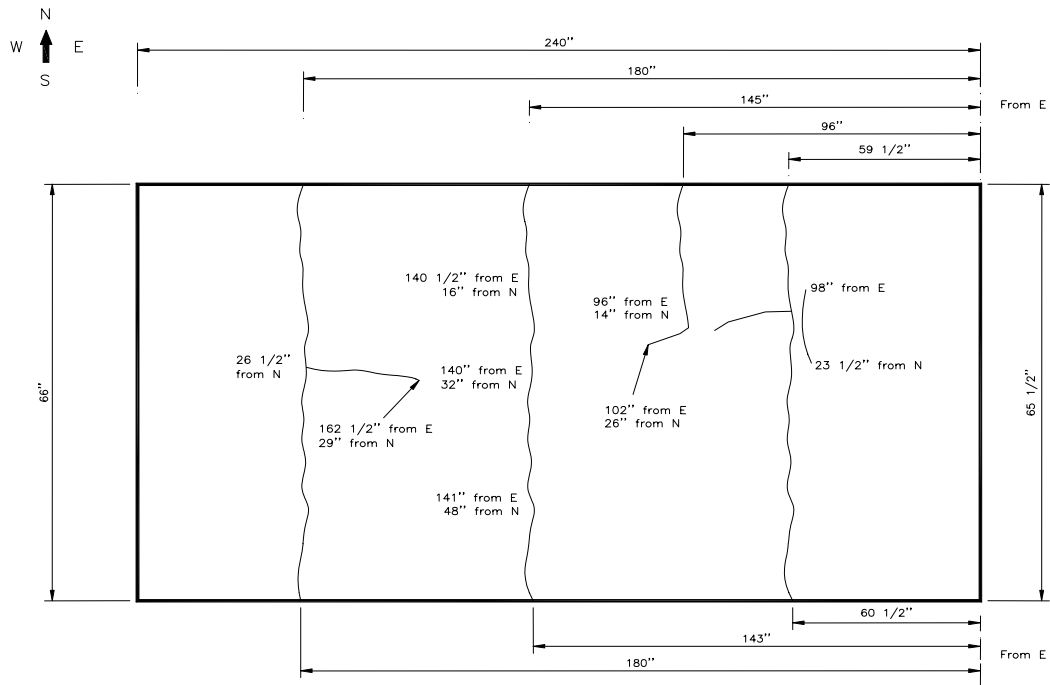
FIGURE 4.23: Crack Mapping for the South Pavement (Exp. #9)

63

FIGURE 4.24: Pumping through Cracks and Joints in the North Lane

FIGURE 4.25: Pumping on the Side of the North Lane

4.2 Experiment #10

 4.2.1 Stresses and Strains in Pavements

 - Vertical Stresses

  Vertical stress in the subbase for experiment #10 was monitored in the same six locations as described in section 3.1.9 for experiment #9, Pressure Cells. The maximum vertical stresses (in psi) are provided in Table 4.8. The pressure transducer located at the west end of the north pavement failed during experiment #9, therefore no data was collected. Figures 4.26 to 4.28 show vertical stress vs. cycles for the west end, midspan and east end locations, respectively. The stress in the west end of the south subbase increases initially, remains constant from 1000 to 17000 cycles, then decreases until the end of the test.

TABLE 4.8: Maximum Vertical Stress (psi)

Cycles	South Slab West end 12" below slab	South Slab Midspan 12" below slab	North Slab Midspan 12" below slab	South Slab East end 26" below slab	North Slab East end 26" below slab
0	2.179	2.521	1.9752	0.7852	1.934
619	3.64	2.5203	1.8495	0.5831	3.1997
2604	3.733	2.6694	2.0436	0.5801	2.4657
5051	3.7955	2.869	3.49	0.5469	1.5871
6882	3.9463	2.7646	4.1928	0.5361	1.3465
9236	3.4854	2.7982	1.0608	0.6123	1.2195
11769	4.132	2.9875	1.0108	0.7204	1.3306
14205	3.8017	2.9784	1.794	0.7205	1.2201
16553	3.8499	3.2861	1.7078	0.7766	1.3934
21355	2.454	3.495	2.8352	0.8402	1.2841
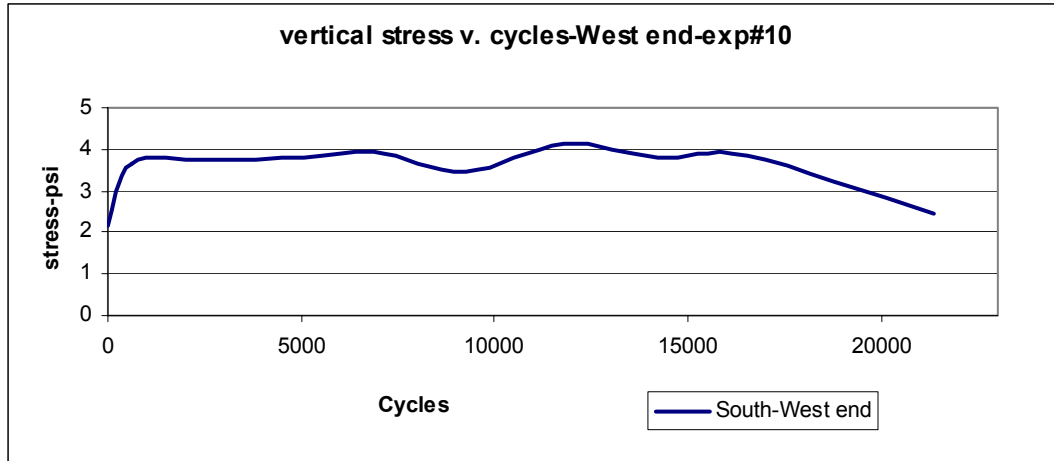
FIGURE 4.26: Vertical Stress vs. Cycles, West End, Exp. #10
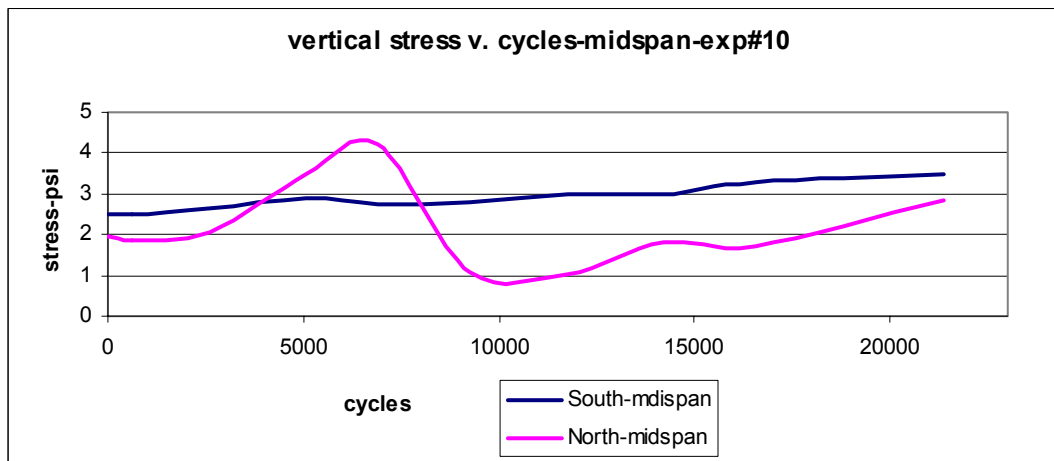
FIGURE 4.27: Vertical Stress vs. Cycles, Midspan, Exp. #10
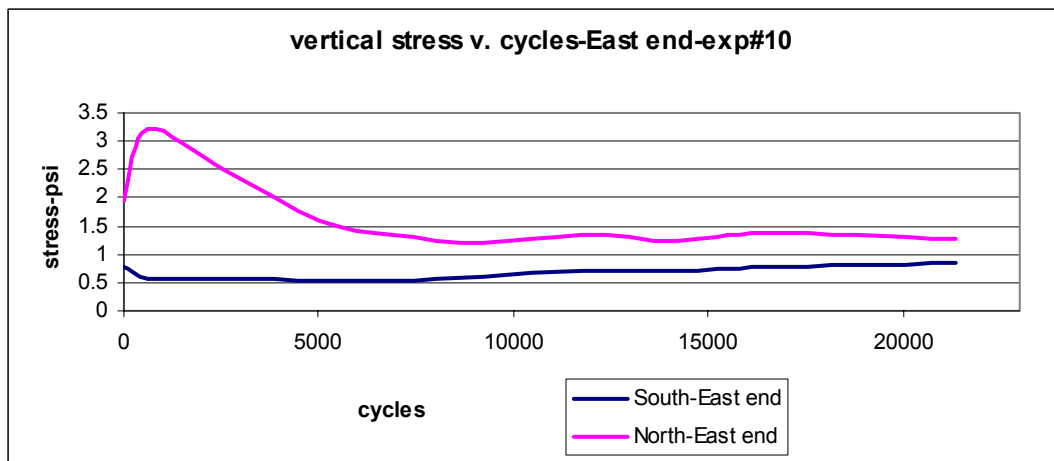
FIGURE 4.28: Vertical Stress vs. Cycles, East End, Exp. #10

The stress for the south pavement for the midspan and east end locations increases slightly over the duration of the experiment. The stress in the north pavement at midspan increases sharply to 4.3 psi at 6500 cycles, then decreases to less than 1.0 psi at 11,000 cycles, then shows an increasing trend to the end of the experiment. The stress at the east end of the north pavement increases above 3 psi at 700 cycles, then decreases to approximately 1.3 psi to the end of the experiment.

- Strains

Strains for experiment #10 were monitored at 12 different locations in both the north and south pavements as described in section 3.1.9 with Table 3.8 and locations shown in Figure 3.11. The maximum strain values for positions #1 and #4 (west end) are provided in Table 4.9. The first four columns of this table give the strains in both pavements for the top and bottom positions as the wheel approaches locations #1 and #4.

TABLE 4.9: Maximum Strains at Positions #1 and #4 (in μ€)

Wheel Approach					Wheel Leaving			
South top	South Bottom	North Top	North Bottom	Cycles	South top	South Bottom	North top	North bottom
-31.78	76.17	-99.42	87.36	0	308.46	-185.96	232.43	-143.59
-25.66	57.95	-102.89	120.15	619	313.66	-199.17	270.82	-154.43
-9.48	52.43	-82.95	99.67	2604	329.61	-205.25	319.87	-171.42
-13.94	51.87	-49.48	90.58	5051	331.05	-203.55	329.96	-166.10
0.00	61.25	-36.27	54.66	6882	354.02	-212.93	335.91	-184.28
25.07	79.46	-23.07	48.75	9236	383.38	-210.16	337.95	-200.31
13.37	61.26	-52.77	171.59	11769	348.27	-259.30	280.97	-287.80
18.00	64.56	-67.00	290.13	14205	364.77	-257.61	252.18	-647.46
10.56	46.34	-57.60	973.00	16553	366.01	-274.11	263.61	-943.67
15.56	44.16	-51.58	1657.20	21355	380.29	-238.96	517.18	1500.00

The last four columns show the strains in both pavements as the wheels have passed locations #1 and #4. Figures 4.29 and 4.30 show the strains at the top and bottom positions for locations #1 and #4 as the wheels approach and after passing, respectively.
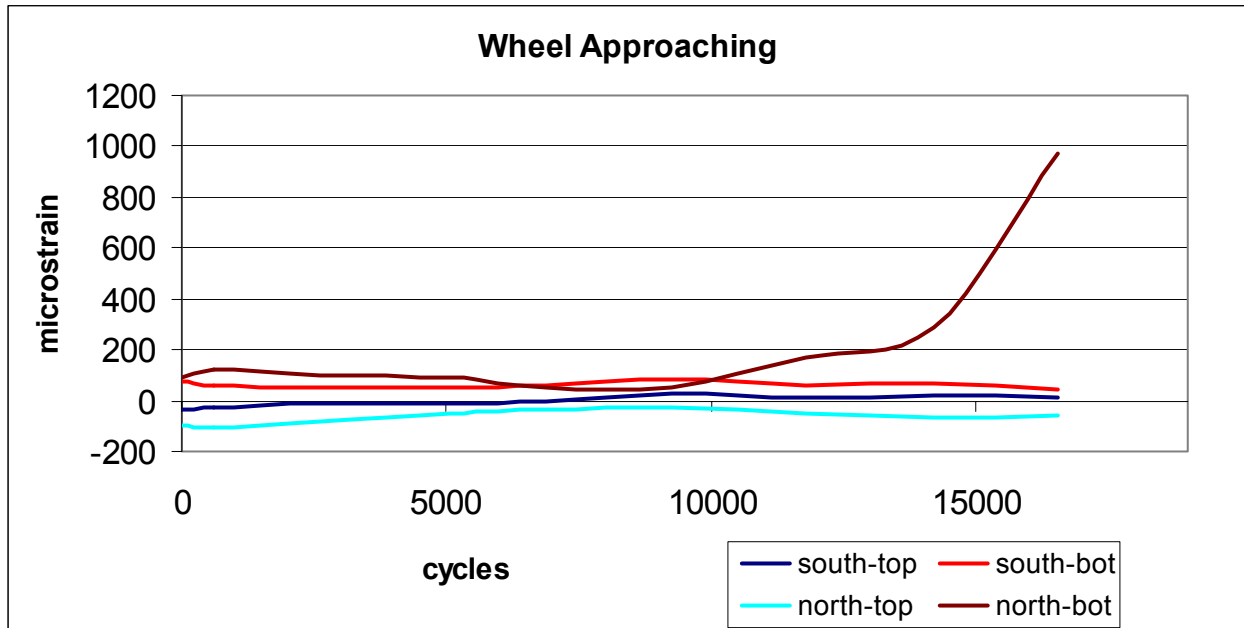
FIGURE 4.29: Strain vs. Cycles for Location #1 and #4 (Wheel Approach)
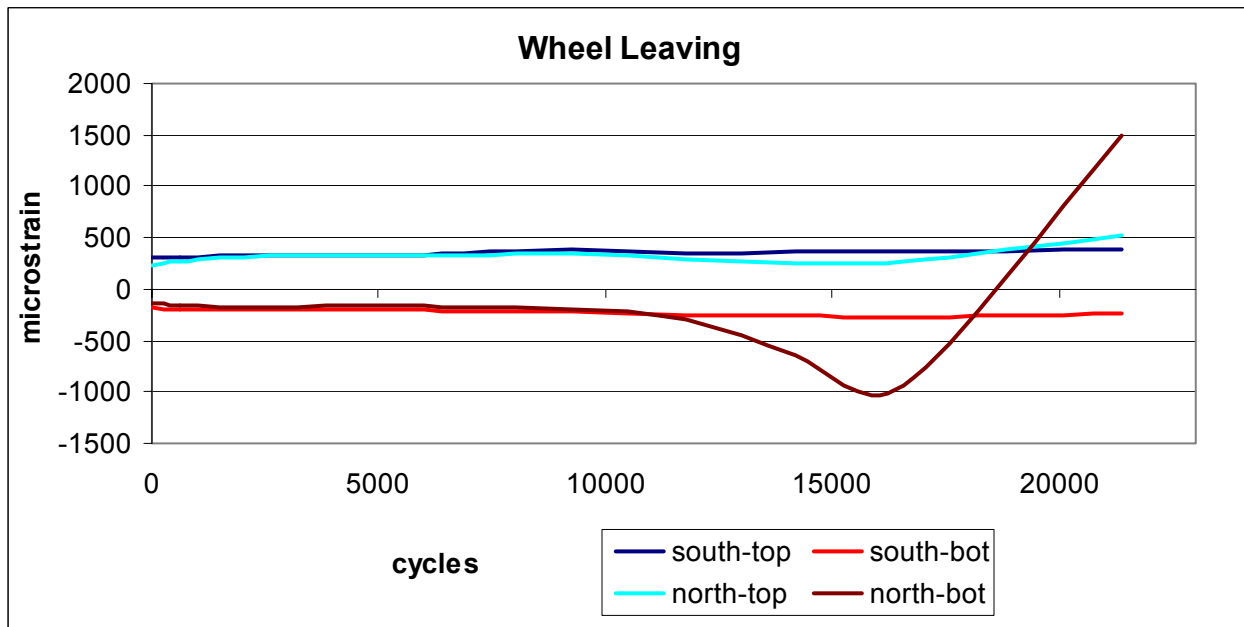
FIGURE 4.30: Strain vs. Cycles for Location #1 and #4 (Wheel Leaving)

Longitudinal and transverse strains were monitored in both pavements at midspan. Tables 4.10 and 4.11 give the strain values for the top and bottom positions in both pavements at locations #2 and #5 for longitudinal and transverse directions, respectively. The first four columns are strain values for wheel approaching and the last four columns are for the wheel leaving.

TABLE 4.10: Maximum Longitudinal Strains, Locations #2 and #5 (in μ€)

Wheel Approach					Wheel Leaving			
South top	South Bottom	North top	North Bottom	Cycles	South Top	South Bottom	North Top	North bottom
89.50	-35.11	63.60	-55.16	0	148.05	392.02	-207.75	452.30
215.50	-7.68	76.55	-126.05	619	312.17	469.04	-215.63	488.14
357.93	18.63	95.55	-146.85	2604	526.05	523.89	-210.27	426.78
417.81	-23.55	-1540.33	-237.66	5051	671.95	535.24	-1969.65	249.91
403.18	-65.67	232.88	-184.18	6882	754.54	514.65	523.32	262.67
496.09	-92.95	524.40	-178.48	9236	803.46	518.52	9.98	235.64
979.70	-20.77	296.41	-181.88	11769	-444.81	583.25	570.66	278.86
1293.54	-98.82	282.25	-193.57	14205	-1046.40	449.59	613.67	240.04
1854.59	-205.52	-373.43	-304.59	16553	-1738.56	287.14	520.96	285.90
2283.35	-317.75	-114.51	-247.34	21355	-3263.35	198.82	1036.63	411.40

Cycles	South top	South Bottom	North top	North bottom
0	-131.97	3503.7	3260.89	0
619	-100.33	4109.81	4426.89	0
2604	-105.46	4851.37	4609.8	0
5051	-109.34	5180	1560.09	0
6882	-132.98	5368.72	-1134.9	0
9236	-170.11	5712.2	-2012.66	0
11769	-198.83	6627.45	3238.57	0
14205	-209.11	7075.4	3053.66	0
21355	-237.04	8746.07	2341.38	0

Figures 4.31 and 4.32 show the longitudinal strains at the top and bottom positions for locations #2 and #5 as the wheels approach and after leaving, respectively. Figure 4.33 shows the transverse strains at the top and bottom positions for locations #2 and #5.
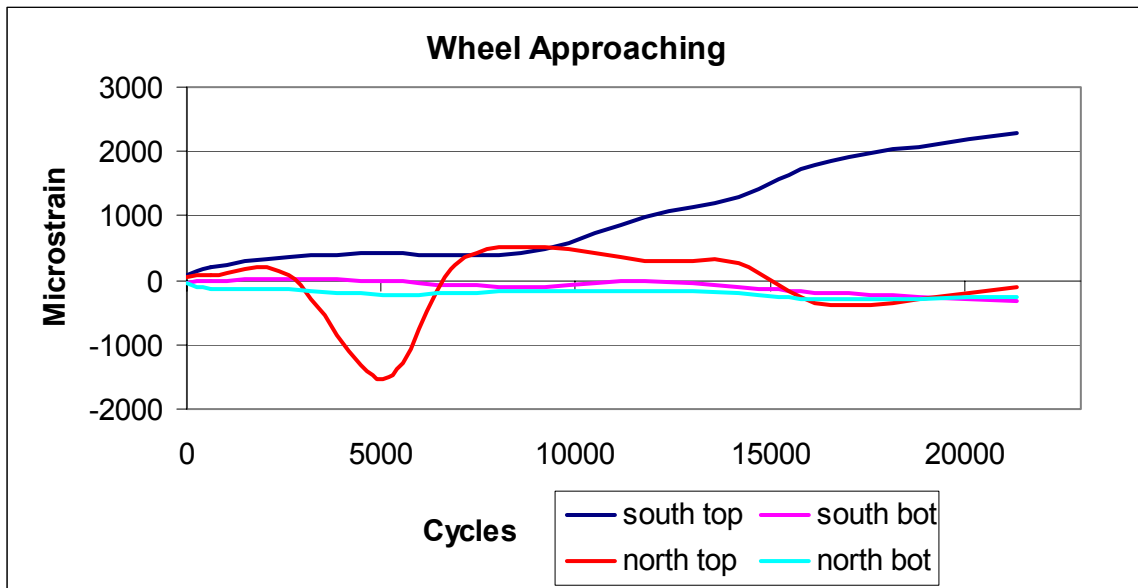
FIGURE 4.31: Longitudinal Strain vs. Cycles (Locations #2 and #5)
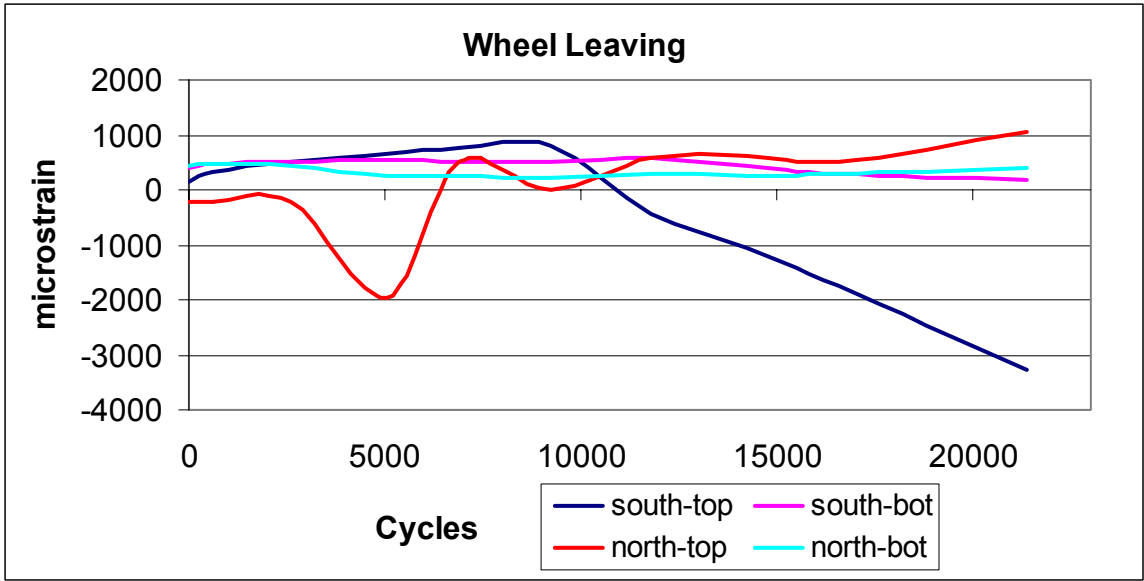
FIGURE 4.32: Longitudinal Strain vs. Cycles (Locations #2 and #5)
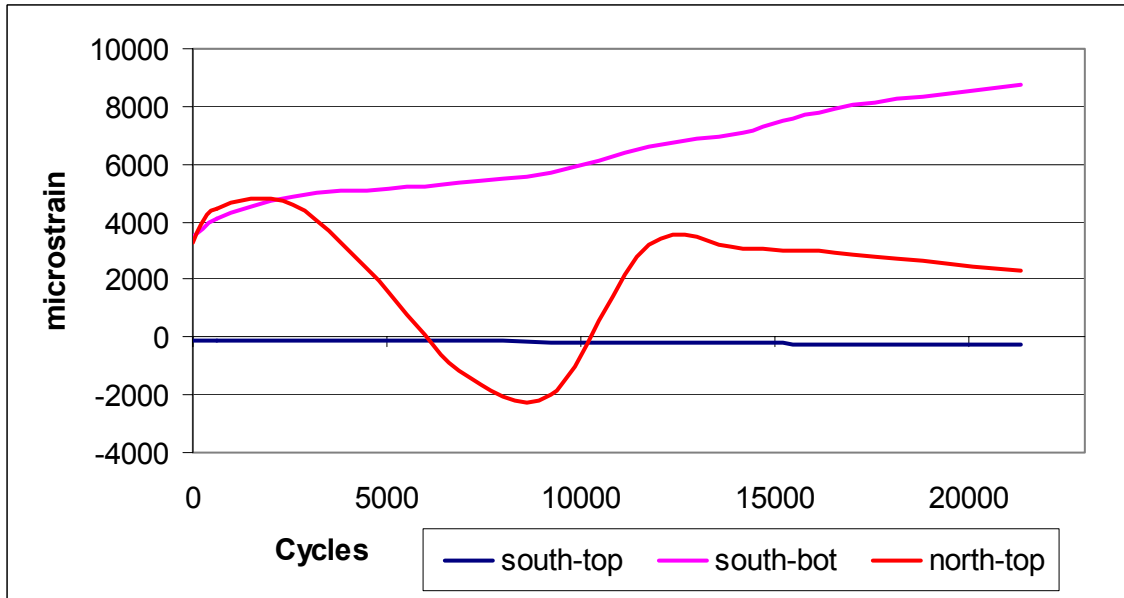
FIGURE 4.33: Transverse Strain vs. Cycles (Locations #2 and #5)

Table 4.12 gives the strain values for the top and bottom positions in both pavements at locations #3 and #6. The first four columns are the wheel-approaching strain values and the last four columns are for the wheel leaving.

71

TABLE 4.12: Maximum Strains for Locations #3 and #6 (in µ€)

Wheel Approach				Cycles	Wheel Leaving			
South top	South Bottom	North top	North Bottom		South Top	South Bottom	North Top	North bottom
231.90	0.00	-78.02	141.24	0	-152.11	0.00	58.08	-95.47
260.18	0.00	-62.13	204.93	619	-132.01	0.00	73.87	-60.09
279.04	0.00	-30.50	144.11	2604	-121.79	0.00	120.27	-138.35
278.48	0.00	-18.18	116.63	5051	-124.04	0.00	144.29	-195.46
344.07	0.00	4.69	146.30	6882	-108.84	0.00	147.80	-166.24
389.93	0.00	19.35	123.39	9236	-94.21	0.00	164.75	-179.88
449.02	0.00	11.72	144.00	11769	-17.95	0.00	164.75	-150.81
511.61	0.00	-4.10	113.07	14205	57.45	0.00	153.61	-176.39
546.76	0.00	-47.47	37.61	16553	28.02	0.00	103.73	-381.04
553.32	0.00	-50.97	-456.59	21355	76.21	0.00	90.23	-1214.15

Figures 4.34 and 4.35 show the longitudinal strains at the top and bottom positions for locations #3 and #6 as the wheels approach and after leaving, respectively.
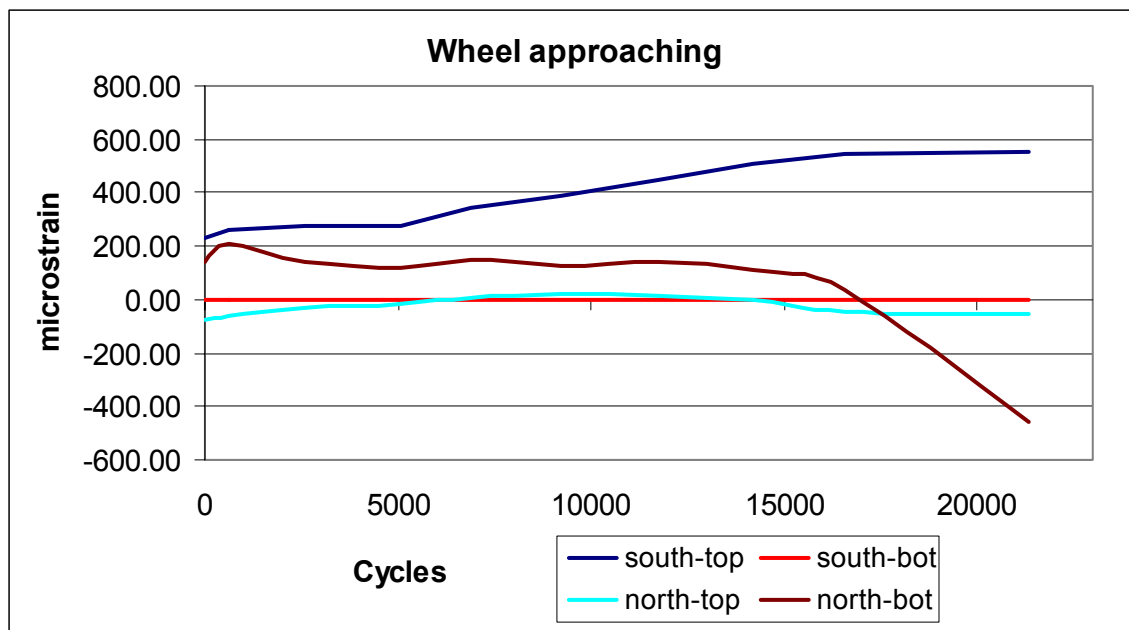
FIGURE 4.34: Strain vs. Cycles for Locations #3 and #6
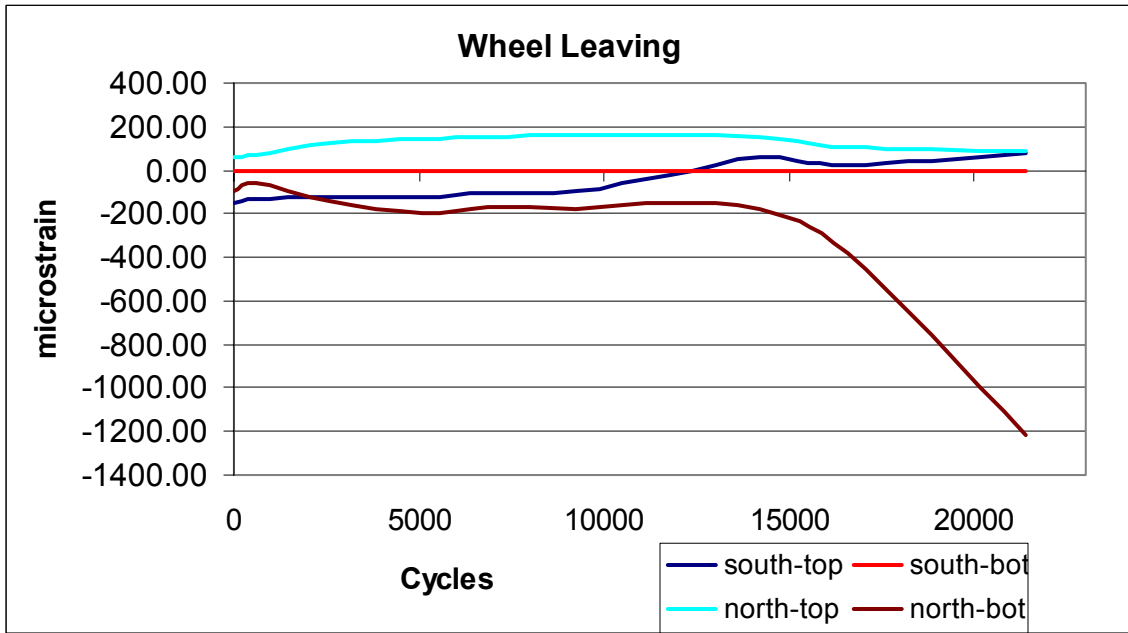
FIGURE 4.35: Strain vs. Cycles for Locations #3 and #6

4.2.2 Vertical Deflection

The vertical deflection in only the north pavement was monitored in experiment #10 using LVDT's. The description and location of each LVDT is described in section 3.2.3 for the rolling wheel loads. A typical deflection response for the north pavement is shown in Figure 4.36. As the wheel travels west to east, LVDT #9 is first to deflect downward and LVDT #1 is last to deflect downward, as observed in Figure 4.36. It is observed that as the wheels travel west to east, for example, LVDT #6 deflects downward as the wheels pass and then deflect upward when the wheels pass the location of LVDT #3. This behavior is observed for other LVDTs as well. The maximum deflections, both upward and downward, for each LVDT are shown in Figures 4.37 and 4.38 for the north pavements, respectively.

73
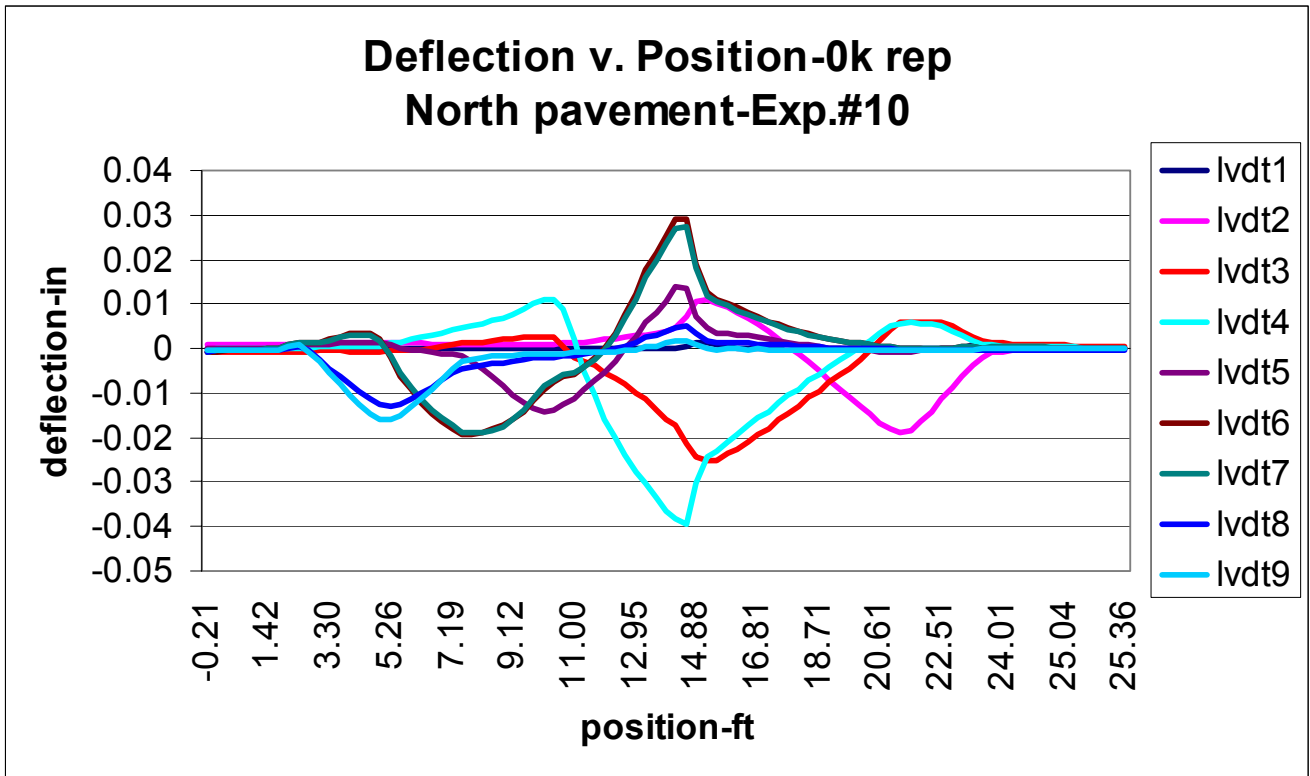
FIGURE 4.36: Deflection vs. Position, North Pavement, 0k cycles
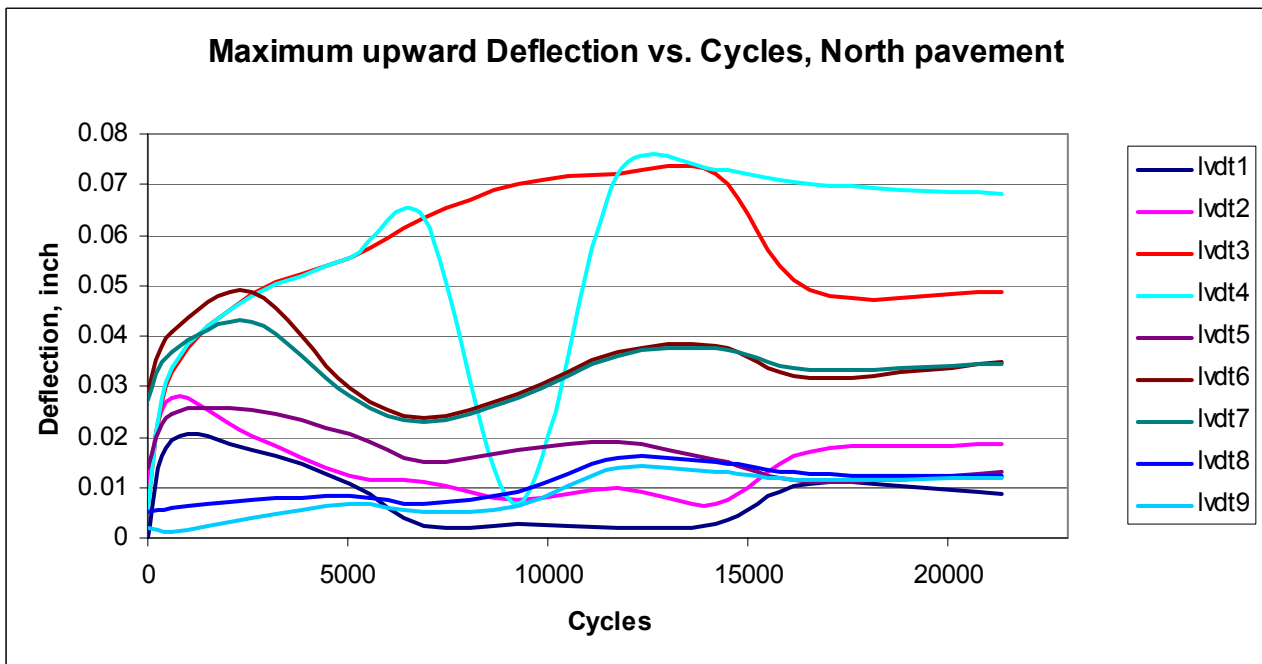
FIGURE 4.37: Maximum Upward Deflections vs. Applied Cycles

74

Maximum downward Deflection vs. Cycles, North Pavement
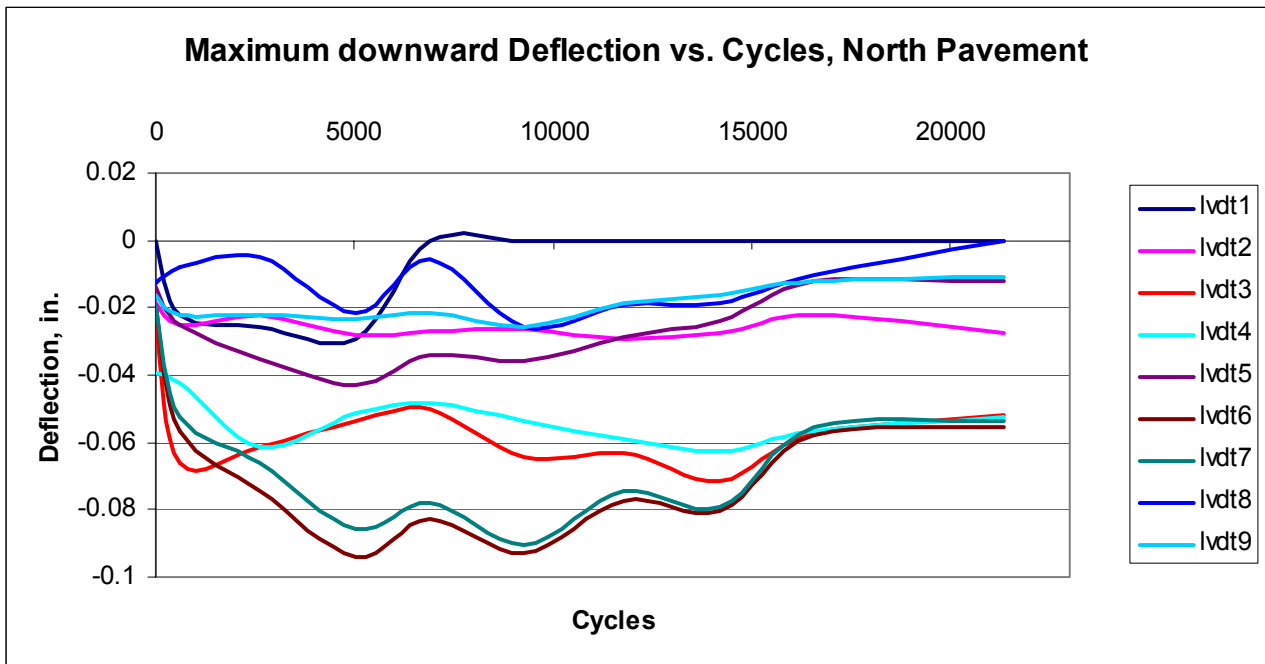
FIGURE 4.38: Maximum Downward Deflection vs. Applied Cycles

4.2.3 Pavement Cracking, Experiment #10

Pavement cracks developed during experiment #10 were monitored and documented for the duration of the experiment. Table 4.13 details the crack developments and the number of applied cycles. Figures 4.39 and 4.40 show the location of the cracks which occurred in the north and south pavements, respectively. The photographs in Figures 4.41 and 4.42 show the deterioration of the concrete around the FRP dowels. Figure 4.41 shows the severe crack development and crack continuation of the FRP dowel retrofitted at the west end, farthest north in the north lane. Figure 4.42 shows the transverse crack at the west end of the north lane, at the end of the test after the FRP dowels and crumbled concrete was removed and the surface broomed.

TABLE 4.13: Experiment #10 Cycles and Crack Descriptions

Cycles	Description/Comments
302,600	-North slab, crack observed on 1 ½" FRP dowel -Pumping steadily from north slab, several locations
309,236	-North slab, longitudinal crack observed originating at FRP plate (stitch) toward west transverse joint -Pumping significant on north edge of north slab, observable from south edge of north slab
314,205	-North slab, faulting and starts to breakup at west end (4th crack) 1" FRP dowel retrofit
316,550	-North slab, substantial joint faulting and deterioration at west end retrofit -Original mid-span section of slab (between 1 ½" and 1" FRP dowels) split longitudinally -No significant signs of distress near the epoxy coated steel dowels
321,355	-Test terminated due to severe distresses in the north lane
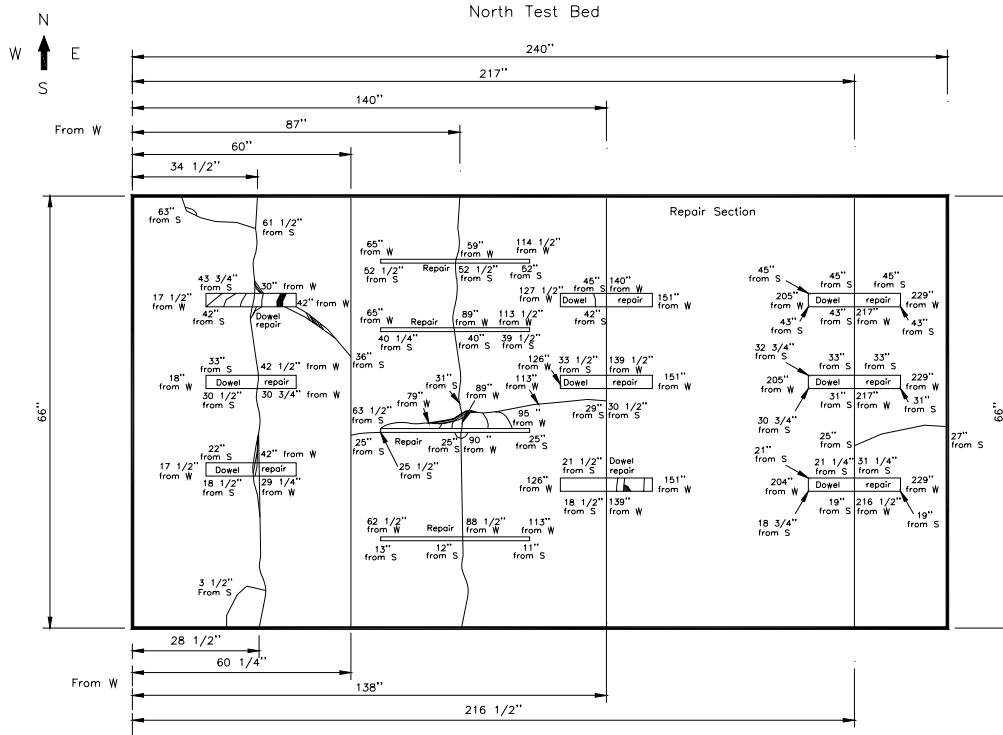
FIGURE 4.39: Crack Mapping in the North Pavement, Exp. #10
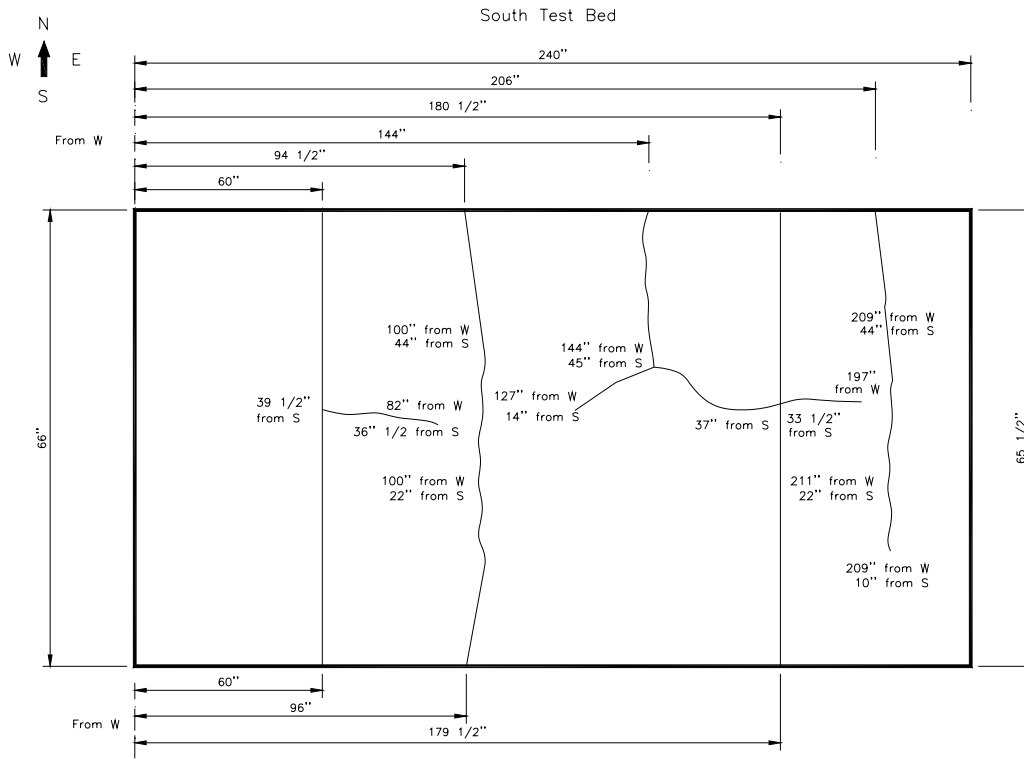
FIGURE 4.40: Crack Mapping in the South Pavement, Exp. #10

FIGURE 4.41: Severe Crack along FRP Dowel in the North Lane

FIGURE 4.42: FRP Dowels after Removal in the North Lane (West End)

Chapter 5

Conclusions and Recommendations

The major conclusions resulting from this research are:

1. ***The unbound permeable base gives a better performance than the unbound semi-permeable base.***

    This conclusion is supported by the following:

    - The surface cracking observed on the semi-permeable base pavement were much more severe than those observed on the permeable base pavement. Even after the PCCP slab in the semi-permeable base pavement was reinforced through the retro-fitting of the dowel bars, this pavement has more distresses and shorter life than the permeable base pavement.

    - The semi-permeable base pavement exhibited severe pumping of the fine materials through the joints, cracks and the side drain, while very little pumping was observed on the permeable base pavement.

    - The vertical compressive stresses in the subgrade soil have very similar values for the two pavements; only slightly higher stresses were recorded in the semi-permeable base pavement.

    - The horizontal longitudinal tensile strains at the bottom of the slabs have very similar values for the plain and fiber reinforced PCC overlays.

    Considering these observations, the use of semi-permeable bases under PCC pavements is not recommended. Longer life for these pavements is obtained if unbound permeable bases are used.

2.   ***When retrofitted to reinforce distressed joints and cracks, conventional 1-in. steel dowels give better performance than the 1 ½-in. FRP dowels.***

This conclusion is supported by the following:

- After 25,000 passes of the ATL machine, more severe deteriorations were observed around the FRP dowels than around the steel dowels.

REFERENCES

1. Melhem, H.G., *Development of an Accelerated Testing Laboratory for Highway Research in Kansas*, Report No. FHWA-KS-97/5, Kansas Department of Transportation, Topeka, KS, November 1997.

2. Melhem, H.G., *Accelerated Testing for Studying Pavement Design and Performance*; FY97-98, Report No. FHWA-KS-99-2, Kansas Department of Transportation, Topeka, KS, May 1999.

3. Melhem, H.G., Sheffield, F., *Accelerated Testing for Studying Pavement Design and Performance*; FY99, Report No. FHWA-KS-99-7, Kansas Department of Transportation, Topeka, KS, July 2000.

4. Swart, R., Melhem, H.G., *Accelerated Testing for Studying Pavement Design and Performance*; FY2000, Report No. FHWA-KS-02-6, Kansas Department of Transportation, Topeka, KS, October 2003.

5. "*Standard Specifications for State Road and Bridge Construction*" Kansas Department of Transportation, Topeka, KS, Edition 1990.

APPENDIX A

ATL #9 INDEX OF DATA FILES: Stored on CD consisting of seven folders of which the first is the Index and which is presented in hard copy herewith.

FOLDER "INDEX OF DATA FILES"

FOLDER "ATL #9" (THIS IS A DATA TEST AND IS NOT USEFUL DATA)

      FILE LOADTEST   8-30-00
                LOADTEST2   8-31-00
                LOADTEST3   8-31-00
                LOADTEST4   8-31-00
                LOADTEST5   8-31-00
                TESTDATA1   8-31-00
                TESTDATA2   9-1-00

FOLDER "ATL9DROPWEIGHTBINARY" (This is a binary file of dropweight data, the channels are 1-9 LVDT, and channel 10 is the load cell; the conversion of the load cell to pounds is "value recorded minus the initial offset multiplied by 8333.33."

      FOLDER   0KREP
                     5KREP
                     10KREP
                     20KEP
                     25KREP
                     40KREP
                     40KREP (AFTER REPAIR)
                     50KREP
                     60KREP
                     80KREP
                     100KREP
                     120KREP
                     180KREP
                     260KREP

FOLDER: "ATL9DROPWEIGHTTXT" This is a text file of the dropweight data conversion of the load cell data to pounds, "value recorded minus the initial offset multiplied by 8333.33" Format of text dropweight (data is taken at 10,000 entries per second), channels are numbered from 1 TO 10, 1 TO 9 are LVDT with positions shown on the figure, channel 10 is for the load cell.

CH 1	*CH 2*	*CH 3*	*CH 4*	*CH 5*	*CH 6*	*CH 7*	*CH 8*	*CH9*	*CH10*
-0.114	-0.258	-0.250	-0.013	0.201	-0.230	0.497	0.156	0.228	-0.004

> **FILE**: 090100 0REP
> 100300 5KREP
> 100500 10KREP

ATL #9 INDEX OF DATA FILES: Stored on CD consisting of 7 folders of which the first is the Index and which is presented in hard copy herewith

> 101100 20KREP
> 110800 40KREP
> 111300 40KREP AR   (AFTER REPAIR) NORTH
> 052101 260KREP

FOLDER : ATL9LVDTRL
This is a test file of the rolling wheel load, this data is taken at a rate of approximately 60 points per second, channels are numbered 1 to 10, 1 to 9 are LVDT's, data is in inches, channel 10 is the position of the rolling wheel, data is in volts. The conversion to wheel position is: (volts + 5.14)/0.1898 = Position in feet, the zero position is the west end of the pit.

> **FILE:** 090100 0REP N
> 090100 0REP S
> 100300 5KREP S
> 100300 5KREP S
> 100500 10KREP N
> 100500 10KREP S
> 101100 20KREP N
> 101100 20KREP S
> 101600 25KREP N
> 101600 25KREP S
> 110800 40KREP N
> 110800 40KREP S
> 111300 40KREP AR (AFTER REPAIR) NORTH
> 111600 50KREP N
> 111600 50KREP S
> 112900 60KREP N
> 112900 60KREP S

122000 80KREP N
122000 80KREP S
012601 100KREP N
012601 100KREP S
021501 120KREP N
021501 120KREP S
032701 180KREP N
032701 180KREP S
052101 260KREP N
052101 260KREP CRACKS N
052101 260KREP NORTH JOINT
052101 260KREP S

FOLDER: ATL#9 STRAINPRESSPOS: This is a text file of the strain and ground pressure data. Strain is read in microstrain and pressure in psi.

DATE	*TIME*	*CHANNEL 0*	*CHANNEL 1*	*CHANNEL 2*
11/29/2000	2:34:34 PM	-35139.3281	-33589.6055	-45699.1523

CHANNEL 3	*CHANNEL 4*	*CHANNEL 5*	*CHANNEL 6*	*CHANNEL 7*
-36331.6602	-49560.457	-41356.1445	-34931.316	-42657.3750

CHANNEL 8	*CHANNEL 9*	*CHANNEL 10*	*CHANNEL 11*	*CHANNEL 12*
-38880.0703	-34751.0820	-42570.1016	-156185.515	-45161.9062

CHANNEL 13	*CHANNEL 14*	*CHANNEL 15*	*CHANNEL 16*	*CHANNEL 17*
-48082.1914	-54256.1641	-32875.9609	-37879.9531	-29535.0898

CHANNEL 18	*CHANNEL 19*	*CHANNEL 20*	*CHANNEL 21*	*CHANNEL 22*
-29460.3574	-40570.2227	-47120.5430	-40009.1875	-47943.3516

CHANNEL 22	*CHANNEL 24*	*CHANNEL 25*	*CHANNEL 26*	*CHANNEL 27*
-41990.1172	1.3605	1.4801	1.1798	-0.9308

CHANNEL 28	*CHANNEL 29*	*CHANNEL 30*	*SPARE*
75.0037	-1.2549	-2.3188	0.0000

FILE: 90500 0KREP
90500 0KREP TEST
100300 5KREP
.   100500 10KREP
101100 20KREP
101600 25KREP
101800 30KREP
102400 35KREP

```
110800 40KREP
111300 40KREP AR   (AFTER REPAIR)
111600 50KREP
112900 60KREP
122000 80KREP
012601 100KREP
021501 120KREP
032701 180KREP
052101 260KREP
```

FOLDER: ATL#9 TEMPERATURE: This is a file for temperature data; Date, Time, 18 channels for thermocouple data (in degrees-F)

DATE	*TIME*	*CH.0*	*CH.1*	*CH.2*	*CH.3*
11/30/2000	1:36:29 PM	265.42	80.52	122.27	68.62

CH.4	*CH.5*	*CH.6*	*CH.7*	*CH.8*	*CH.9*	*CH.10*
71.72	65.47	71.46	73.32	120.96	66.96	70.49

CH.11	*CH.12*	*CH.13*	*CH.14*	*CH.15*	*CH.16*	*CH.17*
101.01	65.24	70.05	65.18	64.78	68.75	121.80

FILE ATL EXP#9
11-30-2000	9:41:45 AM	TO	12-26-00	8:35:14 AM

FILE ATL EXP#9a
12-9-2000	9:10:27 AM	TO	12-18-00	12:58:13 AM
12-26-2000	10:24:16 AM	TO	12-29-00	7:21:19 AM
1-19-2001	3:33:20 PM	TO	2-01-01	5:07:15 PM
2-12-2001	8:52:41 AM	TO	2-15-01	1:05:14 PM
2-19-20001	8:03:31 AM	TO	3-12-01	12:56:51 PM
4-10-2001	8:10:44 AM	TO	4-24-01	11:27:36 AM

APPENDIX B

Permeability

```
***********************************************
*          S O I L P R O P          *
*A program to estimate soil hydraulic properties*
*    from particle size distribution data      *
*                                  *
*     COPYRIGHT  1990  Version 2.1        *
* Environmental Systems and Technologies, Inc. *
* P.O. Box 10457, Virginia 24062-0457        *
*          (703) 552-0685          *
***********************************************


***********************************************
*          ATL #9 CLAY CONTENT 2%       *
***********************************************
```

-------- PARTICLE SIZE DISTRIBUTION DATA --------

```
        % clay  material   => 2.00
        % fine silt       => 2.00
        % medium silt     => 3.00
        % coarse silt     => 5.00
        % very fine sand  => 2.00
        % fine sand       => 3.00
        % medium sand     => 1.00
        % coarse sand     => 2.00
        % very coarse sand => 5.00
        % fine gravel     => 46.00
        % cobbles         => 29.00
```

R^2 for log-normal fit => .8231

```
        theta_s (cc/cc)   => .18
        % error in theta_s => .00
        bulk density (g/cc) => 2.16
        % error in bulk den => 10.00
```

R^2 for V_G model fit => .9286

Irreducible water saturation / water content
estimated from retention data by SOILPROP

86

------ VAN GENUCHTEN RETENTION PARAMETERS -------

	Estimated value	Standard deviation
alpha (1/cm)	2.46	1.03
n	1.37	.771E-01
theta_r(cc/cc)	.154E-01	.393E-02
K_s (cm/d)	.530E+05	.193E+06

--------- PARAMETER CORRELATION MATRIX ----------

	alpha	n	theta_r
alpha	.100E+01		
n	-.895E+00	.100E+01	
theta_r	-.254E+00	.497E+00	.100E+01

Irreducible water saturation / water content
  estimated from retention data by SOILPROP

------ BROOKS-COREY RETENTION PARAMETERS -------

	Estimated value	Standard deviation
h_d (cm)	.295	.108
lambda	.342	.601E-01
theta_r(cc/cc)	.154E-01	.393E-02
K_s (cm/d)	.530E+05	.193E+06

--------- PARAMETER CORRELATION MATRIX ----------

	h_d	lambda	theta_r
h_d	.100E+01		
lambda	.861E+00	.100E+01	
theta_r	.211E+00	.497E+00	.100E+01

```
*************************************************
*              S O I L P R O P            *
*A program to estimate soil hydraulic properties*
*      from particle size distribution data      *
*                                                *
*        COPYRIGHT  1990  Version 2.1          *
*  Environmental Systems and Technologies, Inc. *
*  P.O. Box 10457, Virginia 24062-0457          *
*              (703) 552-0685                  *
*************************************************


*************************************************
*              NO CLAY                    *
*************************************************
```

-------- PARTICLE SIZE DISTRIBUTION DATA --------
     % clay material   => .00
     % fine silt   => .00
     % medium silt   => 5.00
     % coarse silt   => 6.00
     % very fine sand   => 3.00
     % fine sand   => 3.00
     % medium sand   => 1.00
     % coarse sand   => 2.00
     % very coarse sand => 5.00
     % fine gravel   => 46.00
     % cobbles   => 29.00

     R^2 for log-normal fit => .8420

     theta_s (cc/cc)   => .18
     % error in theta_s => .00
     bulk density (g/cc) => 2.16
     % error in bulk den => 10.00

     R^2 for V_G model fit => .9288

  Irreducible water saturation / water content
   estimated from retention data by SOILPROP

------ VAN GENUCHTEN RETENTION PARAMETERS -------

	Estimated value	Standard deviation
alpha (1/cm)	2.65	1.08
n	1.32	.603E-01
theta_r(cc/cc)	.111E-01	.498E-02
K_s (cm/d)	.630E+05	.212E+06

--------- PARAMETER CORRELATION MATRIX ----------

	alpha	n	theta_r
alpha	.100E+01		
n	-.860E+00	.100E+01	
theta_r	-.233E+00	.548E+00	.100E+01

Irreducible water saturation / water content
  estimated from retention data by SOILPROP

------ BROOKS-COREY RETENTION PARAMETERS -------

	Estimated value	Standard deviation
h_d (cm)	.290	.104
lambda	.299	.496E-01
theta_r(cc/cc)	.111E-01	.498E-02
K_s (cm/d)	.630E+05	.212E+06

--------- PARAMETER CORRELATION MATRIX ----------

	h_d	lambda	theta_r
h_d	.100E+01		
lambda	.818E+00	.100E+01	
theta_r	.179E+00	.548E+00	.100E+01